Numerical Modelling for Horizontal Ground Heat Exchangers Optimization

March 2016

Department of Science and Advanced Technology
Graduate School of Science and Engineering
Saga University

Salsuwanda Bin Selamat

Numerical Modelling for Horizontal Ground Heat Exchangers Optimization

By

Salsuwanda Bin Selamat

A dissertation submitted in partial fulfillment of the requirements for the degree of

Doctor of Engineering (Dr.Eng.)
in
Mechanical Engineering

Department of Science and Advanced Technology
Graduate School of Science and Engineering
Saga University
Japan

March 2016

Approval

Department of Science and Advanced Technology
Graduate School of Science and Engineering
Saga University
1, Honjo-machi, Saga 840-8502, Japan

This is to certify that the dissertation submitted by

Salsuwanda Bin Selamat

titled "**Numerical modelling for horizontal ground heat exchangers optimization**" has been approved by the dissertation committee for the partial fulfillment of the requirements for the degree of ***Doctor of Engineering (Dr.Eng.)*** in Mechanical Engineering at March, 2016.

Dissertation Committee:

Chairman
Dr. Akio MIYARA
Professor, Department of Science and Advanced Technology
Saga University

Member
Dr. Shigeru MATSUO
Professor, Department of Mechanical Engineering
Saga University

Member
Dr. Yuichi MITSUTAKE
Professor, Department of Mechanical Engineering
Saga University

Member
Dr. Keishi KARIYA
Associate Professor, Department of Mechanical Engineering
Saga University

ACKNOWLEDGEMENT

All praise is due to The Almighty who blessed me with this life and may He guides me to His right path.

All my profound gratitude is dedicated to my supervisors, Professor Akio Miyara and Associate Professor Keishi Kariya, for their precious guidance and support throughout my study at Saga University. Their genuine interest in the study enhanced my vision and research ability.

This study was made possible from funding from the project on 'Renewable energy-heat utilization technology and development project' of New Energy and Industrial Technology Development Organization (NEDO) of Japan.

I would like to thank my friends and colleagues here in Japan, whom made this journey memorable and exciting. Special thanks to colleagues at Miyara Laboratory for their sincere support throughout my stay here.

Also I would like to show gratitude to those I was sharing valuable social aspects of life with them; Malaysian community, Muslim community, good friends, and all others associated to me during this time.

Special thanks are also due to my scholarship providers; Universiti Malaysia Perlis and Ministry of Higher Education of Malaysia, for granting me this once-in-a-lifetime opportunity.

Those without them I will not exist; my parents whom I can never truly repay for what was provided for my life. I also extend my thanks to my brother, sisters and my in–laws.

Last but not the least to my beloved wife and children whom always keep me going, I love you all.

Dedicated to my beloved Mama and Bapak, my lovely wife and children, my brother and sisters, and the rest of my big family; Malaysia

ABSTRACT

Ground source heat pump (GSHP) systems have been proven to have higher efficiency and more environmental-friendly compared to conventional air source heat pump systems for space heating and cooling applications. Despite its benefits, exorbitant initial cost discourages homeowners and small-medium enterprises to opt for such systems. Horizontal ground heat exchangers (GHE) buried at shallow depth offer relatively low-cost solution that may help promoting these systems usage worldwide. On the downside, horizontal GHE performance is subjected to daily and seasonal variations.

Therefore, optimization of such designs is essential to warrant high efficiency and provide ways for land area and piping materials minimization. The aim of this work was to investigate the effect of different installation layouts, pipe materials and thermal interference on horizontal GHE thermal performance. In this work, possible ways of optimization were explored using three-dimensional CFD simulation in examining short-term response of GHE models. Preliminary analysis involved modelling a slice of ground profile cross-section containing only a unit of GHE for single and parallel operation. Subsequently, real-scale modelling of moderate-size GHE was performed for a more reliable simulation results.

Based on the preliminary analysis for 24 h operation under several operation modes, it was found that the GHE orientation is not so important due to the little effect it has on thermal performance. While the mean heat exchange rate of copper loop increases 48% compared to HDPE loop, the analysis supports the common claim that heat exchange rate is predominantly limited by the thermal conductivity of the ground. With the same amount of circulation work, the mean heat exchange rate increases by 83–162% when operated in parallel loops operations. The performance in these operations can be further optimized to 10–14% increase when spacing between adjacent loops was provided. Similar findings were obtained when the operation was extended for 5-day continuous operation.

The simulation was then performed on real-scale GHE models to predict the outlet temperature and heat exchange rate under continuous 5-day heating operation.

The effect of pipe materials of different thermal properties on heat exchange rate of GHE operation was also studied. The analysis includes comparison of heat exchange rates between straight and slinky configurations. Although the heat exchange per pipe length for slinky configuration is lower, the heat exchange per trench length outperforms the straight configuration due to the greater surface area provided. Copper pipe shows a significant increase in thermal performance in GHE operation attributed by superior thermal properties compared to the commonly used HDPE pipe.

Comparative analysis of real-scale GHE models was extended using different configurations, orientations and pipe materials under cooling operation. All cases tested are able to yield comparable heat exchange rate for an equal trench length. However, the effective period differs one from the other. Additional initial and overhead costs are worthy as slinky GHE prolongs heat transfer process when compared against straight configuration. Pipe materials with superior thermal conductivity also promote longer high efficiency operation. An improvement of 16% is reported when copper pipe is used instead of the conventional HDPE pipes. Effective period can be extended by 14% when GHEs are installed in vertical orientation. Thermal interference in slinky configuration is prevalent during initial operation. In a long run, the effect is observed to be minimal except in vertical orientation. However, it is avoidable beforehand at design stage.

OUTLINE OF THESIS

This study presents the outcomes of numerical modelling of horizontal GHE in several designs and operating conditions for investigation of thermal performance. The thesis includes compilation of the following published and submitted papers that are organized into separate chapters.

I. Selamat S, Miyara A, Kariya K. Analysis of short time period of operation of horizontal ground heat exchangers. *Accepted for publication in Resources* 2015; 4(3):507–23. doi:10.3390/resources4030507.
II. Selamat S, Miyara A, Kariya K. Considerations for Horizontal Ground Heat Exchanger Loops Operation. *Accepted for publication in Transactions of the Japan Society of Refrigerating and Air Conditioning Engineers* 2015; 32(3):345–51. doi:10.11322/tjsrae.15-18RE_OA.
III. Selamat S, Miyara A, Kariya K. Comparison of heat exchange rates between straight and slinky horizontal ground heat exchanger. *Proceeding of 24th IIR International Congress of Refrigeration*, Yokohama, Japan: 2015.
IV. Selamat S, Miyara A, Kariya K. Comparative analysis of horizontal ground heat exchangers modelled using different layouts and pipe materials. *Submitted to Renewable Energy* 2015.

Chapter 1 presents the background including problem statements and overview of GSHP systems. It also defines aims and objectives of the study. This chapter concludes with a summary of the thesis organization.

Chapter 2 presents the literature review summarizing the analysis methods of GHE. It underlines established analytical and numerical models related to the current study. This chapter ends with comparison between analytical and numerical methods for GHE analysis.

Chapter 3 compiled from Paper I presents the simulation results in short time period of operation of exact shape of single and parallel GHE. The time frame of the simulation includes 24 h for short time period of operation and 7 days for discontinuous

9 h and 12 h operation a day.

Chapter 4 compiled from Paper II presents extended analysis of seasonal variations of the developed GHE modelled in continuous 5-day operation. For parallel loops operation, the analysis was carried out only in cooling mode.

Chapter 5 compiled from Paper III presents the numerical modelling of real-scale GHE designs to predict the outlet temperature and heat exchange rate for operation in heating mode. The analysis includes comparison of heat exchange rates between straight and slinky configurations.

Chapter 6 compiled from Paper IV presents the continuity of real-scale GHE analysis in cooling mode in proposing possible ways of optimization. The effective thermal performance and period of GHE and the effect of thermal interference are highlighted in this chapter.

Chapter 7 presents the summary of results of this thesis. Proposals for future research are also presented.

TABLE OF CONTENTS

LIST OF FIGURES

LIST OF TABLES

NOMENCLATURE

Λ	Thermal interference (-)
A	Surface area (m^2)
c_p	Specific heat (J/kg·K)
HER	Heat exchange rate (W)
k	Thermal conductivity (W/m·K)
L	Length (m)
$\dot{m}$	Mass flow rate (kg/s)
ρ	Density (kg/m^3)
T	Temperature (°C or K)
ΔT	Temperature difference (°C or K)
y	Vertical distance (m)

Subscripts

avg	average
eff	effective
i	individual pipe in parallel configuration
LP	per unit pipe length
LT	per unit trench length
P	pipe
T	trench

CHAPTER

1

INTRODUCTION

1.1 Background

The world energy demands, principally in Asia, are predicted to rise by 1.3 times the present amounts by 2030 [1]. It is estimated that in Japan, commercial and residential sector attribute to about 34% of total energy use. Approximately 30% of commercial and residential energy consumption is for space heating and cooling. Building acclimatization combines with hot water supply constitute about 60% in residential and 40% in commercial buildings energy demands [2].

Conventional air source heat pump (ASHP) systems for air-conditioning have been identified as one of the major contributors to heat island phenomena in urban areas. It is reported that ambient temperature rise in 23 of Tokyo wards is half due to artificial exhaust heat build-up from buildings [3]. Heat island average daily density of 3–5 °C during the summer would result in thermal discomfort and increases air-conditioning loads [4]. To compensate the increase in ambient temperature, building energy demands are estimated to increase by 5–10% [5].

Similarly, climate change increases electricity consumption for acclimatization caused by the change in ambient conditions. In order to meet the demands, more fossil fuels are required at power generation plants thus releasing more CO_2 and other harmful emissions. This dampens the effort to mitigate climate change and inadvertently contributes to global warming. Hence, energy efficiency strategies need to be put in

place for HVAC systems.

The Intergovernmental Panel for Climate Change (IPCC) reported that the global mean surface temperature is expected to increase from in the range of 0.3–0.7 °C to 2.6–4.8 °C until 2100 using 1986-2005 baseline. Global CO_2 emissions from fossil fuel combustion are accountable for 31 gigatons of annual total GHG emissions [6,7]. It is emphasized that the global temperature rise should be kept within 2 °C to avoid catastrophic impacts through emission reduction pathway.

As a signatory member of Kyoto Protocol, Japan is committed to reduce its CO_2 emission by 6% based on the 1990 level [8]. While the first commitment period ended in 2012, Japan continues to strive with its own initiatives in reducing greenhouse gases (GHG) emissions. This is emphasized by the Bill of the Basic Act on Global Warming Countermeasures that targets emission reduction of 25% by 2020 and 80% by 2050 based on the 1990 level [9].

The Bill also targets to raise the share of renewable energy to 10% from total primary energy supply by 2020. This becomes increasingly important in the wake of the Fukushima Nuclear Power Plant accident in 2011. In the aftermath, Japan had witnessed a surge in the dependency on coal for power generation. Renewable energy such as hydro, wind, solar, biomass and geothermal provide sources that are clean and sustainable. Reduction in foreign fuel imports also benefits the nation's economy as power generation from these sources can be self-produced.

Besides power generation, renewable sources can be applied as a tool to enhance energy efficiency and environment conservation. A study conducted in Tokyo [10] suggests that GSHP systems would result in 54% equivalent to 39,519 tons of the CO_2 emissions reduction annually. Ground source heat pumps (GSHP) systems tap the stored energy in geothermal reservoir for space heating and cooling. These systems are more efficient than conventional ASHP systems due to relatively stable ground temperature. On the contrary, ASHP systems performance is affected by temporal and seasonal variations.

Geothermal reservoir in deep zones has been used for steam generation in power plant and district heating or even cooling. GSHP systems can also be used in tandem for hot water supply in commercial and residential buildings by reusing heat stored in the ground. The ground can provide thermal energy storage up to several months whether hot or cold for later use. For example, heat as waste product of GSHP systems or from solar collector during warm season can be extracted during cold season.

Other building acclimatization, applications of GSHP systems include road and car park snow melting and swimming pools heating. As of 2013, they are 1513 GSHP systems installations throughout Japan with exponential increase since 2000 [11]. Applications in residential constitute 42% of the total installations but mainly concentrated in colder regions of the country. The cumulative system capacity in Japan is 62,476 kW with total ground heat exchangers (GHE) length of 316,302 m [12].

GSHP systems offer relatively lower operating cost. It is reported that a GSHP installation in Japan reduces the daily power consumption by 39% in cooling mode and 19% in heating mode compared to ASHP system [13]. An installation in Aomori Prefecture shows reduction of 48% in operating cost and 50% in CO_2 emissions for air-conditioning and snow melting compared to conventional system using air chiller, kerosene boiler and electric snow melting [14].

GSHP systems are listed as one of the components in Net Zero Energy Buildings (ZEB) [1]. Despite the benefits of GSHP systems, the usage is still low in public and private sectors. These systems draw huge drawback because of high investment cost pertaining to installation of GHE. Typically, the payback period of investment cost ranges from 5 to 10 years [15] thus causes hesitation among potential system owners. Ways to reduce the payback period through GHE design and sizing optimizations and higher efficiency are critical in promoting such systems.

1.2 Overview of GSHP systems

1.2.1 Geothermal heating and cooling

In the pursuit of sustainable environment, systems with high efficiency and produce less pollution are brought into perspective. Geothermal would provide a solution for energy efficiency and an option of renewable energy. Since 1960, geothermal has been applied in power generation at locations with geothermal resources such as steam, hot springs and hot dry rock [16].

Geothermal systems work with the environment to provide clean, efficient, and energy-saving heating and cooling the year round. Geothermal systems use less energy than alternative heating and cooling systems, helping to conserve our natural resources. Geothermal systems do not need large cooling towers and their running costs are lower

than conventional heating and air-conditioning systems.

A geothermal heat pump system is a heating and/or an air conditioning system that uses the Earth's ability to store heat in the ground and water thermal masses. Geothermal heat pumps are similar to ordinary heat pumps, but use the ground instead of outside air to provide heating, air conditioning and, in some cases, hot water. Because they use the Earth's natural heat, they are among the most efficient and comfortable heating and cooling technologies currently available.

Studies had shown that by switching on to geothermal system, a significant amount of savings could be made in terms of monetary and pollution loads. Geothermal systems save homeowners According to the US Environmental Protection Agency, 30–70% in heating costs, and 20–50% in cooling costs, compared to conventional systems [17]. Geothermal systems also save money in other ways. They are highly reliable, require little maintenance, and are built to last for decades. They add considerably to the value of homes.

Geothermal systems also support the Green Building [18] or more recently ZEB concepts which encompasses the practice of increasing efficiency with which buildings use resources – energy, water, and materials – while reducing building impacts on human health and the environment during the building's lifecycle, through better siting, design, construction, operation, maintenance and removal.

In all types of geothermal systems, the heat from the ground is transferred in storage tanks in buildings, where it is used for domestic hot water or even forced-air heating system. Geothermal systems can also deliver effective air conditioning during hot weather as well as heat during cold weather. Heat pumps are generally classified for heating of buildings according to the type of heat source. Hence, geothermal systems are often interchangeably referred as GSHP systems.

GSHP systems perform better than conventional ASHP systems especially in climates characterized by high daily temperature swings [19]. The ground is warmer during cold seasons and cooler during warm seasons than ambient conditions. The ground temperature remains relatively constant at depth of 2–3 m and below [20]. The effect of seasonal variations is negligible at depth beyond 7–12 m due to thermal inertia at greater depth [21].

1.2.2 Energy efficiency of GSHP systems

Coefficient of performance (COP) is typically used to express the efficiency of a heat pump. COP provides an indication of amount of energy delivered or "work produced" by heat pump with regards to energy supplied to perform the work. Hence, COP is defined as the ratio between the energy of heat pump output and work input. Most heat pumps available in today's market have a seasonally averaged COP of 2 to 3.

In contrast, an electrical furnace that able to convert all of the work supplied to energy used for heating yields a COP of 1. A heat pump system with a COP of 3 tells that with every unit of work used to drive the heat pump, three units of energy is transferred between the heat source and desired space. Heat pumps is able to yield a COP greater than unity by absorbing heat from low temperature source then transferring it to high temperature source.

The COP of a heat pump operating in heating mode is defined by:

$$\mathrm{COP} = \frac{Q_H}{W} \tag{1.1}$$

where Q_H is heating capacity of heat pump and W is power supplied to operate the heat pump.

For cooling mode, the COP is defined by:

$$\mathrm{COP} = \frac{Q_C}{W} \tag{1.2}$$

where Q_C is cooling power of heat pump.

Energy efficiency ratio (EER) is more commonly used to measure room air conditioning efficiency using the ratio between cooling capacity in British thermal unit (BTU) and power input. Hence, EER is expressed analogous to COP using:

$$\mathrm{EER} = 3.413\mathrm{COP} \tag{1.3}$$

where 3.413 is conversion factor from watt to BTU/h.

The efficiency of heat pump is limited by the second law of thermodynamics. Operation of heat pump with the maximum possible COP is the Carnot cycle calculated using:

– in heating mode

$$\mathrm{COP}_{Carnot} = \frac{T_H}{T_H - T_C} \tag{1.4}$$

– in cooling mode

$$\mathrm{COP}_{Carnot} = \frac{T_C}{T_H - T_C} \tag{1.5}$$

where T_H and T_C are temperature of warmer source and cooler source, respectively.

The ratio between sum of heat pump output and work input in an entire season are used to describe the seasonal efficiency. Therefore, seasonal COP or more commonly referred as seasonal performance factor (SPF) of heat pump is defined by:

$$\mathrm{SPF} = \frac{\int Q\, dt}{\int W\, dt} \tag{1.6}$$

where Q is heating or cooling capacity of heat pump and t is operation time.

As ASHP systems are subjected to varying ambient conditions, it is more practical to compare the efficiency over the entire season. In general, the SPF for GSHP units [20] is around 3.5 compared to 2.5 for ASHP in heating mode. In cooling mode, the efficiency GSHP units range from a SPF of 3–5. With the existing GSHP technology, the EER ranges from 15 to 30 [22].

The performance of heat pump relies much on the temperature of the heat source. The COP of ASHP units depends on the conditions of ambient air. If the temperature difference between ambient air and desired space is small, the COP will decrease. Whereas for GSHP units, ground conditions dictates the inlet temperature available in heat pump. The COP will suffer with smaller difference between inlet temperature and temperature of desired space.

The design and sizing of GHE in has critical influence on thermal performance of GSHP systems. The COP decreases at a faster rate if heat is being extracted or rejected to smaller volume of ground. This causes the ground near GHE to be unable to disperse the concentrated heat effectively. As the temperature difference between the heat source and desired space become smaller, more work input is required for heat pump to deliver the output temperature.

This is common in GHE installations involving shallow horizontal pipe buried 1–2 m deep. It is reported [23] that improvement of SPF for horizontal GHE is small compared to ASHP systems in heating operation. However, short-term extreme temperature variations are negligible allowing GSHP unit to meet heating requirement where ASHP is incapable [24]. Despite small difference in COP, greater annual energy savings presents as the aid of auxiliary electric heating is minimized.

1.2.3 Classification of GSHP systems

A broad method used to classify GSHP systems is by the way the working fluid circulates between heat pump unit and heat source or sink. Therefore, GSHP systems can be divided into two general classifications: (1) open loop systems, and (2) closed loop systems [20].

Fig. 1.1 shows GSHP examples that can be used to differentiate between open loop and closed loop systems. Open loop systems use heat in water from a reservoir and return it to the same or different reservoir. In closed loop systems, heat transfer fluid circulates inside pipes buried in and contact with the ground or paced at bottom of water bodies.

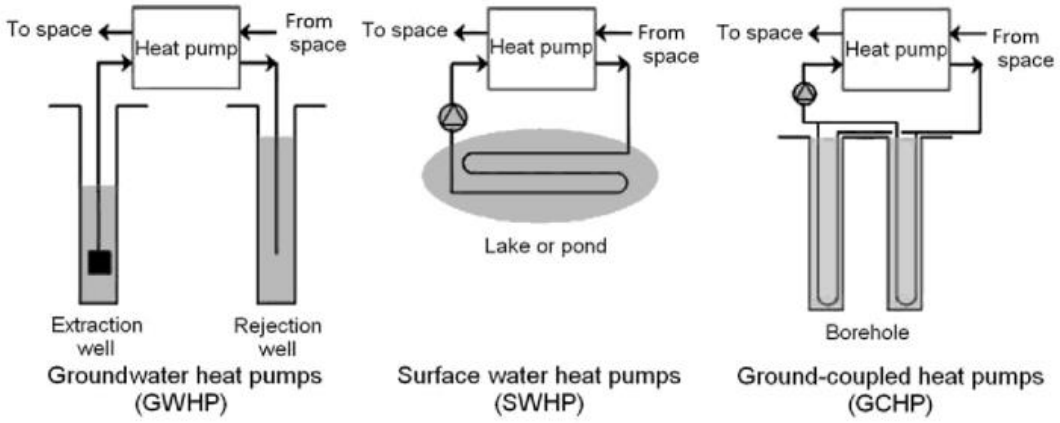

Fig. 1.1. Examples of different GSHP systems [19,25].

Open loop systems draw natural water from standing-column wells or surface-water. Groundwater heat pump (GWHP) systems pump groundwater to heat pump unit for heat exchange process and reject it into separate well or open-water. If standing-column wells are deep enough, some can reach depth of several hundred meters, water is returned at the top of water table of the same well.

Surface water heat pump (SWHP) can benefit from both open loop and closed loop systems. Water can be extracted from other water bodies such as lake and stream and returned at some distance from intake location. Otherwise in closed loop systems, coil pipes are submerged in the water. It is more preferable for circulation pump to be submerged in the water as well rather than placing it slightly above water level [26]. This prevents air from entering thus causing damage to the pump.

Open loop systems normally cost less to install than closed loop systems

especially in SWHP as less excavation is required. However, installation cost and pumping work required could be prohibitive for GWHP systems where water table is too deep. These systems are able to meet huge thermal loads depending on available volume of extraction and temperature difference [20]. Such systems operate using natural water in the absent of use chemical additives fluid.

In places where huge water bodies present, higher efficiency systems are achievable. Deep lake undergoes thermal stratification that keeps temperature at the bottom almost undisturbed. To some extent, heat pump is not necessary in open loop systems whereby cooling requirement of buildings is entirely met by the cold circulating water [19]. Higher thermal performance combined with low energy input to the systems reduces operating cost.

The disadvantage of open loop systems is due to heat pump unit is subjected to fouling, corrosion and blockage. Back-washable filters should be in place to prevent particulates such as grit and debris clogging the systems. Water with conductivity exceeding 450 μS/cm is not recommended due to corrosion and scaling factors [25].

The problems associated with open-loop systems using surface water can be eliminated by using closed loop systems. Lakes or ponds with at least 1.8 m deep and surface area 2500–5000 m^2 are suitable these applications [27]. Coils rest at bottom water bodies and secured to avoid shifting for example by spring ice movement.

Compared to GHE in ground-coupled heat pump (GCHP) systems, closed loop coils in SWHP systems require cheaper installation cost with minimal trenching work. Maintenance of the coils for repair of leakage can be performed relatively easy as the coils are readily accessible. Transporting heat to groundwater and surface water poses affect natural aquifers and water quality. The groundwater pathway between different water bearing strata may change in the presence of underground pipes [28].

The systems operation may affect the groundwater temperature in detrimental ways. Risk of groundwater pollution increases from corrosive pipe materials and release of chemical additives through leakages. Hence, such installations are regulated in some countries such as the US and UK [20]. In the US, the use of groundwater systems is not recommended as water tables are reported to fall over the last 50 years and continue to fall [29].

On the other hand, system owners have more freedom in installing closed loop GHE in GCHP systems. Nonetheless, enforcing agencies are currently figuring out ways to control GCHP installations. Heat transported by GHE perturbs ground

temperature and soil moisture content. Drastic changes on natural conditions of the ground cause harm to soil ecology.

Compared to other systems, GCHP systems are less efficient but the thermal performance in term of heat exchange yield can be conveniently predicted. Systems that use open loop and water source are prone to wide variation involve many unknowns and potential problems. Investigation of ground thermal conductivity through thermal response test and meteorological data allow accurate sizing of the systems, specifically GHE pipe length.

Fig. 1.2 explains the basic principle of GSHP systems utilizing closed loop in heating mode. Generally, closed loop systems consist of three principle elements: (1) earth connection via GHE; (2) heat pump unit; and (3) heat distribution system.

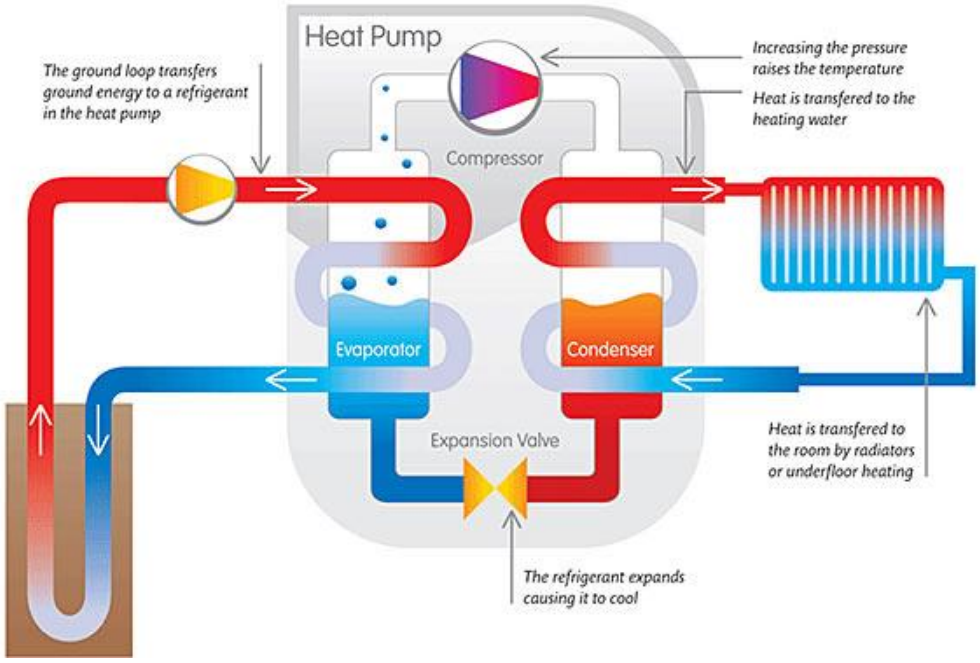

Fig. 1.2. Basic principle of closed loop GSHP systems (Source: www.revolveengineering.ca).

Heat pump unit operates similarly to Carnot vapor-compression cycle of a refrigerant. The refrigerant at evaporator absorbs heat from circulating fluid inside GHE. The compressor drives the refrigerant circulation and compresses it to the pressure that corresponds to the temperature needed at the condenser to supply heat for distribution system. The heat distribution system can either consist of radiant panels, underfloor heating or air handling unit (AHU). Finally, the refrigerant pressure is reduced allowing to it expand and further cool for the next cycle. The systems operate is reversed in cooling process.

Closed loop GHE are mostly constructed from plastic pipe and using water as heat medium. Besides that, use of metal pipes such as copper and steel is not uncommon. Brine solution or water-antifreeze mixtures are often used in conditions where the fluid temperature drops 6 °C [30]. Monoethylene glycol is commonly added to water as it provides freeze protection and increases GHE efficiency as specific heat capacity of mixture is reduced. However, it is considered toxic to living organisms and ecosystems.

Therefore, its usage is not recommended as it can contaminate drinking water supply. Other alternative additives [30] with lower toxicity include propylene glycol and ethanol. Vegetable extracts or organic salts pose less threat as additive while showing equivalent or better hydraulic performance. The same rule of thumb should be applied if corrosion or slime inhibitors are added to prevent biodegradation or biofilm growth. For systems in hot climate regions and dominantly used for cooling, water without any additive addition is recommended.

In some cases, the systems are equipped with auxiliary components. Solar collector panels and cooling towers are installed together in hybrid GSHP systems. Hybrid systems deliver higher energy efficiency and are advantageous to compensate the effect of ground thermal saturation. Refrigerant desuperheaters are commonly added to recover waste heat for supplying domestic hot water.

Other types adopting close loop systems can be classified by heat source or sink and types of working fluid used. Earth-to-air heat exchangers (EAHE) are used for ventilation in agricultural and residential buildings. These installations involved circulating air from desired space through underground ducting or tunnel at shallow depth directly or indirectly using heat pump. In residential application, EAHE systems are used to (1) preheat intake ventilation air in winter; (2) prevent freeze-ups of heat recovery unit of ventilation system; and (3) cool intake ventilation air in summer [31].

Direct-expansion ground heat exchangers (DXGHE) are systems where refrigerant passes through the ground in order to reject or extract heat. The absent of secondary fluid in heat pump allows refrigerant to evaporate in ground loop. The loop is typically made from copper pipe sheathed in polyethylene coating and buried in horizontal configuration at shallow depth.

In European countries, DXGHE are coupled with direct condensation in floor heating systems [32]. The application is limited to smaller units and requires a firm understanding of refrigeration cycle. High capacity pump is required to circulate

refrigerant in small tube over a long distance. Risk of releasing harmful refrigerant gases to the environment is presence in the event of leakage. Depending on local regulations, these systems may require approval and license prior to installation.

1.2.4 Types of GHE configurations

The earth connection is the most critical element in a closed loop GSHP system. This is where heat is being transported between ground and desired space via GHE. Most of the installation cost of GSHP systems is contributed by boreholes drilling or trench excavation works for GHE employment. That being said, GHE installations can be divided into two main categories: (1) vertical or borehole loops and (2) horizontal loops. The types of GHE cannot be recognized hidden beneath ground surface after the installation is complete.

1.2.4.1 Vertical loops

Vertical loops can be GHE pipes installed in a single or multiple boreholes as shown in Fig. 1.3. Hence, the term borehole loops is also interchangeably used for this configuration. The boreholes depth is typically range 20–100 m deep. The depth depends on heating or cooling load requirement, in industrial application the installations can reach up to 200 m deep. Consideration for suitable depth should also include geology factor and land area limitation.

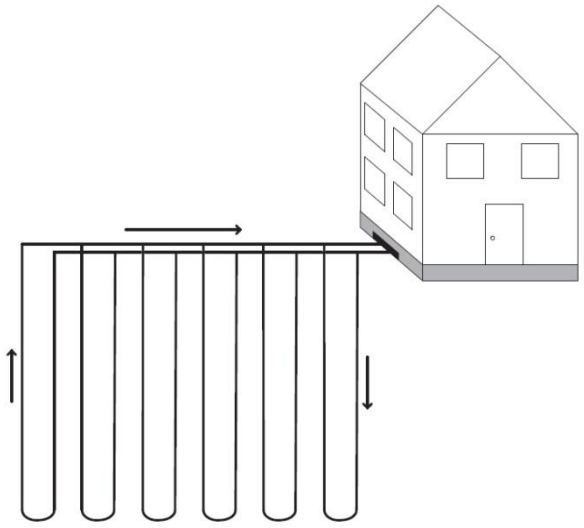

Fig. 1.3. Vertical closed loops GHE [33].

Diameter of each borehole range 100–200 mm where the U-tube shape GHE made from polyethylene or polybutylene of 20–40 mm nominal diameter is installed. One borehole can be installed with more than one U-tube GHE as these pipes do not cost much. The GHE can also be designed as concentric or coaxial pipes where a smaller pipe is enclosed in another larger pipe. Fig. 1.4 shows examples of common vertical GHE designs.

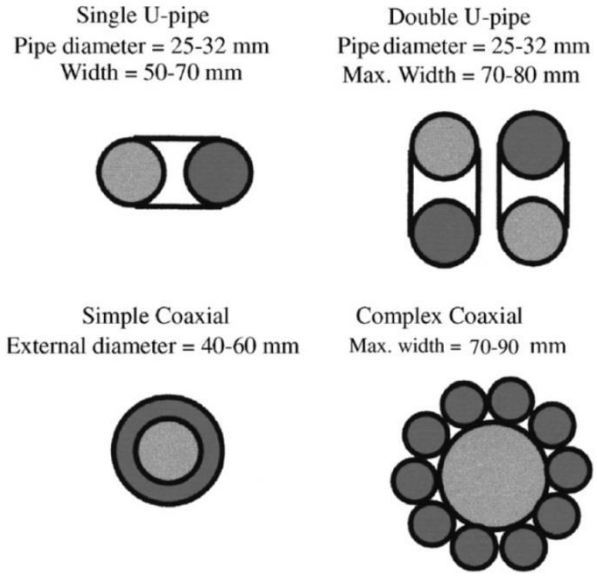

Fig. 1.4. Examples of common vertical GHE designs [34].

In multiple vertical GHE, the individual loop is joined for one or more circuits for connection to heat pump unit. The use of manifold system ensures equal flow distribution in multiple systems. Normally, spacing between boreholes is around 5–6 m to avoid interference from adjacent borehole that may affect overall efficiency. Sand is used for backfilling or grouted with pumpable slurry materials such as bentonite.

Vertical GHE installations benefit from limited land as this configuration reduces installation area. The location deep in the ground provides high and consistent system performance and requires less amount of piping. The major disadvantage of using vertical GHE is high installation cost due to expensive borehole drilling work.

1.2.4.2 Horizontal loops

Horizontal loops are laid and buried typically 1–2 m below ground surface. This configuration offers simplicity of installation compared to vertical loops. Any ground work contractors would be able to perform the required excavation and backfilling

works. This eliminates the requirement of specialist drilling contractor. Therefore, the cost of horizontal GHE installation would be minimal. However, this configuration necessitates abundant land area outside the building footprint.

In case of limited land area available for such installation, straight GHE pipes are arranged in series or parallel dense patterns [32]. This choice of configurations, shown in Fig. 1.5, is commonly used in Western and Central Europe. Usually, the whole top earth layer above the GHE area is completely removed for pipes arrangement and before finally backfilled. In area where land area is abundant, the loops are laid in small trench that occupy larger piece of land as shown in Fig. 1.6.

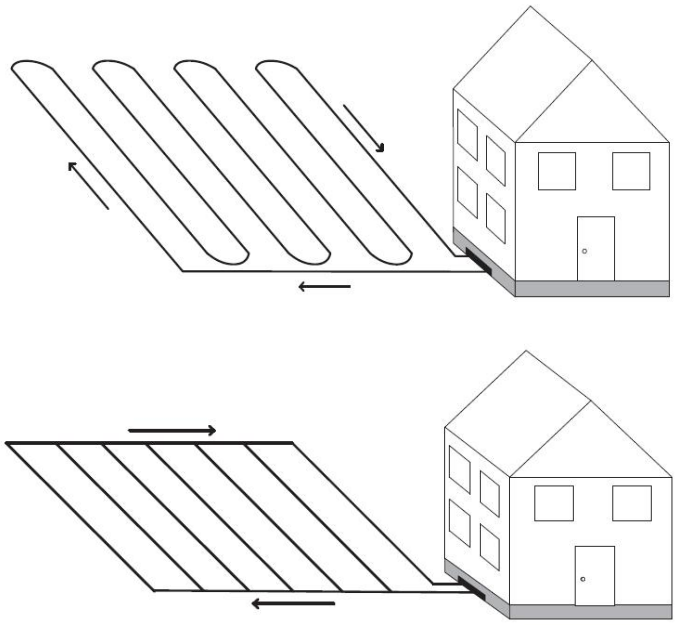

Fig. 1.5. Horizontal GHE in series (*above*) and parallel (*below*) [33].

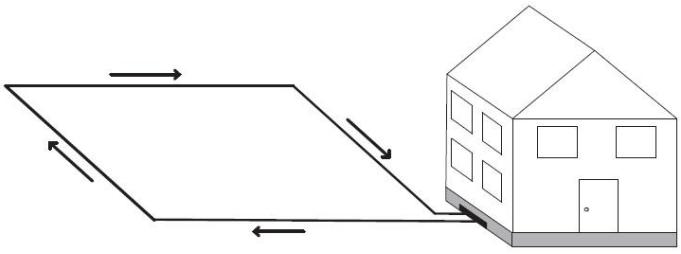

Fig. 1.6. Horizontal GHE in trench configuration [33].

Thermal recharge is the process where the ground recuperates its thermal balance. The main source of thermal recharge in systems using horizontal GHE is solar radiation to the Earth's surface. For installations in cold climate regions, insulations should not be

provided at ground surface above horizontal GHE by for example, locating it under a building. The opposite is true for systems that rely much on cooling operation where thermal recharge is not vital and ground surface interaction is undesirable.

Other GSHP systems that commonly utilize horizontal GHE are DXGHE and EAHE. Apart from ample land area, horizontal GHE are popular in places where aquifer level is high. However, thermal performance of this configuration in shallow depth is affected by temporal and seasonal variations. Amount of pipes needed is higher than in vertical configuration in order to recompense lower system efficiencies. Extra care should be taken while backfilling as it could damage the pipe.

To make full use of available land area for trenching, horizontal GHE can be installed as slinky loops or stretched coils, as shown in Fig. 1.7. Straight return pipe connects the end of the loops back to the heat pump unit. Slinky configuration yields more pipe length per trench length, increasing contact area between GHE and ground. As such, greater amount of pipes is required compared to conventional straight configuration. Typically, slinky GHE require 43–87 m of pipe per kW of heating and cooling capacity [32]. The added pipe length increases circulation pump work thus lowering the system COP.

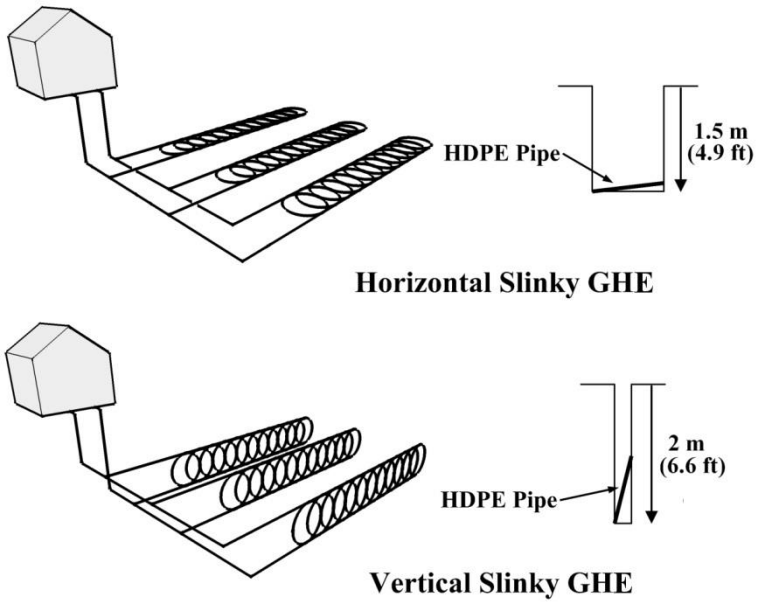

Fig. 1.7. Examples of slinky GHE configuration [35].

Loop pitch is distance between two slinky coils typically range 0.6–1.2 m. Slinky GHE involves installation in two varieties: (1) horizontal; and (2) vertical orientations.

For horizontal slinky GHE, width of trench range 0.8–1.8 m with separation distance in multiple trenches of 2–4 m. For vertical slinky GHE, the loops sit in upright position in narrower trench generally 15 cm wide. Narrower trench requirement in vertical layout could provide a way to reduce the total installation cost.

1.2.5 Ground thermal behavior

Ground temperature, at the surface and profile at various depths, is an important consideration in GSHP systems. Ground surface interaction with climatic conditions affects the temperature distribution along the depth. Therefore, the design of GHE should incorporate these underlying factors in preventing under- or over-sizing of the systems.

Nam et al. [36] present a ground surface heat balance model, as described in Fig. 1.8. Hence, ground surface heat flux can be calculated using the following equation.

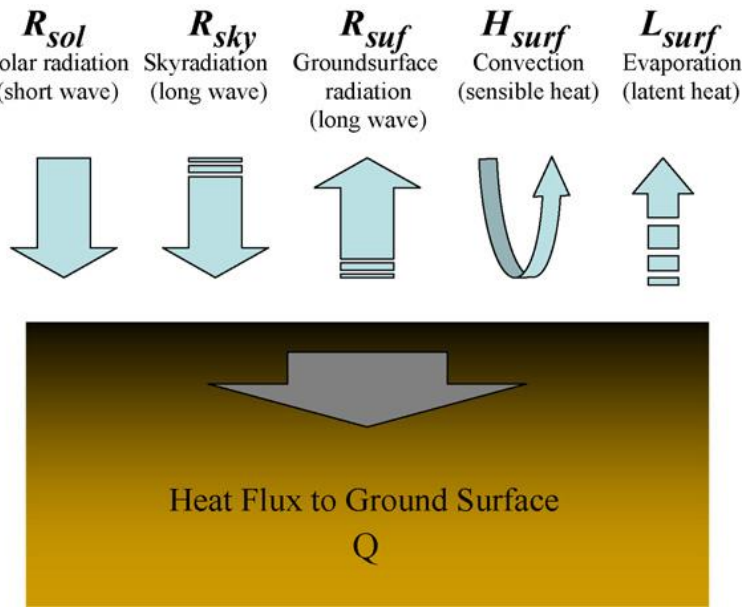

Fig. 1.8. Thermal balance on ground surface [36].

$$Q = R_{sol} + R_{sky} - R_{surf} - H_{surf} - L_{surf} \tag{1.7}$$

where R_{sol} is total solar radiation, R_{sky} is downward atmospheric radiation; R_{surf} is upward wave radiation from the ground surface; H_{surf} is sensible heat flux; and L_{surf} is latent heat flux. Each term on Eq. (1.7) can be obtained using the following equations.

$$R_{sol} = (1 - \alpha_s)(J_{dn} \times \sin(h) + J_{sh}) \tag{1.8}$$

Here, J_{dn} is direct solar radiation on the ground surface; $\sin(h)$ is solar altitude; J_{sh} is sky radiation; and α_s is albedo or reflectivity of solar radiation on the ground.

$$R_{sky} = \sigma(273.16 + T_a)^4(0.526 + 0.076\sqrt{f})(1 - 0.062 \times c) \tag{1.9}$$

Here, σ is Stephen-Boltzmann constant of $5.67 \times 10^{-8}\ \mathrm{W/m^2.K^4}$; f is water vapor pressure near the ground surface in mmHg; c is the degree of cloudiness; and T_a is air temperature.

$$R_{surf} = \sigma(273.16 + T_s)^4(1 - 0.062 \times c) \tag{1.10}$$

Here, T_s is ground surface temperature.

$$H_{surf} = \alpha_c(T_s - T_a) \tag{1.11}$$

$$\begin{aligned} \alpha_c &= 5.8 + 3.9v \quad && v \leq 5\ \mathrm{m/s} \\ \alpha_c &= 7.1v^{0.78} && v > 5\ \mathrm{m/s} \end{aligned} \tag{1.12}$$

Here, α_c is convective heat transfer ratio on the ground surface given by Jurges equation with respect to wind velocity near the ground surface, v.

$$L_{surf} = \beta \times 7 \times \frac{133.15}{1000}\alpha_c(f_{sat}(T_s) - T_a) \tag{1.13}$$

Here, β is moisture availability of the ground surface, and $f_{sat}(T_s)$ is saturated water vapor flux of T_s.

The ground temperature distribution is also affected by the structure and physical properties of the ground and the ground cover for example, bare ground, lawn, snow, etc. The most important ground thermal characteristics are thermal conductivity (k), density (ρ), specific heat (c_p) and thermal volumetric capacity $(C = \rho \times c_p)$. The accumulation and thermal capacity of the ground are functions of the ground moisture contents and the quantity of minerals present.

The temperature distribution at any depth below the earth surface remains unchanged throughout the year with the temperature increasing with depth with an average gradient of about 30 °C/km [34]. The geothermal gradient deviations from the average value are, in part, related to the type of rocks present in each section. Heat flow, which is a gauge of the amount of thermal energy coming out of the earth, is calculated by multiplying the geothermal gradient by the thermal conductivity of the ground. Each rock type has a different thermal conductivity, which is a measure of the ability of a material to conduct heat.

Rocks that are rich in quartz, like sandstone, have high thermal conductivity, indicating that heat readily passes through them. Rocks that are rich in clay or organic

material, like shale and coal, have low thermal conductivity, meaning that heat passes slower through these layers. If the heat flow is constant throughout a drill hole (i.e., water is not flowing up or down the hole), then it is obvious that low-conductivity shale layers will have a higher geothermal gradient compared to high-conductivity sandstone layers.

In the presence of groundwater flow, heat exchange is more complex because the water flow determines the changes of the temperature field in the direction of the water movement, enhancing heat exchange [25]. The hydraulic conductivity of the ground is thus another parameter to consider. This requires determining the groundwater velocity and the well-known horizontal pressure gradient:

$$v = ki \tag{1.13}$$

where, v is the Darcy velocity; i is the pressure gradient; and k is the hydraulic conductivity.

The ground temperature distribution can be distinguished into three zones [37]:

1. *Surface zone* reaching a depth of about 1m, in which the ground temperature is very sensitive to short time changes of weather conditions.
2. *Shallow zone* extending from the depth of about 1–8m (for dry light soils) or 20m (for moist heavy sandy soils), where the ground temperature is almost constant and close to the average annual air temperature; in this zone the ground temperature distributions depend mainly on the seasonal cycle weather conditions.
3. *Deep zone* (below about 8–20 m), where the ground temperature is practically constant (and very slowly rising with depth according to the geothermal gradient).

For positioning the GHE, it is important that the ground is well settled and level. The more water the ground contains, the better the heat transmission. A smaller ground area is required for dense, wet soil than for dry, crumbling ground. Rainwater is very important for the generation of the ground. The ground must settle before heat is collected.

1.3 Aims and objectives of study

GSHP systems offer double-edged benefits in providing high efficiency solution for space heating and cooling while having less impact on the environment. Although the number of GSHP systems installation continues to grow worldwide, the actual usage is admittedly still low. This is particularly true in less developed regions of the world where the awareness of the effectiveness of these systems is amiss.

The main obstacle in promoting GSHP systems usage is the expensive initial costs although the potential savings from operating cost is beneficial in a long run. It is crucial that efforts to reduce the payback period for such installations are enhanced. This study aims to reduce the costs concerning GSHP systems, initial- and operating-wise in order to attract more potential owners especially homeowners and small and medium enterprises.

The main contributor to high initial costs is the earth connection part particularly by installing GHE in vertical configuration. The installation cost can be reduced significantly by installing GHE in horizontal configuration. The major drawback of horizontal GHE is that it requires ample land area and pipe length for comparable performance to its vertical counterpart. Moreover, the performance is inconsistent due to shallow placement in the ground that prone to daily and seasonal variations.

Therefore, the focal point of this study is for horizontal GHE optimization in terms of sizing and efficiency. Optimization in both terms serves the purpose to introduce GSHP systems that are economically and operability balanced. This is achieved within the scope of work that covers the underlying objectives as follows:

1. To develop numerical model of exact shape of single and parallel horizontal GHE in different layouts and pipe materials.
2. To perform simulation based on the developed simplified model with several operating periods and conditions for thermal performance analysis.
3. To investigate the effect of near-surface interaction and thermal interference on thermal performance of GHE.
4. To analyze ground thermal behavior and temperature distribution in accounting the effective thermal performance and period of GHE.

CHAPTER

2

GHE THERMAL ANALYSIS—LITERATURE REVIEW

2.1 Introduction

Ground source heat pump (GSHP) systems utilize ground heat exchangers (GHE) specifically for ground-coupled earth connection. This differs from conventional air source heat pump (ASHP) systems where outdoor units or cooling towers are commonly used. The economic feasibility of a GSHP system for space heating and cooling heavily relies on the installation costs of GHE.

On the other hand, GHE sizing has major influence on operation performance that translates to operating cost. Therefore, understanding on how the proposed GSHP systems would perform is necessary prior to its introduction. This can be achieved by the mean of prediction tools to assess thermal behavior of GHE. Technical and cost-effectiveness optimization can be performed at design and sizing stage once the GHE thermal behavior has been worked out.

The main objective of the GHE thermal analysis is to determine the temperature of GHE working fluid circulating through the heat pump under certain operating conditions [38]. A design goal is then to control the temperature rise in the ground and circulating fluid within acceptable limits over the system lifespan. The “rule of thumb” approximation method was in fashion for a long time, which was discussed by Ball et al. [39].

Rules of thumb can serve well for specific localities where soil and weather

conditions are fairly uniform because design specifications are primarily based on the experience with related installations. However, some systems have suffered from the inability of the "rule of thumb" designers to properly assess the effect of varied design parameters, such as shallower burial depth, lower shank spacing between GHE U-tube legs and larger borehole/trench space in ground surface.

In addition to the rule of thumb method, several models with different complexity have been developed for the design and performance prediction of the GHE in engineering applications. Actually, the heat transfer process in a GHE involves a number of uncertain factors, such as the ground thermal properties, the groundwater flow and building loads over a long lifespan of several or even tens of years. In this case, the heat transfer process is rather complicated and must be treated, on the whole, as a transient one.

GHE thermal analysis can be approached either by analytical and numerical methods. Among other things, they can be used to predict the heat transfer mechanism inside a borehole, the conductive heat transfer from a borehole and the thermal interferences between boreholes. The principle of superposition of several independent elementary heat transfer processes serves as the basis for analytical models. These models usually consider the heat transfer from a GHE in a steady-state and model it using long time-steps [40].

Numerical models employ principle of solving the entire system in small cells or grids and applying governing equations on these discrete elements to find numerical solutions such as regarding pressure distribution, temperature gradients, flow parameters [41]. The models based on short time-step response focus more on the transient heat transfer in GHE. The time step for these models is in the hourly or sub-hourly range. Simulation using numerical models is helpful in designing GHE from scratch as well in troubleshooting or optimization by suggesting design modifications.

2.2 Consideration factors

Performance of GSHP systems depends on working fluid flow rate, depth and length of buried GHE. These allow sufficient conditions for working fluid to reject or absorb the heat to certain extent. The characteristics of GHE such as pipe size and thermal resistance as well as GHE configurations and combination influence on the

overall system efficiency. GHE pipes installed close enough cause heat flow to interfere with each other. The efficiency also depends on rating of applicable other components, for example circulation pump and blower fan.

Apart from temperature difference between the ground and ambient, initial soil temperature and thermal conductivity of soil including backfill material dictates heat exchange process. The ground surface has an impact on long-term temperature variations in the ground, especially when the heating and cooling loads differ from each other [42]. Excess heating or cooling loads can accumulate in the ground, causing the average ground temperature to gradually increase or decrease over time to such an extent that heat transfer through the ground surface becomes significant. Often, the effect of the ground surface is generally simplified and taken to be a constant-temperature boundary condition.

The movement of groundwater affects heat transfer by involving gross heat convection, which is significant for the long-term temperature response of GHE. Whereas a conservative design assumes no benefit from this flow, estimation of the influence of groundwater flow is desirable. The seepage flow of groundwater may be very complex, being vertical, horizontal, or both. Thus it is often simplified to be homogenous and parallel to ground surface. The movement of groundwater in a porous aquifer may also cause heat transfer by thermal dispersion [43].

ASHRAE recommends that all ground-source heat pumps use extended-range heat pump units for most water-to-air configurations [44]. An extended-range heat pump is a unit specifically designed to operate when the entering water has a temperature (leaving the GHE) of –4 °C in the heating mode and 38 °C in the cooling mode. A temperature of –4 °C for the entering water implies a lower average temperature of the fluid in the ground loop, which can cause problems with groundwater freezing.

Heat transfer in a porous medium is often accompanied by moisture transfer [45]. Even though heat transfer due to moisture transfer by GHEs may be a minor contribution, the accompanying variations in the thermal properties of the ground can be large, thereby significantly affecting the thermal process in the ground. An increase in the amount of moisture in dry soil can lead to a large increase in thermal conductivity, while diffusivity generally rises to a maximum (2–3 times the dry value) at a moisture content of 5–10% [46].

2.3 General assumptions

Several assumptions must be made when developing GHE thermal analysis models. The most common ones are given as follows [42]:

Assumption 1: The ground is infinite or semi-infinite in extent, depending on whether or not the influence of the surface is considered.

Assumption 2: The ground has a uniform initial temperature (effective undisturbed ground temperature). If the surface is considered, this initial temperature can be used as a constant-temperature boundary condition for the surface.

Assumption 3: The boundary condition for the wall of borehole or heat transfer pipe is either a constant flux or a constant temperature, with the constant-flux boundary condition being more convenient.

Assumption 4: If the effect of the seepage of groundwater cannot be ignored, the flow is generally assumed to be homogeneous and parallel to the surface.

Assumption 5: Although the ground is usually layered and inhomogeneous, the ground can be treated as a medium with an equivalent thermal conductivity. Analytical models use Assumption 5 almost exclusively. At first glance, this assumption seems to be highly idealized; but several numerical studies have confirmed that it is appropriate for predicting the overall temperature response [47–49]. It should be noted that this equivalence property is also a key parameter used in practical GCHP system design [44].

Assumptions 1–5 are widely used in analytical models of GHE, and they have been verified to some extent by numerical simulations [47–50].

2.4 Analytical models

In view of the complication of this problem and its long time scale, the heat transfer process may usually be analyzed in two separated regions [38]. One is the solid

soil/rock outside the borehole, where the heat conduction must be treated as a transient process. With the knowledge of the temperature response in the ground, the temperature on the borehole wall can then be determined for any instant on specified operational conditions.

Another sector often segregated for analysis is the region inside the borehole, including the grout, the GHE pipes and the circulating fluid inside the pipes. This region is sometimes analyzed as being steady- state or quasi-steady-state and sometimes analyzed as being transient. The analyses on the two spatial regions are interlinked on the borehole wall. The heat transfer models for the two separate regions are: (1) heat conduction outside borehole; and (2) heat transfer inside borehole.

2.4.1 Heat conduction outside borehole

A number of analytical models for the heat transfer outside the borehole have been recently reported, most of which were developed based on either analytical or numerical analysis.

2.4.1.1 Kelvin's line source model

The earliest approach to calculating the thermal transport around a heat exchange pipe in the ground is the Kelvin's line source theory, i.e. the infinite line source [3,25]. According to the Kelvin's line source theory, the temperature response in the ground due to a constant heat rate is given by:

$$T(r,t) - T_0 = \frac{q_l}{4\pi k} \int_{\frac{r^2}{4at}}^{\infty} \frac{e^{-u}}{u} du \tag{2.1}$$

in which r is the distance from the line source and τ the time since start of the operation; T is the temperature of the ground at distance r and time t; T_0 is the initial temperature of the ground; q_l is the heating rate per length of the line source; k and a are the thermal conductivity and diffusivity of the ground.

The solution to the integral term in Eq. (2.1) can be found from the related references [51–53]. Although it is characterized by the simplicity and less computation time, this model can only be applied to small pipes within a narrow range of a few hours to months because of the assumption of the infinite line source [49,54]. It was estimated that using the Kelvin's line source may cause a noticeable error when as

$\frac{at}{r^2} < 20$ [52]. This approach has been widely utilized in some analytical design methods that are currently used to analyze the heat transfer of GHEs [51,53,55].

A number of improvements for this approach have been proposed to account for some complicated factors so that the accuracy can be comparable to that of the numerical methods. Of all these methods employing Kelvin's line source theory, the Hart and Couvillion method may be more accurate than others [53].

2.4.1.2 Cylindrical source model

The cylindrical source solution for a constant heat transfer rate was first developed by Carslaw and Jaeger [46], then refined by Ingersoll et al. [52], and later employed in a number of research studies [56–58]. It is actually an exact solution for a buried cylindrical pipe with infinite length under the boundary condition of either a constant pipe surface temperature or a constant heat transfer rate between the buried pipe and the soil.

In the cylindrical source model, the borehole is assumed as an infinite cylinder surrounded by homogeneous medium with constant properties, i.e. the ground. It also assumes that the heat transfer between the borehole and soil with perfect contact is of pure heat conduction. Based on the governing equation of the transient heat conduction along with the given boundary and initial conditions, the temperature distribution of the ground can be easily given in the cylindrical coordinate:

$$\begin{aligned} &\frac{\partial^2 T}{\partial r^2} + \frac{1}{r}\frac{\partial T}{\partial r} + \frac{1}{a}\frac{\partial T}{\partial t} && r_b < r < \infty \\ &-2\pi r_b k \frac{\partial T}{\partial r} = q_l && r = r_b, t > 0 \\ &T - T_0 = 0 && \tau = 0, r > r_b \end{aligned} \tag{2.2}$$

The cylindrical source solution is given as follows:

$$T - T_0 = \frac{q_l}{k} G(z, p) \tag{2.3}$$

where $z = \frac{at}{r_b}$, $p = \frac{r}{r_b}$.

As defined by Carslaw and Jaeger [46], the expression $G(z, p)$ is only a function of time and distance from the borehole center. The temperature on the borehole wall, where $r = r_b$, i.e. $p = 1$, is of interest as it is the representative temperature in the design of GHEs. However, the expression $G(z, p)$is relatively complex and involves integration from zero to infinity of a complicated function, which includes some Bessel

functions. Fortunately, some graphical results and tabulated values for the $G(z,p)$ function at $p=1$ are available in some related references [52,56]. An approximate method for G was proposed by Hellstrom [59] and presented by Liu et al. [60].

2.4.1.3 Eskilson's model

Both the one-dimensional model of the Kelvin's theory and the cylindrical source model neglect the axial heat flow along the borehole depth. A major progress was made by Eskilson [49] to account for the finite length of the borehole. The basic formulation of the ground temperature is governed by the heat conduction equation in cylindrical coordinates:

$$\begin{aligned} &\frac{\partial^2 T}{\partial r^2}+\frac{1}{r}\frac{\partial T}{\partial r}+\frac{1}{a}\frac{\partial T}{\partial t} \\ &T(r,0,t)=T_0 \\ &T(r,z,0)=T_0 \\ &q_l(t)=\frac{1}{H}\int_D^{D+H} 2\pi k\left.\frac{\partial T}{\partial r}\right|_{r=r_b} dz \end{aligned} \tag{2.4}$$

in which H is the borehole length; D means the uppermost part of the borehole, which can be thermally neglected in engineering practice.

The final expression of the temperature response at the borehole wall to a unit step heat pulse is a function of t/t_s and r_b/H only:

$$T_b-T_0=-\frac{q_l}{2\pi k}g(t/t_s,r_b/H) \tag{2.6}$$

where $at_s=H^2/9a$ means the steady-state time. The g-function is essentially the dimensionless temperature response at the borehole wall, which was computed numerically.

2.4.1.4 Finite line source model

Based on the Eskilson's model, an analytical solution to the finite line source has been developed by Zeng et al. [61] which considers the influences of the finite length of the borehole and the ground surface as a boundary. The solution of the temperature excess is given by:

$$T(r,z,t)-T_0=\frac{q_l}{4\pi k}\int_0^H\left\{\frac{erfc\left(\frac{\sqrt{r^2+(z-h)^2}}{2\sqrt{at}}\right)}{\sqrt{r^2+(z-h)^2}}+\frac{erfc\left(\frac{\sqrt{r^2+(z+h)^2}}{2\sqrt{at}}\right)}{\sqrt{r^2+(z+h)^2}}\right\}dh \quad (2.7)$$

It can be seen from Eq. (2.7) that the temperature on the borehole wall, where $r=r_b$, varies with time and borehole length. The temperature at the middle of the borehole length ($z=H/2$) is usually chosen as its representative temperature. An alternative is the integral mean temperature along the borehole length, which may be determined by numerical integration of Eq. (2.7).

2.4.2 Heat conduction inside borehole

The thermal resistance inside the borehole, which is primarily determined by thermal properties of the grouting materials and the arrangement of flow channels of the borehole, has a significant impact on the GHE performance [38]. The main objective of these semi-analytical models is to determine the entering and leaving temperatures of the circulating fluid in the borehole according to the borehole wall temperature, its heat flow and the thermal resistance.

One-dimensional model. A simplified one-dimensional model has been recommended for GHE design, which considers the GHE U-tube pipe as a single "equivalent" pipe [51,62].

Two-dimensional model. Hellstrom [59] derived the analytical two-dimensional solutions of the thermal resistances among pipes in the cross-section perpendicular to the borehole axis, which is superior to empirical expressions and one-dimensional model.

Quasi-three-dimensional model. On the basis of the two-dimensional model above mentioned, a quasi-three-dimensional model was proposed by Zeng et al. [63], which takes account of the fluid temperature variation along the borehole depth.

2.5 Ring heat source analytical models

Classical models based on line and cylindrical source are not adequate for coil type heat exchangers because the heat transfer coils are disposed in the proximity of the pile circumference because of limitations due to simplifying assumptions of the heat source [64]. The heat source in the line source model is located at the center of borehole. Thus, the line source model might estimate somewhat lower soil temperature rise compared to the others'.

On the other hand, the heat source in the cylindrical source model is located near the borehole wall with a cylindrical face. Then, the cylindrical source model might estimate somewhat higher soil temperature rise compared to the others' [65]. In order to better understand and simulate the heat transfer of buried spiral pipes, researchers have proposed specific analytical models. These solutions are generally based on continuous point source solution and Green's function theory.

2.5.1 Spiral GHE

Recently, Man et al. [66] presented a new solid cylindrical source model evolved from the classical models. Also, the following models for a spiral coil type GHE have been developed: a ring coil source model [67], and a spiral heat source model [64]. However, they do not provide exact solutions for the spiral coil source and cause a computational problem because of the singularity in evaluating $1/(t-t')^{3/2}$ and need double integrations. Further research is thus necessary in order to develop a mathematically more efficient analytical solution for the spiral GHE.

Park et al. [65] describes the development of an efficient spiral source analytical model. Its analytical solution was developed to consider three-dimensional shape effects and radial dimension effects of a spiral GHE given in Fig. 2.1 using Green's function method. Because of the limitation in computation and the complicated formula, the spiral coil source analytical model was transformed by changing the variable into an error function to improve and simplify the computation for engineering applications.

For modeling a semi-infinite interval $z > 0$, a virtual spiral heat source with the same heat rate q_l and negative depth $-h$ is assumed on a symmetric space to the boundary. An analytical solution for variation of temperature of the spiral source

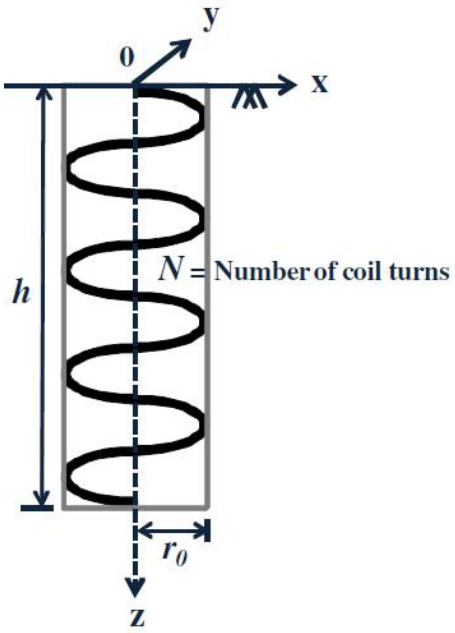

Fig. 2.1. Schematic view of spiral source [65].

problem can then be derived as:

$$\theta(u,t) = \frac{q_l}{4\pi k}\int_0^h \frac{erfc(A_-(u,z')/2\sqrt{at}}{A_-(u,z')} - \frac{erfc(A_+(u,z')/2\sqrt{at}}{A_+(u,z')}$$
$$A_\pm(u,z') = \sqrt{F(x,y,z') + (z \pm z')^2} \tag{2.8}$$
$$F(x,y,z') = x^2 + y^2 - r_0^2 - 2xr_0\cos(\omega z') - 2yr_0\sin(\omega z')$$

where r_0 is the characteristic length, wave number is $\omega = 2N\pi/h$ and u is vector in x, y, z Cartesian coordinates.

2.5.2 Slinky GHE

Li et al. [68] developed and solved analytically a moving ring source model to describe the temperature response of a slinky GHE with groundwater flow. For multiple moving ring source model in an infinite medium as shown in Fig. 2.2, if the temperature rise at point P is caused by multiple ring sources with n unit circles, of which the parameters of the ith ring source are denoted as $(x_i + r_0\cos\sigma, r_0\sin\sigma, z_i')$, the temperature rise at point P is obtained by applying the superposition principle in space:

$$\theta_{inf,P} = \frac{kr_0}{q_r}\sum_{i=0}^{n-1}\Theta_{inf,i}(R_i', Pe, F_0) \tag{2.9}$$

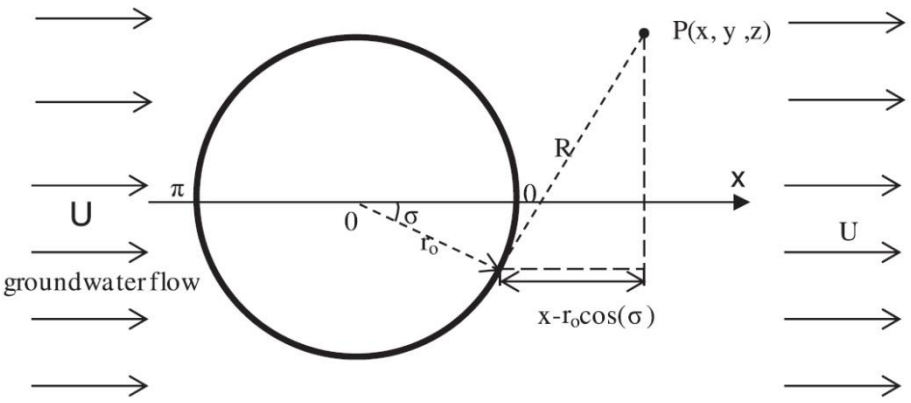

Fig. 2.2. Schematic of the moving ring source in an infinite medium [68].

$$\Theta_{inf} = \theta_{inf}\frac{kr_0}{q_r} = \frac{1}{8}\int_0^{2\pi} \exp\left[\left[Pe\frac{(x-\cos\sigma)}{2}\right] f(R_i', Pe, F_0)\right] d\sigma$$

$$f(R', Pe, F_0) = \frac{1}{R'}\left[\exp\left(-\frac{PeR'}{2}\right) erfc\left(\frac{R'-PeF_0}{2\sqrt{F_0}}\right)\right. \tag{2.9}$$

$$\left. + \exp\left(\frac{PeR'}{2}\right) erfc\left(\frac{R'+PeF_0}{2\sqrt{F_0}}\right)\right]$$

where U is groundwater constant velocity along x-direction, $Pe = \frac{Ur_0}{a}$, $F_0 = \frac{at}{r_0^2}$, $R' = \frac{R}{r_0}$, $Z = \frac{z}{r_0}$ and $X = \frac{x}{r_0}$.

If a slinky GHE consists of n ring source units, of which the parameters of the ith ring source is denoted as $(x_i + r_0\cos\sigma, r_0\sin\sigma, z_i')$, the temperature rise at point P in a semi-infinite medium (Fig. 2.3) is computed by:

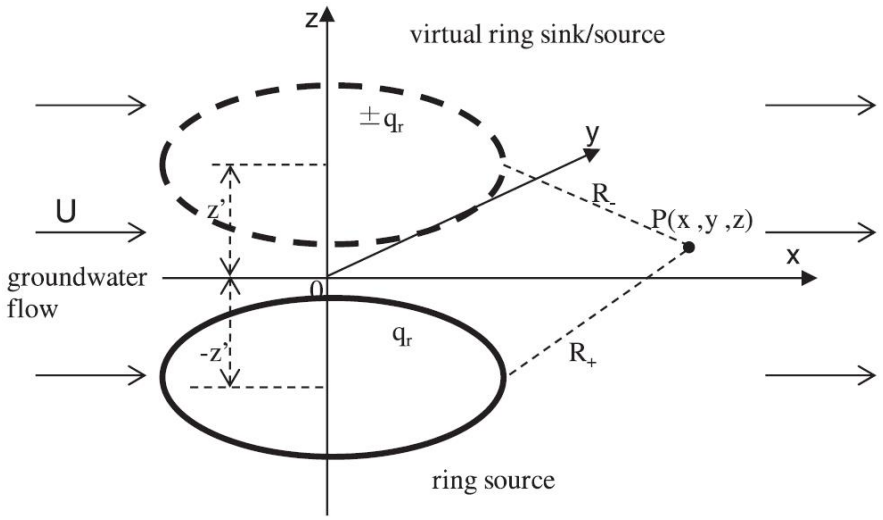

Fig. 2.3. Geography of the moving ring source in the semi-infinite medium [68].

$$\theta_{sf,P} = \frac{kr_0}{q'_r}\sum_{i=0}^{n-1}\Theta_{inf,i}(R'_i, Pe, F_0)$$

$$\Theta_{sf}(R', Pe, F_0) = \theta_{sf}\frac{kr_0}{q_r} = \frac{1}{8}\exp\left(Pe\frac{X}{2}\right)\int_0^{2\pi}[f(R'_+, Pe, F_0) \pm f(R'_-, Pe, F_0)]\,d\sigma \tag{2.10}$$

$$R'_+ = \left(\sqrt{(x-x')^2 + (y - r_0\cos\sigma)^2 + (z - (-z' + r_0\sin\sigma))^2}\right)/r_0$$

$$R'_- = \left(\sqrt{(x-x')^2 + (y - r_0\cos\sigma)^2 + (z - (z' + r_0\sin\sigma))^2}\right)/r_0$$

Xiong et al. [69] formulated an model that relies on analytical ring source solutions to compute temperature response functions for both horizontal and vertical slinky GHE. As Fig. 2.4 shows, point P_i is a fictitious representative point of a cross-section of ring tube i at angle φ. The distance between fictitious point P_i and point P_j is the average value of the distance between the outer point P_{io} and point P_{jo} and the distance between the inner point P_{ii} and point P_i.

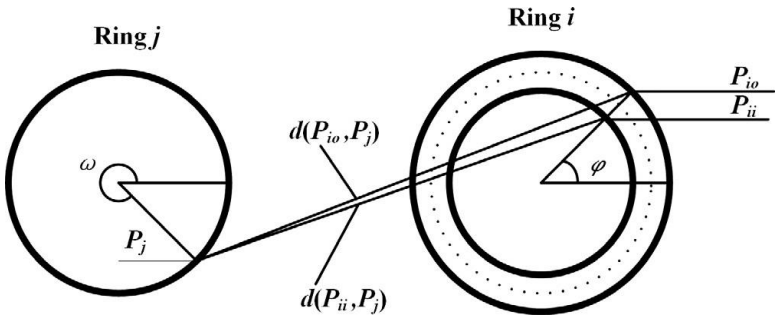

Fig. 2.4. Distance between point P_i and point P_j on ring source j [69].

The average temperature perturbation of the cross-section is assumed as the temperature perturbation of the fictitious representative point P_i. Specially, when i is equal to j, the dashed line in Fig. 2.5 shows the ring source of ring i itself. x_0 and y_0 are Cartesian coordinates of a ring's center. x_0 and y_0 are calculated based on the parameters of the slinky GHE such as the pitch, the distance between slinky tubes, and the number of rings.

The slinky GHE buried underground is treated in a semi-infinite medium with isothermal boundary condition. The solution for this case is obtained by applying the method of images. A fictitious ring source j_o is created for ring j, as Fig. 2.5 shows. For

horizontal slinky GHE, the fictitious ring source j_o is located a distance $2h$ above the ring source j and has the same heat input rate and the opposite sign.

The g-function (temperature response function) methodology is an approach proposed by Eskilson [49] previously discussed in subsection 2.4.1.3 to calculate the vertical borehole temperature response. A g-function can be represented by a set of non-dimensional temperature response factors. The g-function method is widely adopted in solving vertical borehole related problem. Xiong et al. [69] have applied it to the solution of the ring source model.

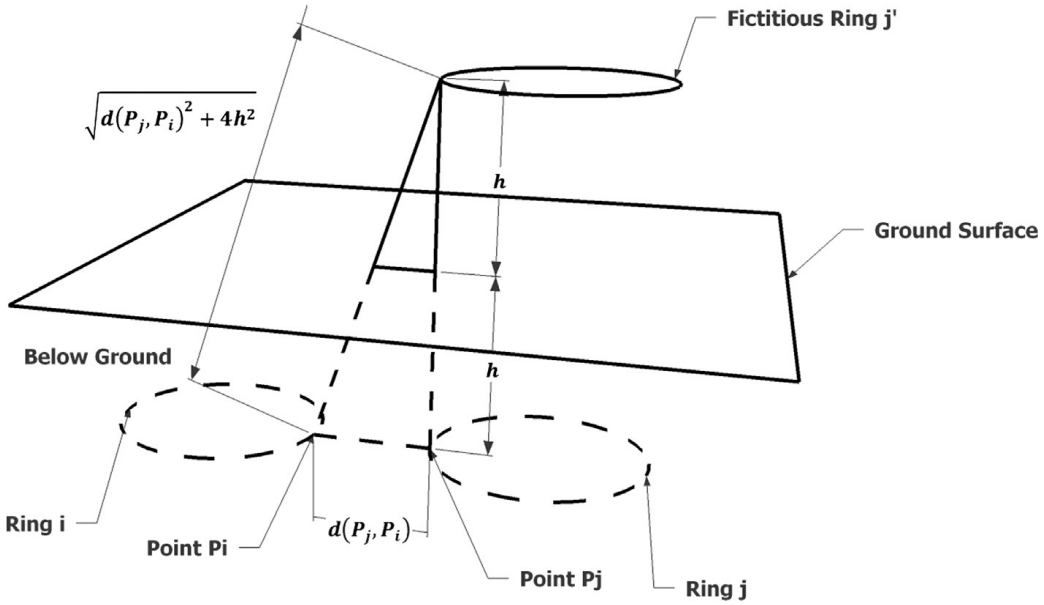

Fig. 2.5. Three-dimensional view of fictitious ring source of ring j [69].

The analytical solution of the temperature response function for slinky GHE in horizontal orientation is given by:

$$g_s(\tau) = \sum_{i=1}^{N_{ring}} \sum_{j=1}^{N_{ring}} \frac{R}{4\pi N_{ring}} \int_0^{2\pi} \int_0^{2\pi} \left[\frac{erfc(d(P_j,P_i)/2\sqrt{a\tau})}{d(P_j,P_i)} - \frac{erfc(\sqrt{d(P_j,P_i)^2+4h^2}/2\sqrt{a\tau})}{\sqrt{d(P_j,P_i)^2+4h^2}} \right] d\omega d\varphi \tag{2.11}$$

$$d(P_j,P_i) = \frac{d(P_{ii},P_j) + d(P_{io},P_j)}{2}$$

$$d(P_{ii},P_j) = \sqrt{\begin{matrix}\left[x_{0i} + (R-r)\cos\varphi - x_{0j} - R\cos\omega\right]^2 + \left[y_{0i} - y_{0j}\right]^2 \\ +\left[z_{0i} + (R-r)\sin\varphi - z_{0j} - R\sin\omega\right]^2\end{matrix}}$$

$$d(P_{io},P_j)=\sqrt{\begin{matrix}\left[x_{0i}+(R+r)\cos\varphi-x_{0j}-R\cos\omega\right]^2+\left[y_{0i}-y_{0j}\right]^2\\+\left[z_{0i}+(R+r)\sin\varphi-z_{0j}-R\sin\omega\right]^2\end{matrix}}$$

Applying the same method as deriving the solutions for horizontal slinky GHE, the analytical solution of the temperature response function for vertical slinky GHE is obtained as follows:

$$\begin{aligned}g_s(\tau)=&\sum_{i=1}^{N_{ring}}\sum_{j=1}^{N_{ring}}\frac{R}{4\pi N_{ring}}\int_0^{2\pi}\int_0^{2\pi}\left[\frac{erfc(d(P_{j'},P_i)/2\sqrt{at})}{d(P_{j'},P_i)}\right.\\&\left.-\frac{erfc(\sqrt{d(P_j,P_i)^2+4h^2}/2\sqrt{at})}{\sqrt{d(P_j,P_i)^2+4h^2}}\right]d\omega d\varphi\\d(P_{j'},P_i)=&\frac{d(P_{ii},P_{j'})+d(P_{io},P_{j'})}{2}\\d\left(P_{ii},P_{j'}\right)=&\sqrt{\begin{matrix}\left[x_{0i}+(R-r)\cos\varphi-x_{0j}-R\cos\omega\right]^2+\left[y_{0i}-y_{0j}\right]^2\\+\left[z_{0i}+(R-r)\sin\varphi-z_{0j}-2h-R\sin\omega\right]^2\end{matrix}}\\d\left(P_{io},P_{j'}\right)=&\sqrt{\begin{matrix}\left[x_{0i}+(R+r)\cos\varphi-x_{0j}-R\cos\omega\right]^2+\left[y_{0i}-y_{0j}\right]^2\\+\left[z_{0i}+(R+r)\sin\varphi-z_{0j}-2h-R\sin\omega\right]^2\end{matrix}}\end{aligned}\tag{2.12}$$

2.6 Numerical modelling

Numerical models can be classified as one-dimensional, two-dimensional and three-dimensional. One-dimensional model is used to derive a relation between pipes inlet and outlet temperatures [34,70]. Most of the researchers opted two-dimensional and three-dimensional models for their studies. Two-dimensional models are advanced than one-dimensional and were adopted during 90s that could calculate temperatures of ground and different depths [34,71].

Three-dimensional models are more dynamic, advanced in technology and used in recent years. Three-dimensional models allow any type of grid geometry that helps to analyze the temperature variations around the pipes and in the depth of ground [34]. Various types of commercial computational fluid dynamics (CFD) tools for numerical modelling are available. EnergyPlus and TRANSYS are used for analysis but not quickly for design [41].

CFD is a popular tool for two-dimensional and three-dimensional studies. Some

popular commercial CFD software are FLUENT, CFX, STAR, CD, FIDAP, ADINA, CFD2000, PHOENICS and others [72].

2.6.1 One-dimensional models

De Paepe and Janssens [73] used a one-dimensional analytical method to examine the influence of the design parameters of the heat exchanger on the thermo-hydraulic performance and devise an easy graphical design method which determines the characteristic dimensions of the ground-air heat exchanger in such a way that optimal thermal effectiveness is reached with acceptable pressure loss. Therefore, the choice of the characteristic dimensions is independent of the soil and climatological conditions. This allows designers to choose the ground-air heat exchanger configuration with the best performance.

Shonder and Beck [74] developed an equivalent diameter model for a single borehole with a U-tube inside. The heat capacity of the U-tube and the fluid is represented by a thin film that immediately surrounds the equivalent diameter of the U-tube. So this model assumes one-dimensional transient heat conduction through the film, the grout, and the ground surrounding the borehole. The finite difference method and the Crank-Nicolson scheme are used to solve this model. Based on this numerical calculation, a parameter estimation procedure is proposed to predict the effective thermal conductivity of different soil formations.

2.6.2 Two-dimensional models

Bojic et al. [75] developed a model in which the soil is divided into horizontal layers with uniform temperature. All the pipes are placed in one layer at the same depth and parallel to each other. The heat transported to the soil by convection from the air and the solar irradiation is calculated. Also an equation describing the heat flow between the airflow in the pipe and the neighboring soil layer is used. All equations used for the soil layers in each time step are steady-state energy equations. This model is a two-dimensional model therefore the influence that pipes have on each other may not be evaluated.

Bi et al. [76] used a two-dimensional cylindrical coordinate system to model a

vertical double spiral GHE. This GHE was designed by the authors for a GSHP system. The underground temperature distribution of the coil was solved numerically and the results were compared to measured temperature data. They concluded that the temperature distribution is important to the performance improvement of the GSHP, and especially for the GHE and that the analytical and experimental results prove that the GHE design is reasonable.

Rottmayer et al. [77] developed a thermal resistance network for borehole GHE. In order to use a two-dimensional finite difference formulation, the circular legs of the U-tube are modified into a pie sector shape with the same perimeter, but the fluid convective heat transfer coefficient is consistent with that of the circular legs. Conduction in the vertical direction is neglected, but the ground temperature in each section is coupled with the fluid temperature. The shape change may alter the short circuit between the two legs, so a geometry factor of the order of 0.3–0.5 is proposed to adjust the influence of shape change on the heat transfer rate calculation.

2.6.3 Three-dimensional models

Gauthier et al. [78] describe a fully three-dimensional model. A simple Cartesian coordinate system is used and the round pipes are replaced with square pipes of equivalent areas. The thermo-physical properties of the ground are considered constant and temperature independent, but actually the ground may not be homogenous. In this way, the influence of different layers in the ground, concrete foundations and insulation can be evaluated. The heat transfer caused by moisture gradients in the ground is assumed to be negligible with respect to that caused by temperature gradients.

Heat transfer in the pipes is dominated by convection in the axial direction but coupled with the temperature field in the ground via the boundary condition on the pipe surface. The model is thoroughly validated with experimental data taken from a GHE storage system installed in a commercial-type greenhouse. Finally, the various parameters that affect the behavior of the GHE storage system are examined.

De Paepe and Willems [79] further refined the above Gauthier et al. [78] approach and the model was used to study the performance of a ground-coupled air heat exchanger in the Belgian climate. A three-dimensional unstructured finite volume model was derived and the FLUENT solver was used to obtain the numerical solutions.

The model considers transient and fully three-dimensional conduction heat transfer in the soil and other materials. The heat transfer by moisture gradients in the soil is neglected and the heat transfer in the pipe is dominated by convection.

The governing equation for the conduction in the soil may be stated as:

$$\rho c_p \frac{\partial T}{\partial t} = k \nabla T \tag{2.13}$$

where ρ is the density, c_p the heat capacity, k the thermal conductivity, T the temperature and t the time.

The boundary conditions for the underground lateral external surfaces of the computational domain are assumed to be adiabatic, thus:

$$\frac{\partial T}{\partial n} = 0 \tag{2.14}$$

where n is the unit vector normal to the surface.

A constant and uniform temperature for the horizontal plane deep underground is imposed. At the ground surface the heat flux from the ambient air to the surface is calculated from:

$$k \frac{\partial T}{\partial n} = h_{surr}(T_{soil} - T_{surr}) \tag{2.14}$$

where T_{surr} is the temperature of the surrounding air and this can be a constant value or a time-dependent function, and h_{surr} is the convection coefficient.

The results show that the influence of the pipe on the temperature of the surrounding soil is limited to a distance of twice its diameter. To make optimal use of the thermal capacity of the soil and to eliminate the influence of the outside air, the tubes have to be buried below a depth of 2.5 m and the length of the tube can be optimized with the calculation model to obtain an efficient heat exchanger.

2.6.4 Numerical models for horizontal GHE

Piechowski [80] proposed a new approach to the simulation of a horizontal GHE is proposed resulting in a better accuracy and at the same time a reduced computational effort. These results come from the concentration of the computational effort at the locations with the largest temperature and moisture gradients, i.e. the pipe–soil interface. The model takes into account heat and moisture transfer in the soil allowing for more accurate predictions of the soil thermal response to the heat fluxes induced by the GHE

operation. This in turn allows for a more accurate prediction of the soil temperature field and the circulating fluid temperature profile.

A comparison of the results obtained by using the implicit and explicit methods of solving the set of governing equations is discussed. The implicit method requires partial linearization of the heat and mass transfer equations but results in a considerably shorter simulation time. The explicit formulation allows for the solution of the fully nonlinear set of heat and mass transfer equations at the expense of increased simulation time. The following analysis shows that the difference between the solutions obtained using these two methods is minimal, thus favoring the implicit formulation.

Wu et al. [81], on the other hand, analyzed the slinky GHE in the UK climate. Florides and Kalogirou [34] evaluated the performance characteristics of a ground coupled heat exchanger. They concluded that atmospheric conditions have a significant impact on GHE performance below and its influence should be considered while designing GSHP systems.

Considering the observations of this research, Wu et al. [81], carried out a CFD simulation to study thermal performance of straight and slinky GHE focusing the effect of coil diameter and coil central interval difference. The following transient three-dimensional sensible heat transfer model (FLUENT) was employed:

$$\frac{\partial(\rho T)}{\partial t} + \nabla \cdot \left(\rho \vec{V} T - \frac{k}{c_p} \nabla T \right) = \frac{q}{c_p} \tag{2.14}$$

where $\vec{V}$ is the fluid flow velocity.

For comparison, an experimental setup including four slinky GHE was utilized. After an observation of two months, it was found that COP reduces from 2.7 to 2.5 i.e. heat extraction of both, straight and slinky GHE decreases over time. Amongst the two, specific heat extraction of straight GHE is greater than the slinky GHE, whereas, the latter's ability of heat extraction per unit length is higher. The study concluded that specific heat extraction is independent of coil diameter and an inverse relation exists between the coil interval distance and heat extraction per unit length.

While Wu et al. [81] numerical study focuses on the short-term (140 hours) thermal performances of slinky GHE, Chong et al. [82] presented a numerical study with the consideration of the long-term operations (60 days). Similar to Wu et al. [81] work, a three-dimensional CFD model was built for the parametric analysis. The ground surface is set as a convective type boundary with a wind speed of 3 m/s and ambient air temperature at 5°C. The temperature variation at the ground surface is therefore not

considered.

In this model, only one or two loops of a slinky GHE were modeled by using FLUENT due to the computation burden. Therefore, the thermal interactions between loops are ignored or partially ignored. This CFD model was applied to simulate the slinky GHE with different parameters, namely, five different loop pitches, three different loop diameters, and three different soil thermal properties.

The comparisons show that the different loop diameters and loop pitches can result in either more excavation work or a larger amount of pipe material. Soil thermal properties are of great importance for the thermal performance of a slinky GHE. In addition, the cyclic operation of a GSHP system can largely increase the heat transfer rate when compared to the continuous operation.

Fujii et al. [83] presented another study of slinky GHE. In this study, slinky GHE were simulated by using finite-element CFD software, FEFLOW. In the numerical simulations, the slinky GHE was modeled as a thin plate. The size of the thin plate was determined by keeping the flow volume and the trench size the same as the slinky pipe values. However, in this case, the surface area of the thin plate heat exchanger is much larger than the slinky GHE surface area.

To solve this, the thermal conductivity of the tube is reduced to account for the extra surface areas. A relationship between the modified thermal conductivity and the loop pitch was derived. The numerical simulation results were validated against the recorded data of three short-term thermal response tests and a long-term air-conditioning test.

2.7 Comparisons between analytical and numerical models

Numerical methods, such as finite-difference, control-volume, and finite-element methods, are elaborate enough to describe all the underlying physical mechanisms. However, they are impractical for engineering applications for three reasons [42]:

(1) They are time consuming for year-round and/or life-cycle simulations, particularly in large applications where all the time and space scales are important and must be tackled.
(2) It is very difficult for in-house programming to develop a general grid

generation program for various configurations of ground channels; and it is thus very difficult to develop for the model for simulation of GHE

(3) In the literature, a majority of numerical models are implemented in commercial software, such as FLUENT and FEFLOW.

Although the numerical models can offer a high degree of flexibility and accuracy especially on short-term scales compared with the analytical models, most of them using polar or cylindrical grids that may be computationally inefficient due to a large number of complex grids [38]. Besides, the numerical models are inconvenient to be incorporated directly into a design and energy analysis program, unless the simulated data are pre-computed and stored in a massive database.

The analytical models are usually found based on a number of assumptions and simplifications in order to solve the complicated mathematical algorithms; therefore, the accuracy of analytical results is slightly reduced due to the assumption of the line source at the center of the borehole, which neglects the physical size of the U-tube in the borehole [84]. However, the required computation time of the analytical model is much less compared with the numerical models. Another advantage is that the straightforward algorithm deduced from the analytical models can be readily integrated into a design/simulation program.

While line source theory has been widely adopted in modelling GHE, the simplifications of the original heat and mass transfer problem result in the neglect of several important issues, such as: moisture transport in the ground, ground freezing and the ground surface effect [35]. Until very recently, most of the analytical models used for GHE thermal analysis overlook the short-term response of GHE. The solutions either completely ignored it or they used oversimplified assumptions. In reality, however, the short-term variations have significant effects on the performance of the heat pump and the overall system [40].

Short-term response of the ground is also critical during heat flux build up stages and for cases with both heating and cooling demands. Studies regarding hourly or sub-hourly thermal energy use and the electrical demands of the ground coupled heat pump system also require the short-term response of the ground to be considered. Short-term response of a GHE requires more stringent assumptions and the GHE cannot be simply modelled as a line or a cylindrical source.

The actual geometry of the GHE is therefore usually retained when determining

its short-term response. This can be achieved through CFD simulation where solutions of the GHE modelled are obtained by solving mathematical equations with the help of numerical analysis. Compared with the classical line and cylindrical source models, the numerical models usually give a better approximation of the ground heat and mass transfer process.

Numerical models are attractive when the aim is to obtain very accurate solutions or in parametric analysis. Therefore, numerical models for GHE usually contribute to a more comprehensive analysis of GSHP systems. It has been found that CFD has been conveniently employed for GHE thermal analysis in the design and optimization phase [72].

CHAPTER

3

ANALYSIS OF SHORT TIME PERIOD OF OPERATION OF HORIZONTAL GHE

3.1 Introduction

Ground source heat pump (GSHP) systems have been proven to have higher efficiency compared to conventional air source heat pump (ASHP) systems for space heating and cooling applications. This is due to the relatively stable subterranean temperature in which GSHP systems exploit to extract and reject heat, whereas ASHP systems are exposed to large fluctuation in ambient temperature and climate conditions. GSHP installations do not require large cooling towers or could be coupled with one for greater efficiency. Hence, their running costs are lower than ASHP systems. Garber et al. [85] suggest that potential savings from a GSHP system largely depend on projected HVAC system efficiencies and gas and electricity prices. The risk analysis performed shows that a full-size GSHP with auxiliary back up is potentially the most economical system configuration.

The thermal performance of GSHP depends on many parameters such as short term weather variations, seasonal variations, moisture content of soil, and thermal conductivity of soil among others that would affect the temperature of ground [86]. GSHP systems extract and reject heat by means of ground heat exchangers (GHE). GHE can be generally classified into two widely installed closed-loop types which are borehole and horizontal configurations. Borehole GHE are pipes installed typically 15–120 m deep in the ground. Meanwhile, pipes are laid and buried in trenches 1–2 m deep

in horizontal GHE installations. Borehole GHE, commonly installed where availability of land area is scarce, provides high and steady thermal performance as less temperature fluctuation occurs along with depth. Moister soil and possible underground water flow in deep region would also contribute to higher heat exchange rate.

While borehole GHE are favorable, this type of installation may hinder small and medium enterprises and homeowners due to high capital costs involved. Furthermore, only specialized contractors are well-equipped in terms of equipment and skills for borehole drilling operations. On the other hand, the installations of horizontal GHE are relatively cost-effective operation and rather straightforward which mainly involve excavation of shallow trenches. Horizontal GHE installations would be convenient where land area is abundant. The drawback of such shallow installations is that it is prone to unstable thermal performance due to temporal weathers and seasonal variations. Pulat et al. [87] performed economic analysis by comparing experimentally GSHP system using horizontal GHE to conventional heating methods and it was shown that the GSHP system is more cost effective than all other conventional heating systems. Naili et al. [88] conducted in-field analysis that showed the utilization of horizontal GHE is appropriate for cooling building in Tunisia, which is characterized by a hot climate.

Numerical modelling has been used in many studies to accurately predict the thermal performance of GHE. This is useful in achieving optimum design and economic feasibility before the commissioning of GSHP systems. Nam et al. [36] developed a numerical model that combines a heat transport model with ground water flow for borehole GHE and was validated with experimental results. The heat transfer rate for an actual office building operation in Tokyo, Japan was predicted using this model. Jalaluddin and Miyara [89,90] investigated the thermal performances of borehole GHE under different operation mode including discontinuous 2 h operation in cooling mode and alternative operation mode between cooling and heating process to provide hot water supply. Discontinuous and alternative operation modes help to alleviate the heat buildup around the borehole thus increasing the heat exchange rate.

The operation of horizontal GHE has been studied in several research papers. Flaga-Maryanczyk et al. [91] presented comparable results between experimental measurements and numerical simulation of horizontal GHE operation at a cold climate for a passive house ventilation system. CFD simulation performed by Tarnawski et al. [92] shows that straight horizontal GHE in GSHP system offers relatively low thermal

degradation of the ground environment, lower cost of heating and cooling, and higher operating efficiency than electric resistance heating or ASHP system. Energy consumptions in the GSHP system is primarily contributed by heat pump unit i.e., compressor and fan compared to the small requirement to drive the circulation pump for horizontal GHE.

Benazza et al. [93] studied horizontal GHE that were laid out concentrically for cooling purposes in continuous and cyclic operating mode by modeling the air and ground temperature using a simple harmonic function. It was reported that the cyclic operation allows a certain thermal discharge during the shut-up period providing an increase of the heat exchange rate compared to continuous operation.

Rezaei-Bazkiaei et al. [94] suggest that by backfilling horizontal GHE trenches with an intermediate layer of material having different thermal characteristics have the potential to enhance heat exchange rate. An aggregate made from recycled tire acted as insulating layer in cold climate areas thus enhancing heat extraction and a high conductive intermediate layer of saturated sand helped to dissipate heat during cooling operation. Simms et al. [95] examined the performance of horizontal GHE in soil with heterogeneous thermal conductivity. The analysis supports the assumption of homogeneity when modelling and designing horizontal GHE as the effect of heterogeneity was found to be minimal relative to uncertainty of the mean soil thermal conductivity. Soil continuum was used to examine heat transfer interference between adjacent pipes which may reduce the thermal performance of the system.

Recent studies show that spiral or slinky pipes are increasingly gaining attention compared to conventional straight polyethylene pipes as greater pipe length per trench length can be achieved thus increasing surface area for heat transfer. Li et al. [68] adapted moving ring source model to solve analytically the temperature response of a spiral heat exchanger with groundwater flow. The effect of different water velocities on the soil temperature variation during the operation of a spiral heater with different water velocities were studied experimentally. Wu et al. [81] compared the thermal performance between horizontal GHE operation in straight and slinky configurations. The specific heat extraction rate for both the straight and slinky GHE operation was comparable initially but the performance decreasing along with operating time at different rates. Although the heat extraction rate per pipe length of the straight GHE would be higher than that of the slinky GHE loops, the heat extraction per trench length of the latter was significantly higher than that of the former.

Congedo et al. [96] reported that slinky GHE loops configuration provides greater heat exchange area compared to straight pipes. This presents an opportunity in optimizing GHE design by allowing the length of pipes and trench excavation work hence the required land area to be reduced. Their analysis covered for system operation in both summer and winter. It was determined that the thermal conductivity of the ground and the velocity of working fluid inside the GHE are the key factors that affect the heat exchange rate. Fujii et al. [83] performed numerical modelling of slinky GHE loops operation by using time-varying parameter, i.e., ground heat flux as surface boundary condition to improve the analysis accuracy. In their model, the geometry of the GHE was simplified to a thin plate. The simulation results were found agreeable with the experimental thermal response tests and long-term air-conditioning tests.

Chong et al. [82] investigated the effect of loop pitch and loop diameter on the thermal performance of slinky GHE loops. A cost-benefit analysis was presented to evaluate the effect of the required amount of pipe material and excavation costs on thermal performance. The analysis indicates that a maximum increase about 16% in heat exchange rate is attainable using smaller loop pitch compared to larger loop pitch configurations, as a result of increased heat transfer area per trench length. Although the excavation work required in installing smaller loop pitch is reduced, the material cost is significantly increased close by twofold. It is also worth noting that the effect of loop diameter on thermal performance is to a lesser extent compared to the change in loop pitch.

In this work, the numerical modelling of slinky GHE loops in several operations was simulated by incorporating time- and position-varying parameters, which would provide a realistic condition. The simulation includes short time period of operation of exact shape of single and parallel GHE loops. The effect of different pipe material, parallel operation and spacing between adjacent parallel loops on heat exchange rate are also discussed.

3.2 Description of numerical model

The analysis carried out in this work was performed using a commercial CFD software FLUENT. Heat transfer can be predicted using the software by solving three conservation equations for continuity given in Eq. (3.1), momentum in Eq. (3.2) and energy in Eq. (3.3) [97].

$$\frac{\partial \rho}{\partial t} + \nabla \cdot (\rho \vec{v}) = 0 \tag{3.1}$$

where ρ is the density of fluid and $\vec{v}$ the local velocity. The operator ∇ referred to as grad, nabla, or del represents the partial derivative of a quantity with respect to all directions in the chosen coordinate system. In Cartesian coordinates, ∇ is defined to be $\frac{\partial}{\partial x}\vec{\imath} + \frac{\partial}{\partial y}\vec{\jmath} + \frac{\partial}{\partial z}\vec{k}$.

$$\begin{gathered}\frac{\partial}{\partial t}(\rho \vec{v}) + \nabla \cdot (\rho \vec{v}\, \vec{v}) = -\nabla p + \nabla \cdot (\bar{\bar{\tau}}) + \rho \vec{g} + \vec{F} \\ \bar{\bar{\tau}} = \mu \left[(\nabla \vec{v} + \nabla \vec{v}^T) - \frac{2}{3} \nabla \cdot \vec{v} I \right]\end{gathered} \tag{3.2}$$

where p is the static pressure, $\bar{\bar{\tau}}$ is the stress tensor, and $\rho \vec{g}$ and $\vec{F}$ are the gravitational body force and external body forces, respectively. μ is the molecular viscosity, I is the unit tensor, and the second term on the right hand side of stress tensor is the effect of volume dilation.

$$\frac{\partial}{\partial t}(\rho h) = \nabla \cdot (k \nabla T) \tag{3.3}$$

where h is sensible enthalpy $\int_{T_{ref}}^{T} c_p dT$, k is thermal conductivity, and T is temperature. For convective transport, additional terms on the right hand side due to convection and viscous dissipation are included in Eq. (3.3) to indicate presence of flow.

The time step used in the transient analysis was in minute basis. However, based on the initial run, the heat exchange rate was found to peak within the first 5 minutes of each flow cycle hence the time step was reduced to every second during this period. By using smaller time step size during the start and the end of the each flow cycle, the analysis accuracy could be further improved. The time frame of the simulation includes 24 h for short time period of operation and 7 days for discontinuous 9 h and 12 h operation a day.

3.2.1 Simulation model

The analysis domain consists of 3D meshing with the dimension of 20 m x 1.1 m x 20 m as given in Fig. 3.1. A slice of the ground profile cross-section containing only a single unit of horizontal GHE loop was modelled to reduce the computational processing for the numerical modelling. Detailed meshing of the GHE including configurations in parallel loops operation can be referred in Fig. 3.2.

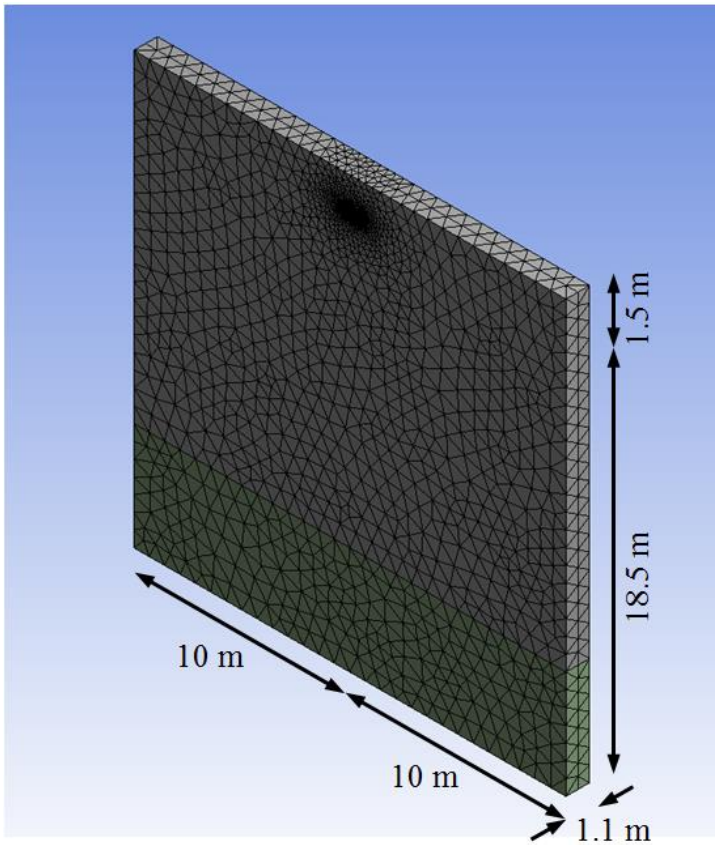

Fig. 3.1. Simulation model.

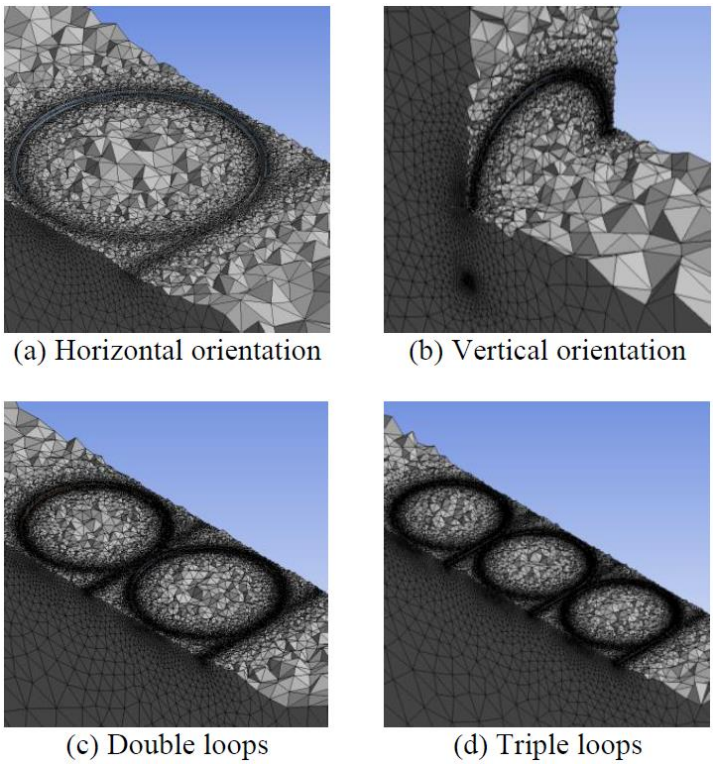

Fig. 3.2. Section view of detailed meshing of GHE at 1.5 m depth. The center of loop in vertical orientation as shown in (b) is at 1.5 m depth.

The GHE loop with 1 m loop diameter was positioned horizontally at 1.5 m below the ground surface with inlet at one side of the vertical wall and outlet at the opposite. By setting loop diameter and loop pitch to be equal, a reasonable compromise between thermal performance and installation costs was assumed [82]. The GHE was of 39 mm inner diameter and 43 mm outer diameter size high density polyethylene pipe (HDPE), typically used in GHE installations, with density of 955 kg/m^3, specific heat of 2300 J/kg.K and thermal conductivity of 0.461 W/m.K. Another pipe material, copper with density of 8978 kg/m^3, specific heat of 381 J/kg.K and thermal conductivity of 387.6 W/m.K was also tested while maintaining the loop dimension.

The ground was composed of clay to the depth of 15 m and sandy-clay below 15 m. The ground properties according to the type of soils are presented in Table 3.1. The 10 m distance from the horizontal boundaries to the center of the GHE and 20 m domain deep were considered adequate to eliminate the heat flow influence from outer ground. The ground was assumed to have no underground water flow and compressed sufficiently that rain infiltration can be neglected.

3.2.2 Initial and boundary conditions

Climatic factors dictate the energy transfer at the ground surface and affect the subsurface heat flow. Heat balance approach can be used to determine the relationship of all heat fluxes at the ground surface [98]. The net heat into/out of the soil or ground heat flux, q_5 can be written as a mathematical expression given in Eq. (3.4).

$$q_5 = aq_1 - q_2 - q_3 - q_4 \tag{3.4}$$

where aq_1 is net short-wave radiation received, q_2 is net long-wave radiation from

Table 3.1. The properties of ground [99].

Parameters	Value
Clay (temperature: 293 K; water content: 27.7%)	
Density, ρ_{clay}	1700 kg/m^3
Specific heat, $C_{p,clay}$	1800 J/kg·K
Thermal conductivity, k_{clay}	1.2 W/m·K
Sandy-clay (temperature: 293 K; water content: 21.6%)	
Density, $\rho_{sandy\text{-}lay}$	1960 kg/m^3
Specific heat, $C_{p,sandy\text{-}clay}$	1200 J/kg·K
Thermal conductivity, $k_{sandy\text{-}clay}$	2.1 W/m·K

surface under condition of cloud, q_3 is convective heat flow to the air and q_4 is heat flux due to evaporation with positive sign in case of condensation.

Hence ground heat flux can be defined as the process where heat is transported between the Earth's surface and subsurface through conduction. The heat conduction in the ground would in turn govern the subsurface temperature profile. Due to GHE shallow position, ground heat flux has strong influence on the heat transport at the ground surface. Time- and position-varying parameters were applied as initial and boundary conditions to mimic heat transfer phenomena in the ground.

The simulation for 24 h of operations was performed based on the conditions on 1 August 2013 and extended to 7 August 2013 for discontinuous 9 and 12 h a day operation. A 3-hourly ground heat flux data obtained from Global Land Data Assimilation System (GLDAS) available at Goddard Earth Sciences (GES) Data and Information Services Center (DISC) at the same site shown in Fig. 3.3 was used to define the ground surface boundary condition.

The subsurface temperature profile from recorded experimental data at a site in Saga University, Japan as shown in Fig. 3.4 was fitted into Eq. (3.5) and defined as the analysis domain initial condition.

$$T_y = 27.7 + 7.7y + 2y^2 + 0.25y^3 + 0.02y^4 + 6 \times 10^{-4}y^5 + 8 \times 10^{-6}y^5 \quad (3.5)$$

where T_y is ground temperature at the vertical distance of y.

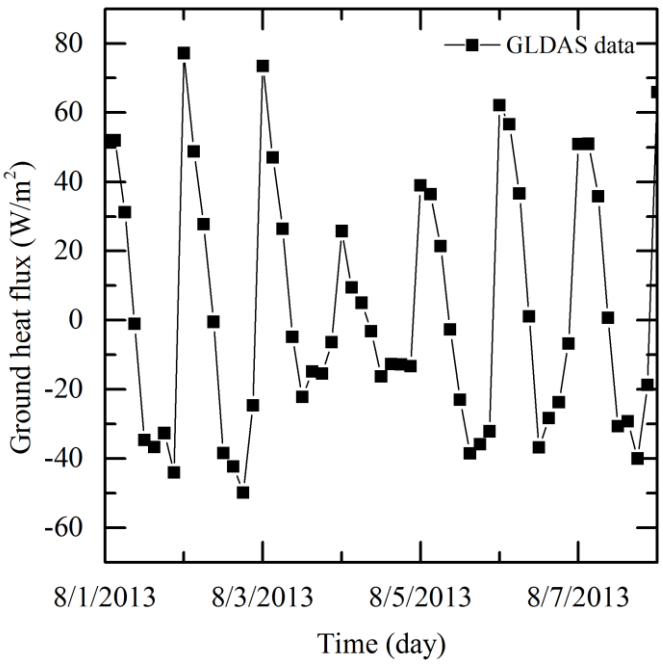

Fig. 3.3. Ground surface heat flux boundary.

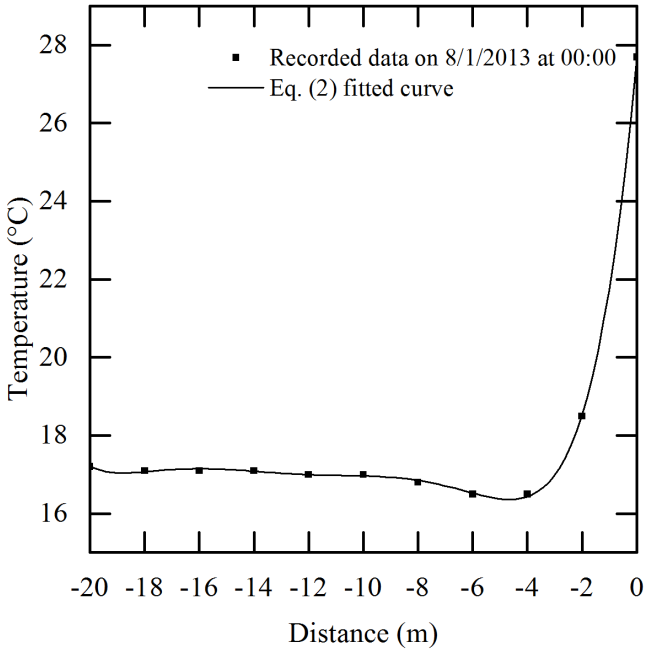

Fig. 3.4. Depth-varying temperature for initial condition of analysis domain.

All vertical walls and bottom were considered to have no influence on the analysis domain thus treated as adiabatic boundaries. Water was used as working fluid inside the GHE. A linear increase/decrease of inlet flow rate was applied during ramp time of 10 s during flow start-up/shut-off. The inlet flow rate was fixed at 4 LPM while in operation and classified as transition flow with Reynolds number of 3300. This is the equivalent to the total flow rate in parallel loops operation. The inlet temperature was fixed at 35 °C for operation in cooling mode and 20 °C for operation in heating mode.

3.2.3 Method similarities with previous validated models

Jalaluddin and Miyara [90] performed numerical modelling for several types of vertical GHE with different operation mode. The output results of the CFD code were validated against experimental data [89] with good agreement between the two analysis. The present work adopted a similar approach in carrying out the modelling of horizontal GHE. The similarities between the present work and previously validated models are: (1) the numerical modelling were performed using the same CFD platform, FLUENT; (2) three-dimensional hybrid mesh generation method was applied in the GHE models; (3) the CFD code utilized similar setup for the main parameters; and (4) the properties and measured data used were taken from the pertaining experimental site.

3.3 Results and discussion

The thermal performance of horizontal GHE was assessed by the heat exchange rate at the interface between the pipe surface and surrounding ground. The total surface heat flux along the pipe or simply, heat exchange rate, *HER*, was obtained from CFD solution. The heat exchange rate expressed in per unit pipe length, HER_{LP} is calculated using Eq. (3.6) for single loop and $HER_{LP,total}$ using Eq. (3.7) for parallel loops.

$$HER_{LP} = HER \times A/L_P \tag{3.6}$$

$$HER_{LP,total} = \sum HER_{LP,i} \tag{3.7}$$

where $HER_{LP,i}$ is the total surface heat flux along pipe i, A is the surface area along the pipe which equals 0.63 m^2 and L_P is the pipe length which equals 4.24 m.

3.3.1 Continuous 24 h operation

In this work, continuous cooling operation was investigated similar to the method in conducting thermal response test for borehole with the exception the inlet temperature was set constant. Table 3.2 summarizes the mean heat exchange rate for continuous 24 h operations. The results for parallel loops operation is discussed in Section 3.4.

Fig. 3.5 shows comparisons between the orientations of GHE on heat exchange rate during 24 h operation period. The heat exchange rate in horizontal and vertical orientations was comparable with the latter slightly higher than the former. Generally, the heat exchange rate peaks within the first 5 min of operation before having a steep decrease until 4 h of operation as the ground warms up. Subsequently the heat exchange rate continues to decrease in a lesser degree until the operation ends as energy is dissipated throughout the ground. The mean heat exchange rate for vertical orientation is only 0.8% higher compared to that in horizontal orientation. Correspondingly at the end of the 24 h operation, the heat exchange rate for vertical orientation is slightly 0.7% higher compared to that in horizontal orientation.

The effect of GHE orientation on thermal performance is insignificant although the trench depth increases by one third. Burying the GHE in vertical orientation means extra trenching work is required and this adds to the installation cost. On the other hand, GHE in horizontal orientation are easier to install. Vertical orientation is suggested in

Table 3.2. Summary of mean heat exchange rate in continuous 24 h operation in cooling mode.

Operation	Material	Orientation	Spacing between adjacent loops (m)	Heat exchange rate at 24 h (W/m)	Mean heat exchange rate (W/m)
Single loop	HDPE	Horizontal	–	29.6	38.8
	HDPE	Vertical	–	29.8	39.1
	Copper	Horizontal	–	33.5	57.5
Double loops	HDPE	Horizontal	0 m	54.2	71.8
	HDPE	Horizontal	0.5 m	58.8	82.1
	HDPE	Horizontal	1.0 m	59.8	82.5
	HDPE	Horizontal	2.0 m	58.9	82.1
	HDPE	Horizontal	4.0 m	58.9	82.1
Triple loops	HDPE	Horizontal	0 m	77.5	101.7
	HDPE	Horizontal	0.5 m	86.5	114.1
	HDPE	Horizontal	1.0 m	86.6	114.2
	HDPE	Horizontal	2.0 m	88.5	115.4
	HDPE	Horizontal	4.0 m	86.8	114.5

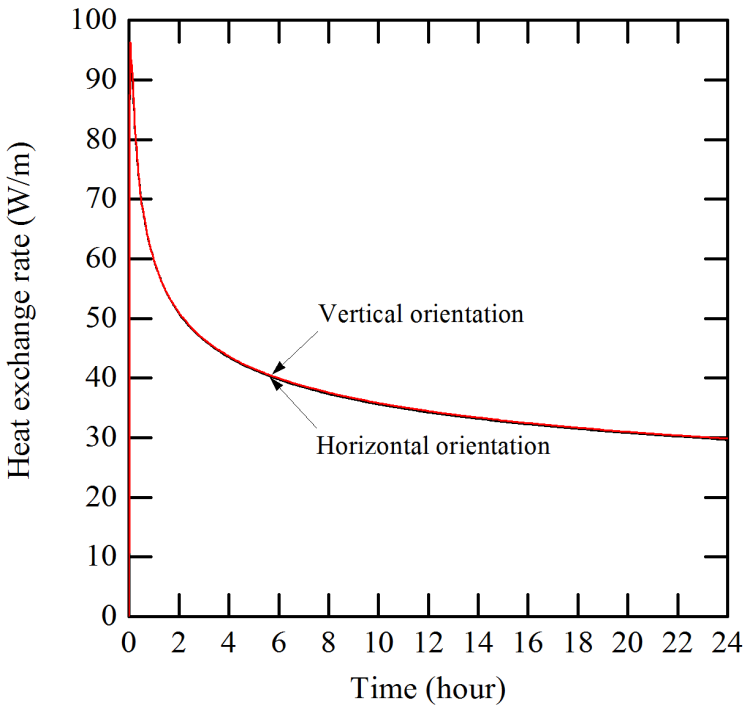

Fig. 3.5. The effect of different orientations on heat exchange rate.

installation where land area is limited. Further analysis of GHE operation beyond this point was investigated in horizontal orientation.

The effect of different pipe material on heat exchange rate was investigated and compared as shown in Fig. 3.6. It can be observed that for copper loop, the heat exchange rate peaks to over 150 W/m compared to that in HDPE loop at 95 W/m during the early operation period. Soon afterward, the heat exchange rate decreases in a much rapid manner. This might be because low temperature gradient presence in copper loop wall as opposed to high temperature gradient in HDPE loop wall. After 1 h of operation, the heat exchange rate begins to gradually decrease as the effect of heat buildup in the ground prevalent. The mean heat exchange rate for copper loop is 48% higher compared to that in HDPE loop. At the end of the 24 h operation, the heat exchange rate for copper loop is 13% higher compared to that in horizontal orientation.

The prospect of using higher thermal conductivity materials such as copper as GHE loop becomes viable as coating could be applied on the outer surface of the pipe as a protection from the elements. The analysis is in agreement that pipe material with higher thermal conductivity suggests higher heat exchange rate. Although the thermal conductivity of copper is over 800 times higher than that of HDPE, the common claim that heat exchange rate is predominantly limited by the thermal conductivity of the ground is observed.

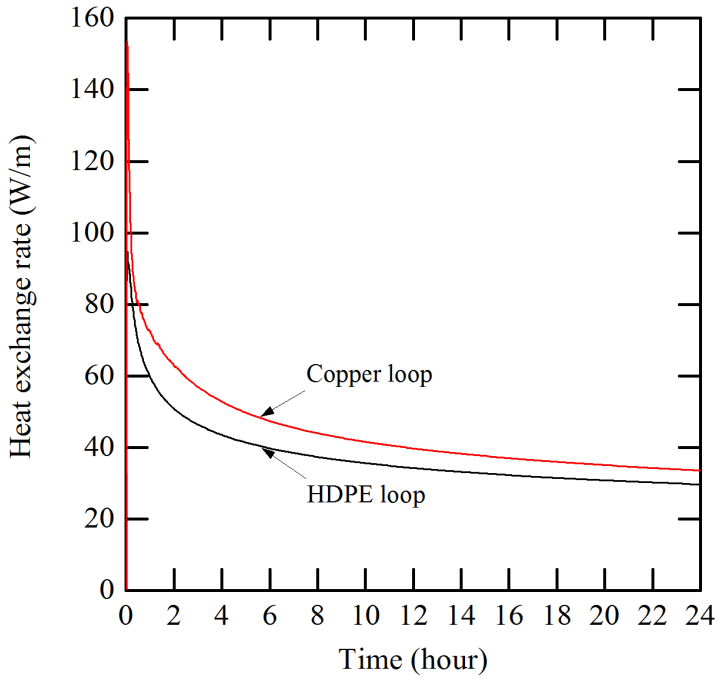

Fig. 3.6. The effect of different pipe material on heat exchange rate.

3.3.2 Discontinuous and alternate 2 h operation

In discontinuous 2 h operation, the GHE was simulated in cooling mode for 2 h and followed by 2 h of no operation or off period in which water flow rate was shut-off completely. Meanwhile, in alternate 2 h operation, the GHE was simulated in cooling mode for 2 h and the subsequent 2 h in heating mode. Heat exchange rate for both operations was compared against that in continuous cooling operation as shown in Fig. 3.7. As discussed earlier, the heat exchange rate was high at beginning of operation and gradually declined due to the effect of heat buildup in the ground along with operating time.

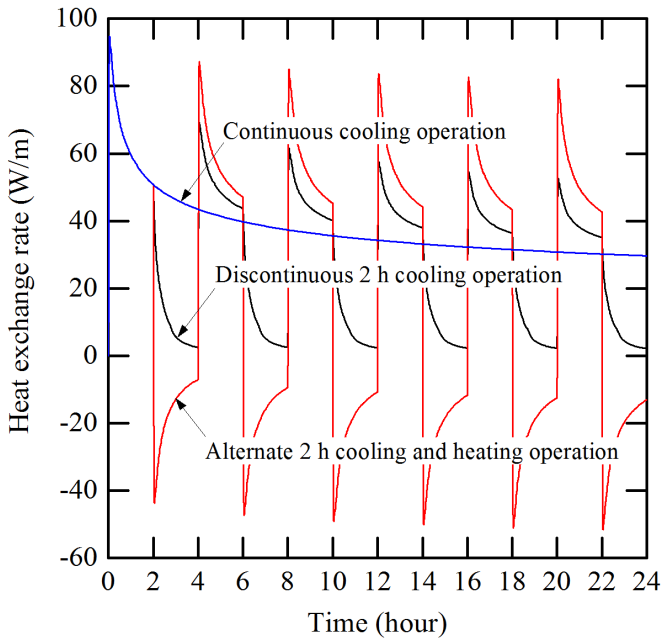

Fig. 3.7. Heat exchange rate in discontinuous 2 h operation in cooling mode and alternate 2 h operation between cooling and heating mode.

Table 3.3 summarizes heat exchange rate for the short time period of operations at the end of cooling cycle. At the end of 22 h operation time, the heat exchange rate in discontinuous 2 h and alternate 2 h operations shows 16% and 42% increase respectively compared to that in continuous operation. At the same time, alternate 2 h operation performed 22% higher than discontinuous 2 h operation. The off period lessen the effect of heat buildup by dissipating the energy thus improving the heat exchange rate in the next flow cycle. Thus the ground is allowed to recuperate its thermal

Table 3.3. Summary of heat exchange rate in discontinuous 2 h operation in cooling mode and alternate 2 h operation between cooling and heating mode.

	Heat exchange rate (W/m)					
Operation time (hour)	**2**	**6**	**10**	**14**	**18**	**22**
Continuous	50.9	39.8	35.6	33.1	31.5	30.2
Discontinuous 2 h	50.9	43.6	40.2	39.0	36.4	35.1
Alternate 2 h	50.9	47.1	45.3	44.2	43.4	42.8

condition during this period while water inside the GHE is still rejecting heat at a much lesser extent. Alternating cooling and heating modes further increases the alleviation of heat buildup. The cooler water flow helps to extract heat thus reducing the thermal saturation in the ground.

3.3.3 Discontinuous 9 h and 12 h operation a day

In this section, an office building operating in cooling operation was analyzed. Two operation hours were applied from 09:00 to 18:00 for 9 h operation and from 09:00 to 21:00 for 12 h operation a day during a seven days period. As described previously, the same flow conditions was applied with flow rate set at 4 LPM during operation and 0 LPM during off period. The inlet temperature was fixed at 35 °C. Table 3.4 summarizes the heat exchange rate in discontinuous 9 and 12 h operations in cooling mode.

Table 3.4. Summary of heat exchange rate in discontinuous 9 and 12 h operation in cooling mode at the end of each cycle.

	Heat exchange rate (W/m)						
Operation time (day)	**0.75**	**1.75**	**2.75**	**3.75**	**4.75**	**5.75**	**6.75**
Continuous	36.4	27.6	24.4	22.5	21.1	20.0	19.1
Discontinuous 9 h	36.4	32.1	30.0	28.3	27.1	26.1	25.3
Operation time (day)	**0.875**	**1.875**	**2.875**	**3.875**	**4.875**	**5.875**	**6.875**
Continuous	34.2	27.1	24.1	22.3	20.9	19.6	19.0
Discontinuous 12 h	34.2	29.8	27.5	25.9	24.7	23.7	22.9

The heat exchange rate was compared against that in continuous operation as given in Fig. 3.8. Near the end of day 7, the minimum heat exchange rate in 9 h operation increases by 33% and in 12 h operation, 21% compared to continuous operation. As can be observed, the extended period of off period increases the heat exchange rate in the next flow cycle.

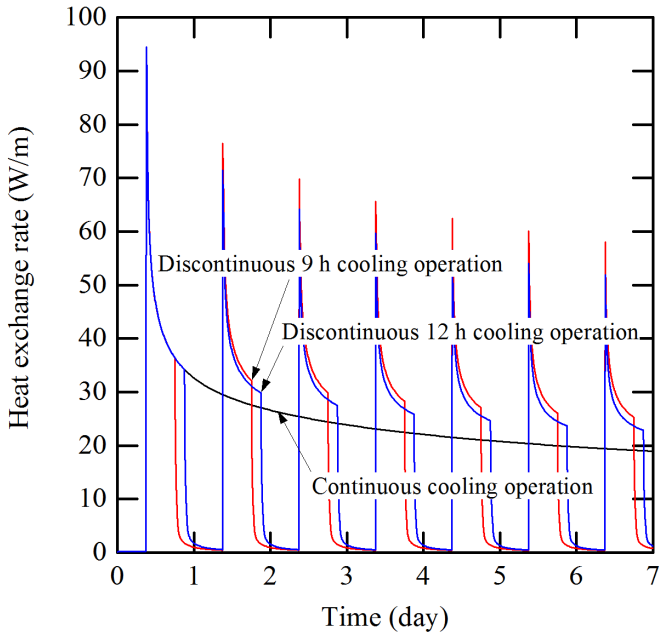

Fig. 3.8. Heat exchange rates in discontinuous 9 h and 12 h operations in a day.

3.3.4 Parallel loops operation

In the interest of predicting thermal performance of parallel loops, double and triple loops operation were simulated in cooling mode. Initially, each identical loop was positioned close to one another in which edge-to-edge loops spacing between them equal 0 m. Each configuration was in continuous 24 h operation with the total flow rate set at 4 LPM, equals the pumping work for single loop operation. Heat exchange rate in parallel loops operation was compared against that in single loop operation as presented in Fig. 3.9. The results summarized in Table 3.2 are recalled. Compared to single loop operation, the mean heat exchange rate for double loops operation improved by 83% meanwhile for triple loops operations, 162%.

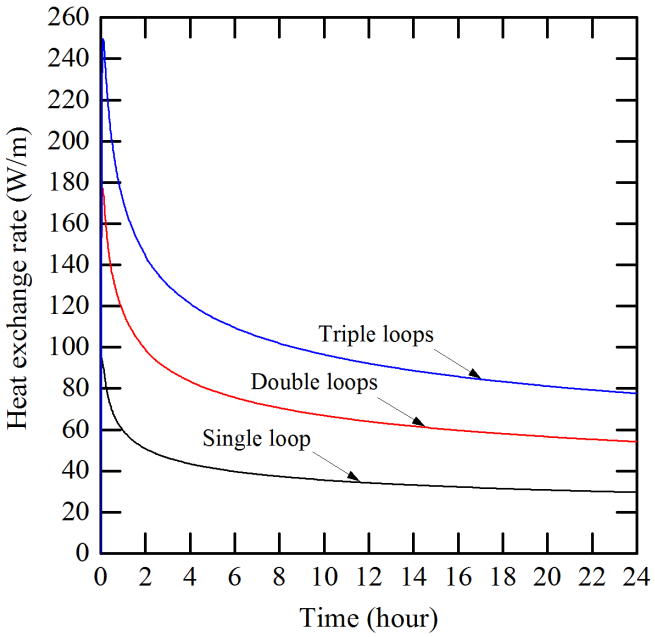

Fig. 3.9. Heat exchange rate in parallel loops operation with no spacing compared to single loop operation.

With the same circulation pump work, parallel loops operation promotes higher efficiency compared to single loops operation as heat transfer area is multiplied in this configuration. Hence it is more sensible to install and operate GHE in parallel consisting of short series rather than one long series of loops. Parallel loops operation also benefits GSHP systems whereby less amount of pressure is required to overcome friction losses through each individual series thus minimizing pressure drop. However, it is worth noting that the turbulence inside the loops is reduced in distributed flow. Installations with parallel loops GHE requires additional initial costs concerning amount of pipe material and excavation works. Surplus land area is also required for such installations. However, in a long run, these extra investments would pay off due to higher thermal performance that is attainable.

It is reckoned that heat transfer from adjacent parallel loops interfere with each other causing a decrease in overall thermal performance. Further investigations were carried out to determine the effect of spacing between adjacent loops on heat exchange rate. Spacing of 0.5 m, 1.0 m, 2.0 m and 4.0 m were imposed between the nearest adjacent loop walls as shown in Fig. 3.10. Fig. 3.11 and Fig. 3.12 show the effect of spacing on heat exchange rate for double and triple loops operation respectively.

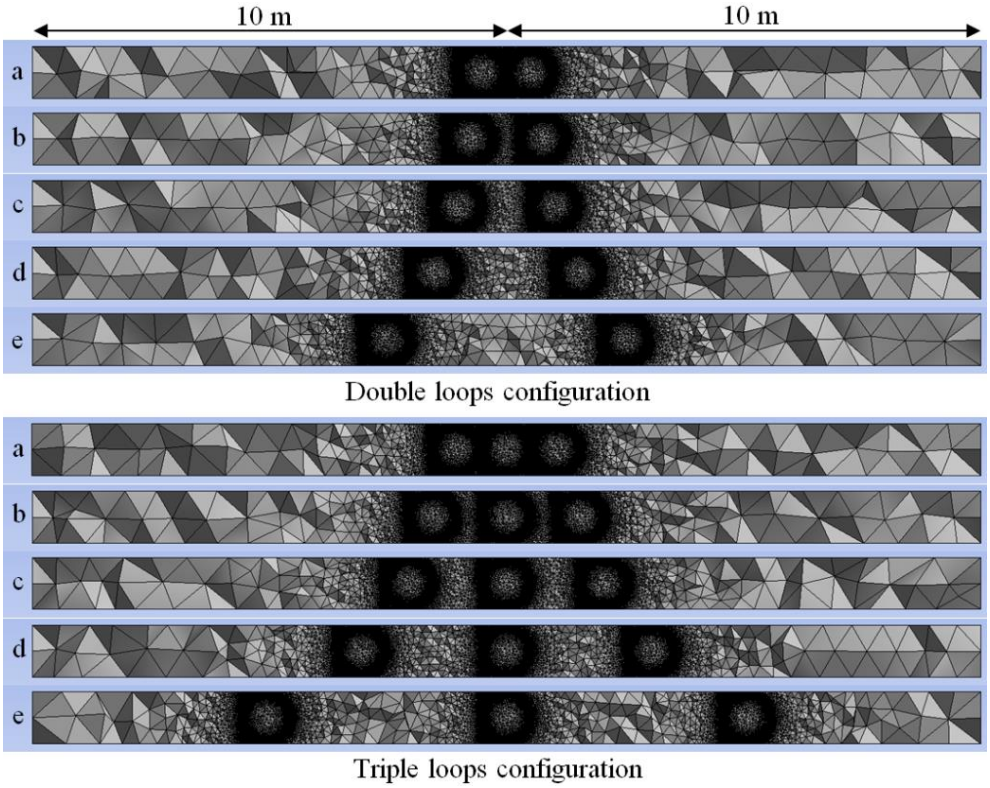

Fig. 3.10. Top section view at 1.5 m deep of spacing in parallel loops operation. (a) 0 m (b) 0.5 m (c) 1.0 m (d) 2.0 m (e) 4.0 m.

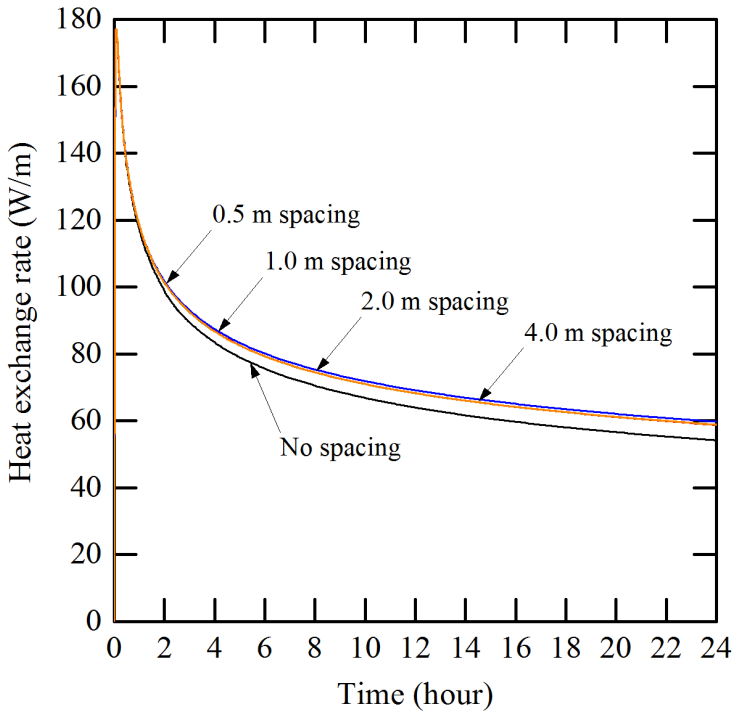

Fig. 3.11. The effect of spacing on heat exchange rate in parallel double loops operation.

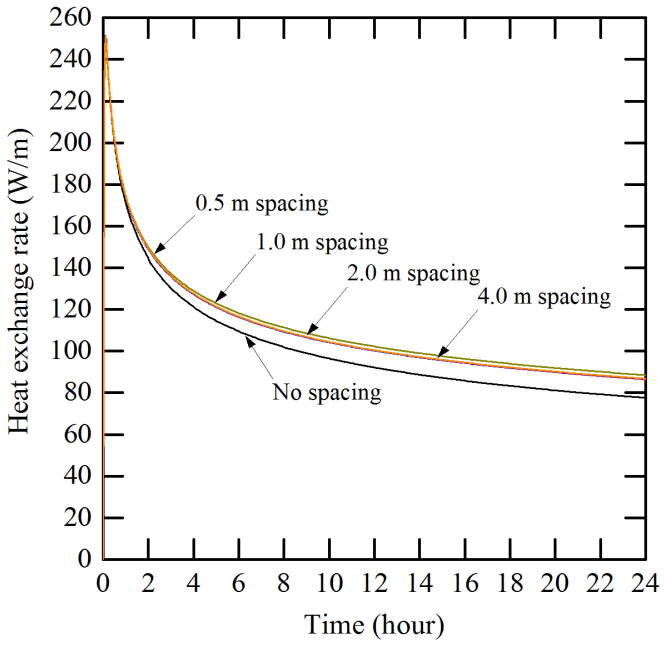

Fig. 3.12. The effect of spacing on heat exchange rate in parallel triple loops operation.

With a minimum spacing of 0.5 m provided, the increase of heat exchange rate becomes noticeable. For double loops operation, the optimum separating distance between adjacent loops is 1.0 m where the mean heat exchange rate increases by 10% compared to that in no spacing. For triple loops operation, the optimum spacing is at 2.0 m with the mean heat exchange rate increase of 14%. Although the differences are negligible, heat transfer should increase with greater loops spacing as less thermal interference between loops. The minor discrepancy in this analysis is thought to be caused by varying cell size in the modelling, particularly between the loops, in order to optimize the mesh size.

3.4 Conclusions

In this research, numerical simulation of horizontal GHE was performed for short time period of operation in discontinuous, alternate and parallel loops and the results were compared against to that in continuous operation. Time- and position-varying parameters were used in the analysis to predict realistically the thermal performance of each operation. The prediction of thermal performance prior to the introduction of a GSHP system is important to determine the economic feasibility of a system design.

The orientation of GHE installation is not as important as it has minor effect on

thermal performance. The thermal performance for vertical orientation provides a slight improvement of 0.8% in mean heat exchange rate compared to horizontal orientation. The analysis shows that although the trench depth increased by one third in vertical orientation, the heat exchange rate only improved marginally compared to that in horizontal orientation. As a matter of fact, installation of GHE in vertical orientation requires extra trenching work and it increases the initial cost. However, vertical orientation would be a practical solution in a proposed installation where land area is limited.

The analysis suggests that the higher thermal conductivity material used as GHE loop, the higher the heat exchange rate. This can be observed in the increase of mean heat exchange rate for copper loop by 48% compared to HDPE loop. As the pipe material was substituted with one having over 800 times higher thermal conductivity, the increase of thermal performance was disproportionate to the increase of thermal conductivity of the tested materials. In spite of higher heat exchange rate is achievable using more conductive pipe material, the analysis supports the common claim that the heat exchange rate is predominantly limited by the thermal conductivity of the ground.

In discontinuous operation, heat is still being rejected by the water inside the loop at a lesser rate while the ground is allowed to restore its thermal balance before the next cycle starts. In discontinuous 2 h operation, the heat exchange rate was 16% higher when the last cycle stops at 22 h operation time compared to in continuous operation. In a more practical comparison for a typical office building discontinuous cooling operation, the heat exchange rate increases by 33% in 9 h a day operation and 21% in 12 h a day operation compared to continuous operation near the end of day 7. The effect of heat buildup in the ground is further lessen by operating the loop in alternate cooling and heating modes. The cooler water flow during heating mode reduces thermal saturation in the ground thus further improves heat exchange rate.

The thermal performance of double and triple loops operation was 83% and 162% respectively higher compared to that in single loop operation with the same amount of pumping work supplied. While greater heat contact area is provided in parallel loops configuration, the pipe material cost increases in tandem and consequently requires more land area for such installation. The thermal performance in parallel operations can be further optimized to 10–14% increase when spacing between adjacent loops was provided. It is reckoned that spacing between adjacent parallel loops is provided to minimize the interference of heat flow that would penalize the overall thermal

performance.

Numerical simulation of GHE involving discontinuous operation should address the thermal behavior at the boundary conditions particularly during off period. In order to further improve the analysis, a dynamic approach is suggested to be imposed on the temperature inlet during this period to reflect a more accurate condition. It is also suggested to extend the operation period in the analysis to reach better understanding of the overall thermal performance.

CHAPTER

4

CONSIDERATIONS FOR HORIZONTAL GHE DESIGNS AND OPERATION

4.1 Introduction

Despite the growing number of ground source heat pump (GSHP) systems worldwide [100–103], efforts in enhancing such system in order to promote its usage especially in developing countries is essential. Cost-effective as well as efficient horizontal slinky ground heat exchanger (GHE) loops may also appeal small businesses and homeowners to opt for GSHP systems. Design and operating strategies to boost GHE loops efficiency is valuable to accomplish this cause. Enhanced-surface pipe shows higher heat transfer not only by increasing surface area but inducing turbulence compared to smooth pipe in heat exchangers [32,72,104,105].

GHE constructed from superior thermal conductors such as copper [106,107] is expected to exhibit high thermal performance. The longevity of this material can be significantly extended as it is commercially available in protective coating as in composite pipe that able to withstand robust environment. Parallel loops operation has the potential to provide high efficiency system. Mihalakakou et al. [108] reported that multiple earth-to-air heat exchangers can provide an effective system used for heating. A reasonable compromise between thermal performance and installation costs was assumed by setting loop diameter and loop pitch to be equal in slinky configuration [82].

In this work, comparisons between thermal performance of GHE loops modelled

in different orientations and using pipe materials of different thermal properties was investigated. The effect of distributing the flow into a group of loops in parallel and heat interference from adjacent loops are also discussed.

4.2 Methodology of numerical modelling

4.2.1 Simulation model

The analysis domain consists of 3D meshing with the dimension of 20 m x 1.1 m x 20 m as shown previously in Fig. 3.1. A slice of the ground profile cross-section containing only a single unit or a group in parallel of the slinky-loops was modelled. Four main geometries and its detailed meshing as shown in Fig. 4.1 are horizontal orientation referred as Case 1 and Case 3, vertical orientation (Case 2), double parallel (Case 4) and triple parallel (Case 5).

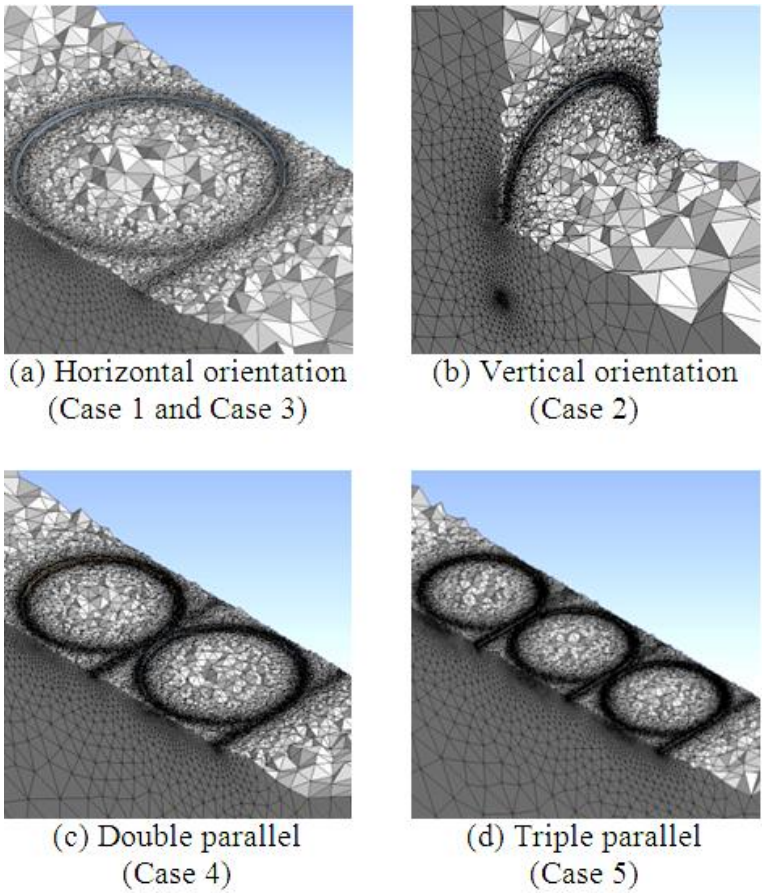

Fig. 4.1. Section view of detailed meshing of GHE at 1.5 m deep.

The loops with 1 m loop diameter were positioned horizontally at 1.5 m below the ground surface. In Case 2, the center of the loop was positioned at 1.5 m depth. Water as working fluid flows from one side of the lateral wall and exits through the other. The 10 m distance from the horizontal boundaries to the center of the loops and 20 m domain deep were considered adequate to eliminate the influence from ground.

The pipe was of 20 mm inner diameter and 23 mm outer diameter size. The geometry used in Fig. 4.1a is for comparison of pipe materials with different thermal properties in single loop operation. In all cases except Case 3, HDPE pipe with density of 955 kg/m^3, specific heat of 2300, J/kg·K and thermal conductivity of 0.461 W/m·K was used. In Case 3, copper pipe with density of 8978 kg/m^3, specific heat of 381 J/kg·K and thermal conductivity of 387.6 W/m·K was also tested. The numerical simulation carried out in this research was performed using a commercial computational fluid dynamics software Fluent.

4.2.2 Meteorological and geological factors

Ground heat flux is the process responsible of transporting heat between the Earth's surface and ground through conduction. The heat conduction in the ground governs the subsurface temperature profile. Due to the loops shallow position at 1.5 m below the surface, ground heat flux has strong influence on the thermal performance of GHE. In order to achieve a realistic and reliable analysis, time- and position-varying parameters were applied as initial and boundary conditions to mimic the heat transfer phenomena in the ground.

The analysis was performed based on the conditions on 1 January 2013 for heating mode and 1 June 2013 for cooling mode. The simulation was initialized using ground temperature profile using data recorded at a site in Saga University, Japan. 3-hourly ground heat flux data at the same site was applied on the ground surface. The data used as initial and boundary conditions are shown in Fig. 4.2. The ground was composed of clay to the depth of 15 m and sandy-clay below 15 m. The properties of ground were presented previously in Table 3.1. All lateral walls and bottom were considered to have no influence on the analysis domain thus treated as adiabatic boundaries.

Based on simulation results, the ground isotherm shows that a relatively smaller

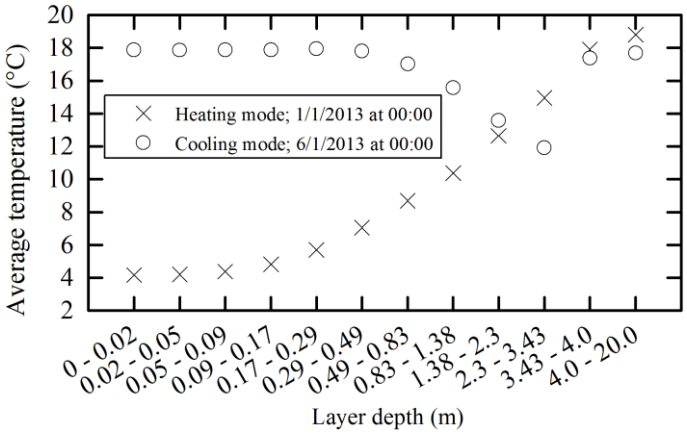

(a) Initial ground temperature profile

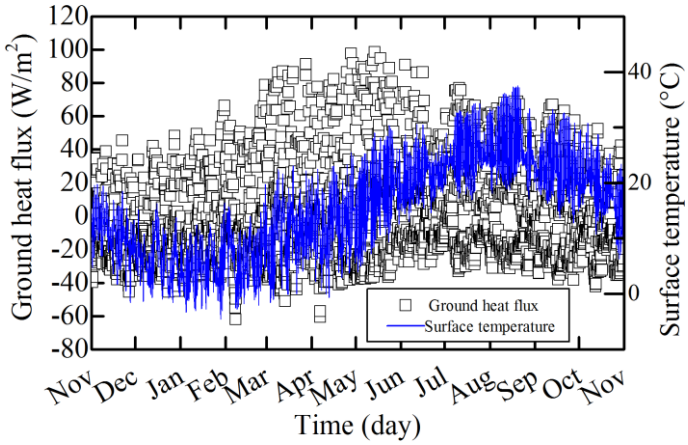

(b) Annual ground heat flux and surface temperature

Fig. 4.2. Data used as initial and boundary conditions (Source: GES DISC).

region of the ground was affected by the loop, about 1 m from the pipe center, compared to ample dimension provided for the simulation domain. The 10 m far-field distance from the center of the loop, or at least 5 m from the outer loops as in triple parallel loops, and 20 m deep simulation domain were considered sufficient to minimize the effect of boundary temperature when all side and bottom walls were considered adiabatic.

4.2.3 Loops operating conditions

The inlet flow rate was set at 4 LPM during single loops operation. The same flow rate was equally distributed in parallel loops operation. A linear increase of flow rate was applied during ramp time of 10 seconds during flow startup. The flow inside the

pipe can be regarded as transition flow with Reynolds number of 3300 in single loop configuration. The flow in parallel configurations was laminar since the same flow rate was equally distributed in each pipe. In all cases, the simulation was performed using laminar model with second order discretization scheme.

The inlet temperature was fixed at 7 °C for operation in heating mode and 27 °C for operation in cooling mode. The simulation applied the initial conditions at 00:00 of day 1 and the results are presented as the operation began on 09:00 the same day. The GHE loops were operated in continuous operation for 5-day in heating mode during winter and cooling mode during summer. For parallel loops operation, the analysis was carried out only in cooling mode. The simulation was performed in time step size of 1 second during the first 5 minutes after the flow begins. Subsequently, the simulation was per minute basis until the operation ended.

4.3 Results and discussion

The thermal performance of GHE loops was assessed by the heat exchange rate along the pipe. The mean surface heat fluxes at the interface between the pipe surface and surrounding soil were calculated during the simulation. The heat exchange rate expressed in per unit pipe length HER_{LP} is calculated using Eq. (3.6) for individual loop. The total heat exchange rate in parallel loops operation $HER_{LP,total}$ is calculated using Eq. (3.7). The surface area along the pipe, A equals 0.63 m^2 and L is the pipe length which equals 4.24 m.

4.3.1 Single loops operation

Fig. 4.3 shows the comparison of heat exchange rates during 5-day continuous operation in Case 1, Case 2 and Case 3. Generally, the heat exchange rate in all cases peaks early at the beginning of operation. Then, the operation experiences a rapid drop in thermal performance before it begins to decrease gradually until the operation ends. The loops reject heat to or extract heat from the ground causing a temperature change in the surrounding soil during the operation.

The temperature difference between surrounding soil and loops decreases causing the amount of heat transfer becoming less as the ground warms up. This results heat

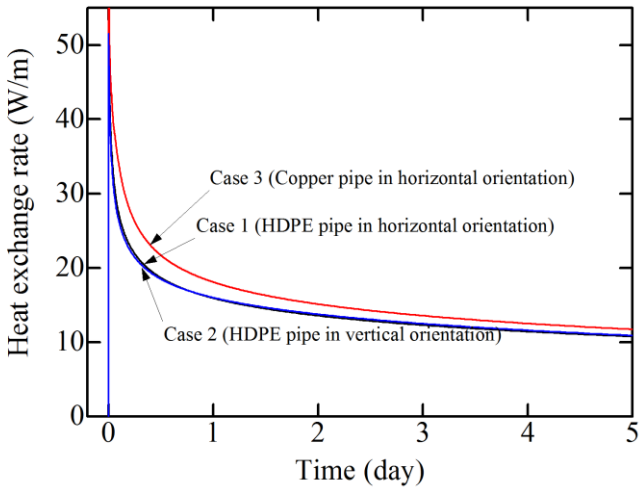

(a) Cooling mode

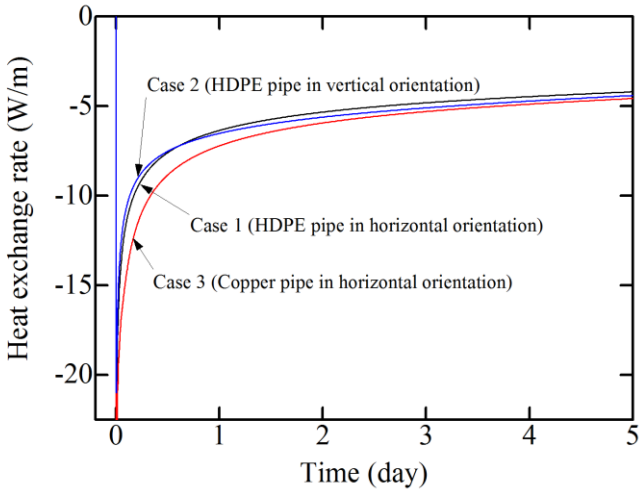

(b) Heating mode

Fig. 4.3. Comparison of different orientations and materials.

exchange rate to decline in a steep manner due to the effect of heat buildup becomes dominant. Subsequently as energy is dissipated throughout the ground, heat exchange rate continues to decrease at a much lesser degree.

The effect of different orientations on heat exchange rate can be analyzed by comparing the results of Case 1 in horizontal orientation and Case 2 in vertical orientation. Based on the analysis, Case 2 performs slightly higher than in Case 1 in both heating and cooling mode although the difference is insignificant. Within the first 5 minutes of operation, the heat exchange rate in Case 1 peaks at 54 W/m while in Case 2 at 52 W/m in cooling mode. The heat exchange rate in Case 1 peaks at 23 W/m while in Case 2 at 21 W/m respectively in heating mode.

As the operation continues, the heat exchange rate for Case 2 has a slightly

steeper drop compared to Case 1. The heat exchange rates begin to stabilize towards the end of day 1 with the result of Case 2 almost equal to Case 1 despite being close. At the end of operation, both heat exchange rates are about the same at 11 W/m in cooling mode and 4 W/m in heating mode. Similarly, the mean heat exchange rate for both cases were about 15 W/m in cooling mode and 6 W/m in heating mode.

Although the thermal performance between Case 1 and Case 2 is marginal, the order of heat exchange rates is reserved after about 18 h of operations. Ground temperature profiles in these cases were used to examine this phenomenon. Reference axes along the depth direction indicated by the vertical lines as in Fig. 4.4 were used to obtain the temperature profiles at 6 h and 24 h of cooling operation. The reference axes were offset by 0.25 m from the loop origin to avoid intersecting the pipes i.e., in vertical orientation.

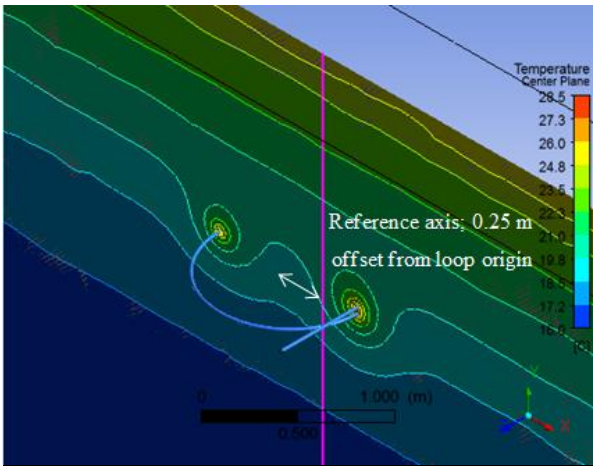

(a) Case 1

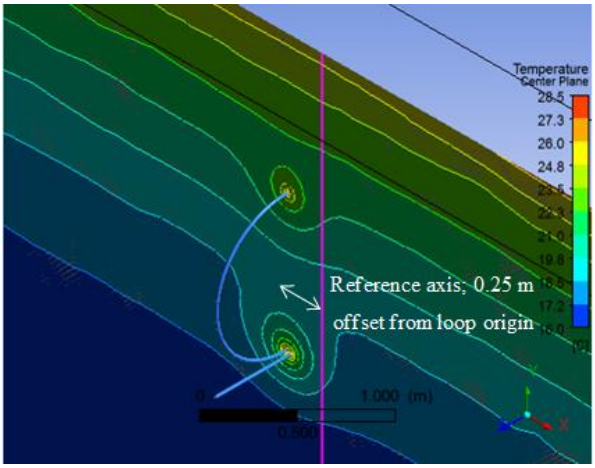

(b) Case 2

Fig. 4.4. Section view of 3D temperature distribution after 24 h of cooling operation.

Fig. 4.5 shows that in Case 1, the ground around the loop was slightly cooler than in Case 2 explaining the slightly higher heat exchange rate in the former at 6 h of cooling operation. At 24 h of cooling operation, the ground temperature around the loop lying flat at 1.5 m deep in Case 1 was warmer than the 19.6 °C mean ground temperature around the loop standing 1–2 m deep in Case 2 explaining the higher heat exchange rate in the latter. It is also worth noting that the straight portion, about 26% of the loop in Case 2 is located at the bottom of the trench.

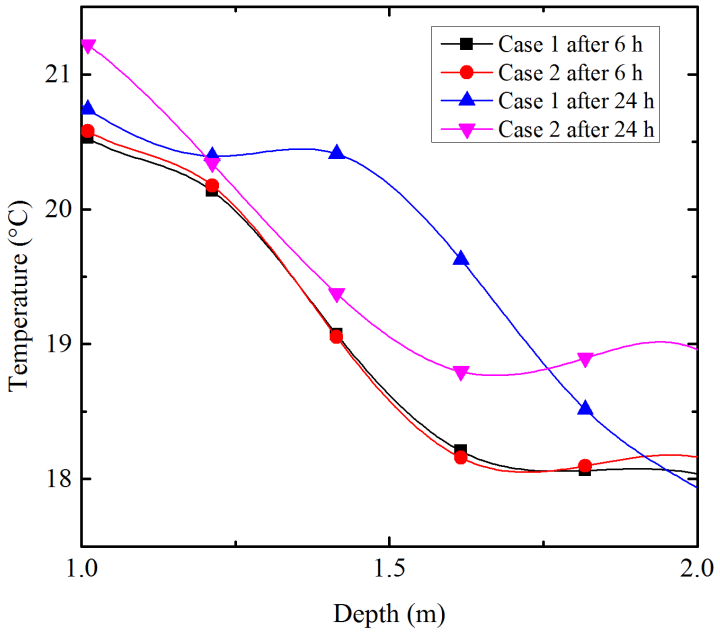

Fig. 4.5. Comparison of ground temperature profiles along reference axis after 6 h and 24 of cooling operation.

Despite this phenomenon, it can be concluded that the effect of loops orientation is minimal although trench depth increases by one third in vertical orientation. Although burying the loops in vertical orientation requires a narrower trench this also means extra excavation work is required in the depth direction. On the other hand, loops in horizontal orientation are easier to install whereby the loops are laid and buried while minimizing the risk of distorting its figure. Therefore, it is suggested that the loops are to be installed in vertical orientation only in the event of land area becomes a limitation.

Copper pipe in horizontal orientation as modelled in Case 3 exhibits a significant improvement in heat exchange rate compared to other cases discussed previously. The heat exchange rate in Case 3 peaks at 87 W/m in cooling and 39 W/m in heating mode. Consequently the thermal performance declines at a much rapid rate before it begin to

stabilize to some extent higher than that in Case 1. This can be justified as the presence of low temperature gradient in copper pipe wall as opposed to high temperature gradient in HDPE pipe wall. However, this results heat buildup in the ground to become dominant at a faster rate.

Hence the high thermal performance in Case 3 cannot be sustained and soon followed by drastic drop. In the end, Case 3 shows heat exchange rate about 12 W/m in cooling mode and 5 W/m in heating mode. The mean heat exchange rate for Case 3 was about 18 W/m and 7 W/m in cooling and heating mode, respectively. This is an improvement of close to 20% in both operation modes compared to Case 1. It is worth noting that although pipe material with higher thermal conductivity suggests higher heat exchange rate, this analysis supports the common claim that heat exchange rate is predominantly limited by the thermal conductivity of the ground.

4.3.2 Parallel loops operation

In the interest of predicting thermal performance in parallel loops operation, further simulation were carried out for double and triple loops operation in cooling mode. Initially, each identical loop was positioned close to one another in which edge-to-edge spacing was set at 0 m. The results in parallel loops operation was compared against single loop operation as presented in Fig. 4.6. The heat exchange rate for double loops operation referred as Case 4 peaks at 100 W/m meanwhile for triple loops operation, Case 5 at 141 W/m.

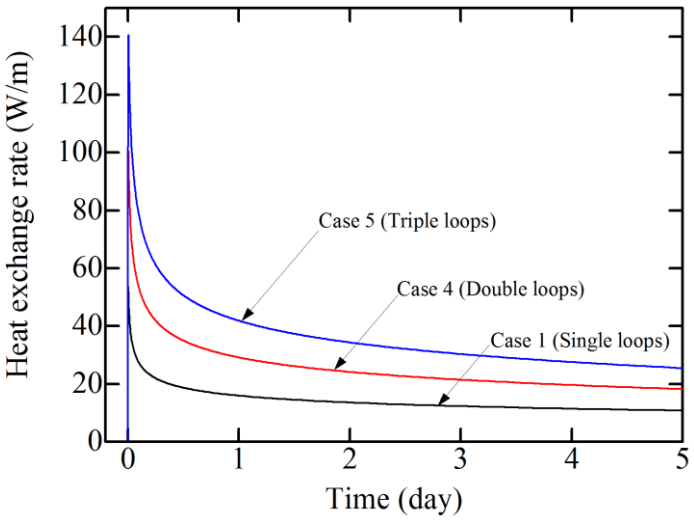

Fig. 4.6. The effect of parallel loops operation.

At the end of operation, as the thermal performance decreases and stabilizes as a result of heat buildup and subsequently dissipated in the ground, the heat exchange rate for double loops operation is about 18 W/m and 25 W/m for triple loops operation. Table 4.1 summarizes mean heat exchange rate for operations in all cases. Case 4 shows an increment of 77% in term of mean heat exchange compared to Case 1. Meanwhile an improvement of 148% is observed in Case 5 compared to Case 1.

Table 4.1. Summary of mean heat exchange rates.

Operation	**Spacing (m)**	**Mean heat exchange rate (W/m)**	
		Cooling	**Heating**
Case 1	-	15.2	6.1
Case 2	-	15.3	6.2
Case 3	-	18.1	7.3
Case 4	0	27.0	-
	0.5	29.4	-
	1.0	30.1	-
	2.0	29.7	-
	4.0	29.5	-
Case 5	0	37.8	-
	0.5	42.5	-
	1.0	42.8	-
	2.0	43.1	-
	4.0	42.4	-

It is perceptible that with the same circulation pump work, parallel loops operation promotes higher efficiency compared to single loops operation. The increased thermal performance in parallel loops operation is unsurprising as heat transfer area is multiplied in this configuration. It is more sensible to install and operate GHE in parallel consisting of short series rather than one long series of loops. Parallel loops operation also benefits GSHP systems whereby less amount of pressure is required to overcome friction losses through each individual series thus minimizing pressure drop.

It becomes apparent that installations with parallel loops configuration requires additional initial costs concerning amount of pipes and excavation works. Abundant land area is also required for such installations. However, these extra investments would pay off due to higher thermal performance would be attainable in a long run. It is evident that heat flow from adjacent loops in parallel operations interferes with one

another penalizing the overall thermal performance. This heat interference or thermal "short-circuiting" disrupts the effective heat transfer in GHE as a result of varying temperature of the flow inside the loops [109].

Further investigations were carried out to determine the effect of spacing between adjacent loops on thermal performance. Edge-to-edge loops spacing of 0.5 m, 1.0 m, 2.0 m and 4.0 m were imposed as previously shown in Fig. 3.10. The effect of spacing distance on heat exchange rate is shown in Fig. 4.7 for double loops operation and Fig. 4.8 for triple loops operation.

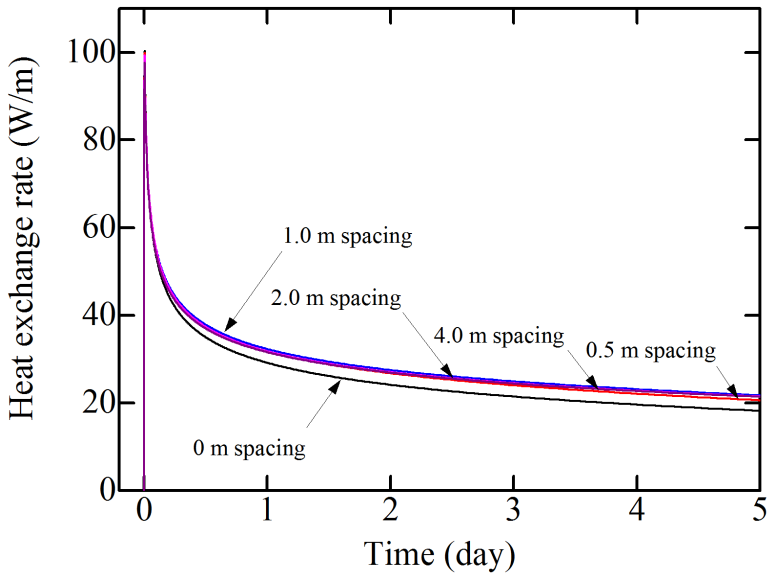

Fig. 4.7. The effect of spacing distance in double loops operation.

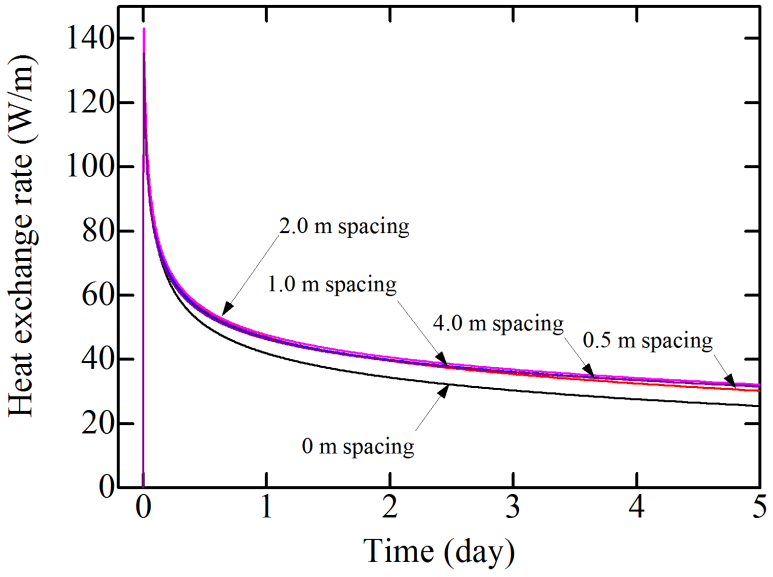

Fig. 4.8. The effect of spacing distance in triple loops operation.

As can be seen in both figures, the thermal performance is significantly improved when the minimum spacing of 0.5 m is imposed. A further improvement is observed in 1.0 m spacing while beyond this point the effect of spacing becomes insignificant. As summarized in Table 4.1, the mean heat exchange rate for double loops operation increases by 9–11% when spacing is imposed. On the other hand, the increase in triple loops operation is 12–14%.

It can be contested that despite the difference in thermal performance in 1.0 m spacing and beyond is negligible, however the mean heat exchange rate is not in increasing order as spacing increases. One can argue that based from other numerical or analytical analysis that thermal performance increases with separation distance as the effect of thermal interference becomes less. The discrepancy in this analysis is thought to be caused by varying cell size, particularly between the loops. This meshing method was used to generate a reasonable number of elements in the model.

4.4 Conclusion

The prediction of thermal performance of GHE prior to the introduction of GSHP system is important. This would be prudent in determining the economic feasibility of a system design. Through this study, it is found that orientation of GHE loops is unimportant as it has minor effect on thermal performance.

The analysis shows that although the trench depth increased by one third in vertical orientation, there was no significant improvement on heat exchange rate compared to that in horizontal orientation. In reality, loops installation in horizontal orientation can be more convenient. In case where land space is limited, it is suggested that the loops are installed in vertical orientation where narrower trench is desired.

The analysis supports the common claim that the ground thermal resistance has more significant effect compared to the pipe thermal resistance on thermal performance of GHE. Although a much higher thermal conductivity i.e., copper were compared against the conventional HDPE as pipe material, the increase in thermal performance was disproportionate while still considered worthy.

Nowadays copper pipe with protective coating are commercially produced and marketed for application in harsh conditions. This enables GSHP installers to opt for GHE with higher efficiency. While parallel loops operation shows high thermal

performance compared to single loops operation, heat flow from adjacent loops causes thermal interference thus affecting the effective heat transfer. It is reckoned that adequate loop separation is provided to thermal interference that would penalize the overall thermal performance.

CHAPTER

5

MODELLING OF REAL-SCALE STRAIGHT AND SLINKY HORIZONTAL GHE

5.1 Introduction

Horizontal ground heat exchangers (GHE) configuration in ground source heat pump (GSHP) system offers relatively low initial costs and ease of installation, compared to vertical borehole configuration [32]. The installation of horizontal GHE mainly involves excavation of shallow trenches 1–2 m deep where pipes are laid and then buried. That being said, horizontal GHE installations would be convenient where land area is abundant. Horizontal GHE in slinky loop configuration provides greater heat transfer compared to straight pipe thus making it more advantageous to be installed in such arrangement. GSHP system owners can choose to install horizontal GHE loop either in horizontal or vertical orientations.

The loop diameter determines the width of the trench in horizontal orientation. In vertical orientation, a narrower trench is desired although this would mean the bottom of the loop sits deeper in the ground. Due to horizontal GHE loop being placed in shallow trenches, the thermal performance is likely to be influenced by the varying conditions at the ground surface [34]. Knowledge of climate interaction and ground thermal properties are increasingly important in designing such installation.

The design that yields the optimal thermal performance permitted by the availability of land area for trenching is desirable. Conversely, the design should achieve a sensible balance between thermal performance and cost-effectiveness i.e.,

initial and operating costs. Despite the growing number of GSHP systems worldwide [100], efforts in enhancing such system in order to promote its usage in developing countries are essential. High efficiency as well as cost-effective horizontal GHE loop operation may also appeal small businesses and homeowners to opt for GSHP system usage. Design and operating strategies to boost the efficiency of horizontal GHE loop is valuable to accomplish this cause.

Enhanced-surface pipe shows higher heat transfer not only by increasing surface area but inducing turbulence compared to smooth pipe in heat exchangers [110]. GHE constructed from superior thermal conductors such as copper [106] is expected to exhibit high thermal performance. The longevity of copper pipe can be significantly extended nowadays as it is commercially available in protective coating to withstand in robust environment.

In this work, the analysis of horizontal GHE operation was performed to predict the thermal performance in terms of heat exchange rate and outlet temperature. The GHE were modelled in different configurations i.e., straight and slinky loops. The effect of pipe materials of different thermal properties on heat exchange rate of GHE operation was also studied.

5.2 Descriptions of numerical modelling

5.2.1 Simulation model

The numerical simulation carried out in this research was performed using a commercial computational fluid dynamics software FLUENT. Heat transfer can be predicted using the software by solving three conservation equations for continuity, momentum and energy. The analysis domain consists of a 3D meshing with an approximate dimension of 8 m trench length in the direction of the GHE, 6 m wide perpendicular to the GHE and 5 m depth, as shown in Fig. 5.1.

The summary of the CFD numerical model and setup is listed in Table 5.1. The GHE buried at 1.5 m depth were modelled in two different configurations (1) straight loop with a spacing of 1.0 m, referred to as in Case 1 and Case 2; and (2) slinky loop with both loop diameter and pitch of 1.0 m, referred to as in Case 3 and Case 4.

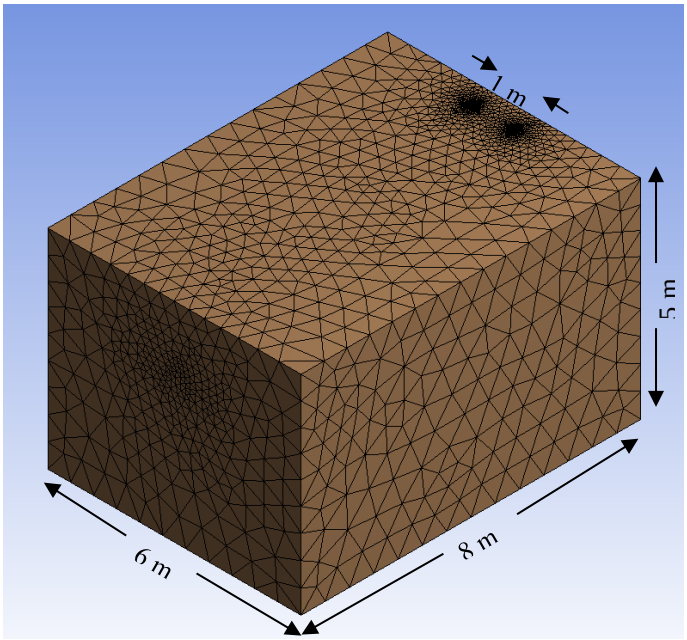

Fig. 5.1. Simulation model.

Table 5.1. Summary of CFD numerical model and setup.

Parameter	**Value**
Boundary meshing	
- GHE and GHE-soil interface regions	Hexahedral
- Soil region	Tetrahedral
Number of cells	
- Case 1 and Case 3 (Straight loop)	8,660,439
- Case 2 and Case 4 (Slinky loop)	22,430,514
Number of nodes	
- Case 1 and Case 3 (Straight loop)	1,768,645
- Case 2 and Case 4 (Slinky loop)	5,461,892
Solver	Transient 3D
Numerical model	Turbulent flow using k-ε model
Numerical scheme	Coupled algorithm
Discretization scheme	Second order upwind

By setting loop diameter and pitch to be equal in slinky configuration, a reasonable compromise between thermal performance and installation costs was assumed [81,82]. A close-up section view at 1.5 m depth of detailed meshing of both configurations is presented in Fig. 5.2. The working fluid flows through one of the vertical pipe then circulates inside the loop before rises through the other vertical pipe.

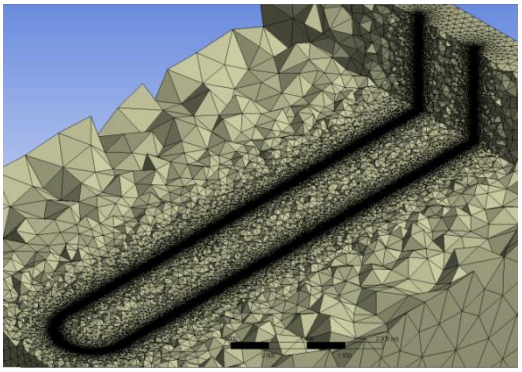

a) Straight loop

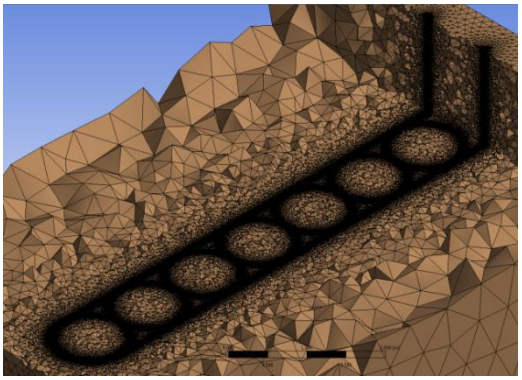

b) Slinky loop.

Fig. 5.2. Close-up section view at 1.5 m depth.

The total pipe length for straight loop is 18 m and for slinky loop is 40 m. The 5 m distance perpendicular to the edge of GHE and 5 m deep were considered adequate to eliminate the influence from ground. In Case 1 and Case 3, the loop was of high density polyethylene pipe (HDPE). On the other hand, the pipe material in Case 2 and Case 4 was composite pipe. The pipe consists of copper as inner layer that is protected with a thin coating of low density polyethylene (LDPE) bringing the overall thickness equivalent to the HDPE pipe thickness. The sizing and properties of pipe materials used in the cases is listed in Table 5.2.

Table 5.2. Pipe sizing and properties.

Case	Pipe material	Inner diameter (mm)	Wall thickness (mm)	Density (kg/m^3)	Specific heat (J/kg·K)	Thermal conductivity (W/m·K)
1 and 3	HDPE	19	2.5	955	2300	0.461
2 and 4	Copper (inner)	19	1.5	8978	381	387.6
	LDPE (outer)	-	1.0	920	3400	0.34

5.2.2 Initial and boundary conditions

Ground heat flux is the process responsible for transporting heat between Earth's surface and subsurface through conduction. Heat conduction in the ground governs the subsurface temperature profile [98]. Due to loop shallow position, ground heat flux has strong influence on the heat transport at the ground surface. In order to achieve a realistic and reliable analysis, time- and position-varying parameters were applied as initial and boundary conditions to mimic heat transfer phenomena in the ground.

The simulation was performed based on the conditions on 1-January-2013 for operation in heating mode. A 3-hourly ground heat flux data at the same site was applied on the ground surface as shown in Fig. 5.3a. The simulation was initialized using subterranean temperature profile using data recorded at a site in Saga University, Japan as shown in Fig. 5.3b. The ground was composed of clay with the density of 1700 kg/m^3, specific heat of 1800 J/kg·K and thermal conductivity of 1.2 W/m·K. All lateral walls and bottom were considered to have no influence on the analysis domain thus treated as adiabatic boundaries.

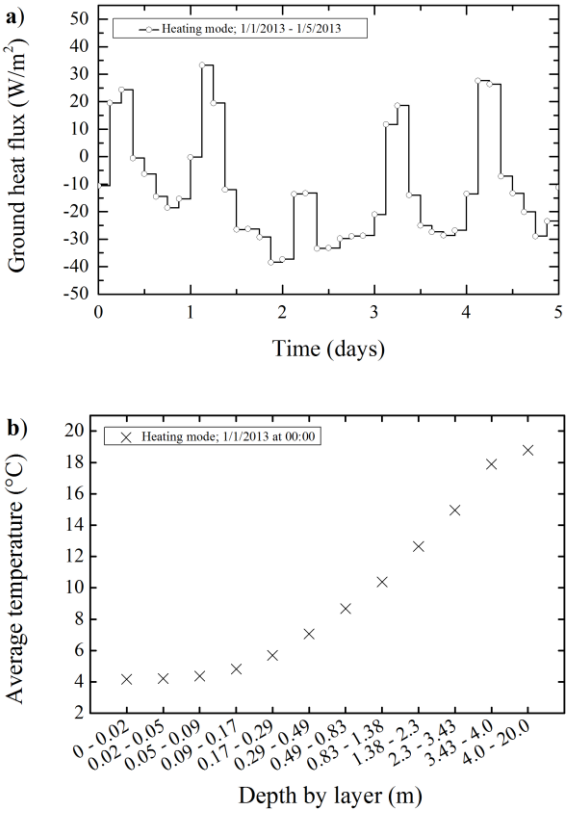

Fig. 5.3. Initial and boundary conditions used in the simulation. a) 3-hourly ground heat flux data b) Subterranean temperature profile.

Water was flowing constant at 4 LPM inside the loop during operation. The pressure distribution in GHE as shown in Fig. 5.4 shows that pressure loss is minimal regardless of its configurations. The loop operation were investigated similar to the method in conducting thermal response test with the exception of fixed loop inlet temperature was imposed. The inlet was set constant at 7 °C in the heating mode operation. The transient analysis was performed for 5-day continuous operation. The simulation of loop operation was carried out per minute basis and the results are reported in a daily basis.

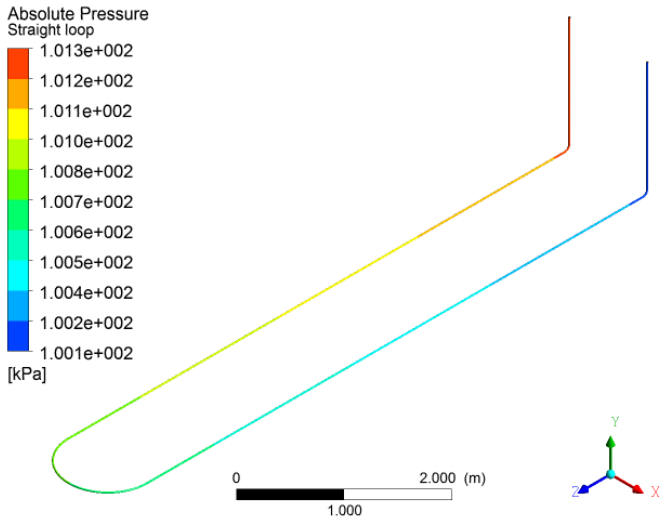

a) Straight loop

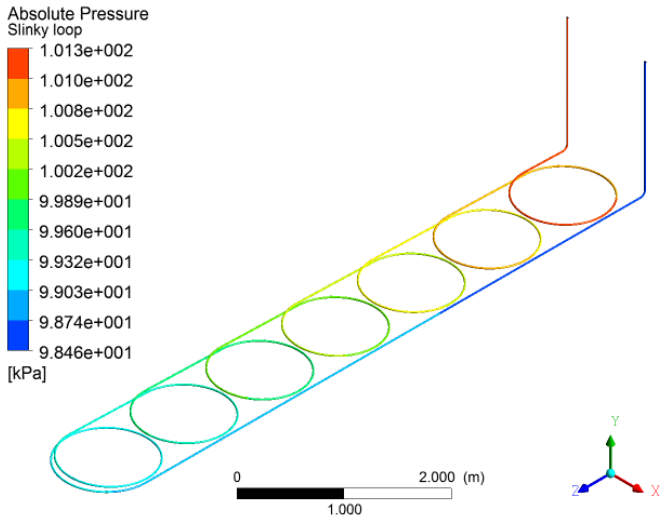

b) Slinky loop

Fig. 5.4. Pressure distribution in GHE.

5.2.3 Transport equations for realizable *k-ε* model

The realizable *k-ε* model [97] differs from the standard *k-ε* model in two important ways: (1) the realizable *k-ε* model contains an alternative formulation for the turbulent viscosity and (2) a modified transport equation for the dissipation rate, *ε*, has been derived from an exact equation for the transport of the mean-square vorticity fluctuation. The term "realizable" means that the model satisfies certain mathematical constraints on the Reynolds stresses, consistent with the physics of turbulent flows.

The modeled transport equations for *k* and *ε* in the realizable *k-ε* model are given in Eq. (5.1) and Eq. (5.2), respectively.

$$\frac{\partial}{\partial t}(\rho k)+\frac{\partial}{\partial x_j}(\rho k u_j)=\frac{\partial}{\partial x_j}\left[\left(\mu+\frac{\mu_t}{\sigma_k}\right)\frac{\partial k}{\partial x_j}\right]+G_k+G_b-\rho\varepsilon-Y_M$$

$$G_k=\rho\overline{u_i'u_j'}\frac{\partial u_j}{\partial x_i}$$

$$G_b=\beta g_i\frac{\mu_t}{Pr_t}\frac{\partial T}{\partial x_i} \tag{5.1}$$

$$\beta=-\frac{1}{\rho}\left(\frac{\partial\rho}{\partial T}\right)_p$$

$$Y_M=2\rho\varepsilon M_t^2$$

where, G_k represents the generation of turbulence kinetic energy due to the mean velocity gradients and G_b is the generation of turbulence kinetic energy due to buoyancy. Y_M represents the contribution of the fluctuating dilatation in compressible turbulence to the overall dissipation rate. M_t is the turbulent Mach number, defined as $\sqrt{k/a^2}$ where $a\left(\equiv\sqrt{\gamma RT}\right)$ is the speed of sound.

$$\frac{\partial}{\partial t}(\rho\varepsilon)+\frac{\partial}{\partial x_j}(\rho\varepsilon u_j)=\frac{\partial}{\partial x_j}\left[\left(\mu+\frac{\mu_t}{\sigma_\varepsilon}\right)\frac{\partial\varepsilon}{\partial x_j}\right]$$
$$+\rho C_1 S\varepsilon-\rho C_2\frac{\varepsilon^2}{k+\sqrt{v\varepsilon}}+C_{1\varepsilon}\frac{\varepsilon}{k}C_{3\varepsilon}G_b+S_\varepsilon$$

$$C_1=\max\left[0.43,\frac{\eta}{\eta+5}\right] \tag{5.2}$$

$$\eta=S\frac{k}{\varepsilon}$$

$$S=\sqrt{2S_{ij}S_{ij}}$$

where, C_2 and $C_{1\varepsilon}$ are constants. σ_k and σ_ε are the turbulent Prandtl numbers for *k* and *ε*, respectively. S is the modulus of the mean rate-of-strain tensor.

5.3 Results and discussion

5.3.1 Comparison of loop outlet temperature

A GSHP system operates at the highest efficiency when the temperature difference of circulating water inside the heat pump is maximized. The GHE outlet temperature is received by the heat pump which later rejects it as GHE inlet temperature. Hence it is desirable for a GHE to transfer heat to the ground as much as possible for a heat pump to operate efficiently.

Fig. 5.5 compares the simulated loop outlet temperature in heating operation respectively. It is recalled that the loop inlet temperature was set constant at 7 °C during the heating operation. Generally in all cases, the loop outlet reaches the highest temperature within hours of operation. A heat pump operates at an optimum range within this period.

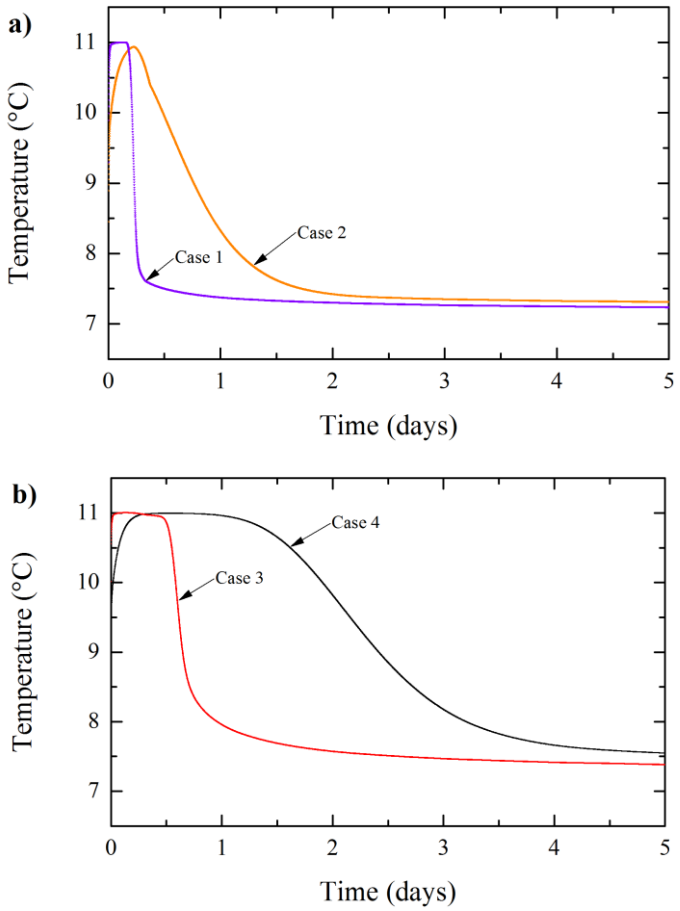

Fig. 5.5. Comparison of loop outlet temperature. a) HDPE pipe (Case 1) and composite pipe (Case 2) in straight configuration b) HDPE pipe (Case 3) and composite pipe (Case 4) in slinky configuration.

Subsequently the efficiency of the heat pump begins to decrease as the outlet temperature drops rapidly. This is due to the effect of thermal saturation within the pipe wall and consequently at ground region surrounding the loop. This effect reduces the amount of heat that can be rejected to or extracted. The outlet temperature begins to drop at a much lesser rate as energy is being dissipated throughout the ground.

The effect of different pipe materials is compared between HDPE pipe (Case 1 and Case 3) and composite pipe (Case 2 and Case 4). It is observed that HDPE pipe reaches optimum outlet temperature quicker than composite pipe. However, the outlet temperature in HDPE pipe deteriorates drastically compared to composite pipe. It can be explained that the high thermal resistance in HDPE wall encourages heat transfer at the beginning of operation. However, as the operation continues the high thermal resistance in the pipe causes the temperature difference between inner wall of the pipe and water flow becomes minimal. Composite pipe allows heat to travel within the pipe wall at a faster rate thus reducing the effect of thermal saturation within pipe wall.

It is also observed that as the thermal saturation at surrounding ground becomes dominant, the effect of different pipe materials is negligible. At the end of the operation, the outlet temperature is about the same regardless of the pipe materials used. The analysis shows that the effect of different pipe materials is more significant in slinky configuration. The time before the temperature difference between outlet and inlet reaches 1 °C in Case 1 is about 6 h compared to about 18 h in Case 3 for HDPE pipe. Whereas the time taken before reaching the same temperature difference in Case 2 is about 1 day compared to about 3 days in Case 4 for composite pipe.

5.3.2 Comparison of thermal performance

The thermal performance of horizontal GHE was expressed in heat exchange rate through the water flow [90] calculated using Eq. (5.3).

$$HER = \dot{m} c_p \Delta T \tag{5.3}$$

where $\dot{m}$ denotes mass flow rate of circulating water, c_p is specific heat, ΔT is temperature difference between the loop inlet and outlet of circulating water.

Specific heat exchange rate is used to describe the GHE performance per length of pipe, calculated using Eq. (3.6) and per length of trench, using Eq. (5.4).

$$HER_{LT} = HER / L_T \tag{5.4}$$

where L_P denotes pipe length and L_T is trench length.

Trench length is far shorter than pipe length in comparison especially in slinky configuration. Therefore it is understandable that heat exchange rate per trench length is higher compared to heat exchange rate per pipe length in any of the same case. Fig. 5.6 shows the comparisons of heat exchange rate of GHE using HDPE pipe in different configuration. Fig. 5.7 presents the comparisons of heat exchange rate of GHE using composite pipe. As discussed in previous sub-section, thermal performance deteriorates significantly as operation continues due to heat build-up in pipe wall and ground region surrounding the loop.

It becomes apparent that despite a large difference in optimum heat exchange rate per pipe length between straight and slinky configuration, the specific heat exchange rate is about the same if expressed per trench length. Both configurations and pipe materials are found capable in exploiting the ground temperature by rejecting or extracting heat in a comparable amount during the early stage of operation.

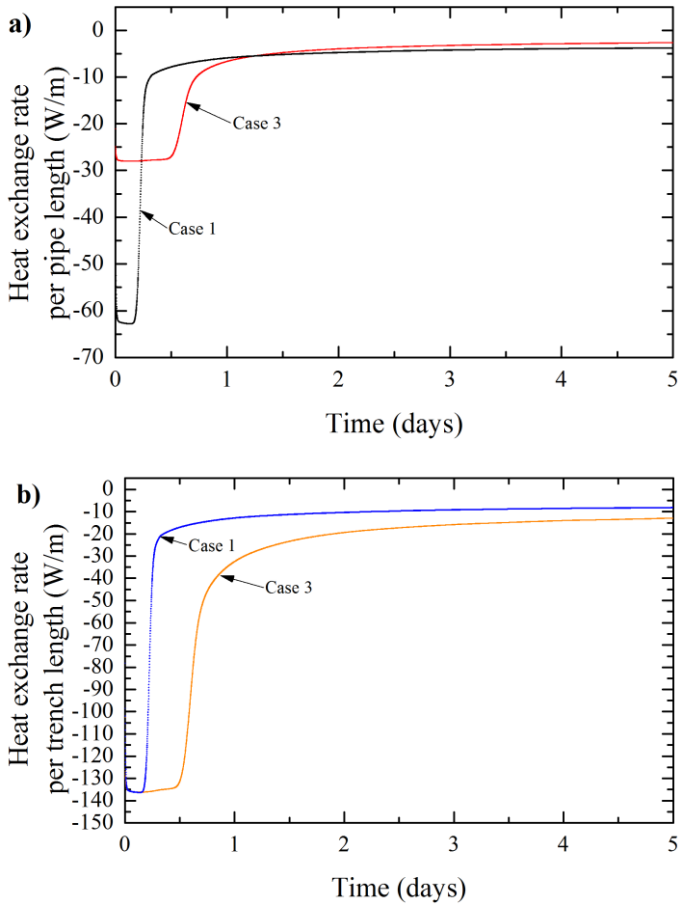

Fig. 5.6. Comparison of thermal performance of GHE using HDPE pipe between straight configuration (Case 1) and slinky configuration (Case 3). a) Heat exchange rate per pipe length b) Heat exchange rate per trench length.

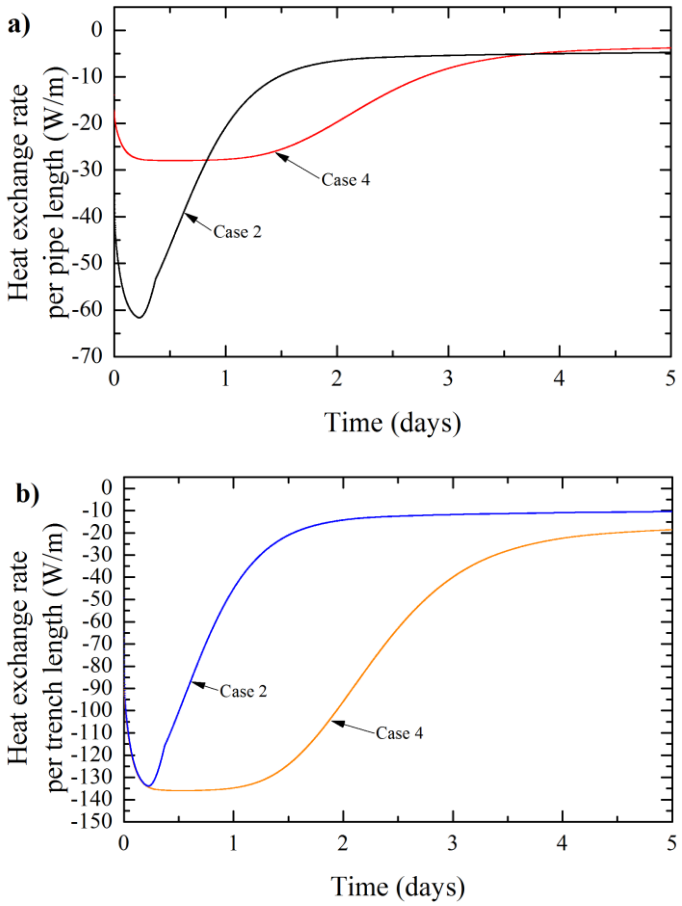

Fig. 5.7. Comparison of thermal performance of GHE using composite pipe between straight configuration (Case 2) and slinky configuration (Case 4). a) Heat exchange rate per pipe length b) Heat exchange rate per trench length.

The greater contact area and pipe material of superior thermal properties help to prolong the optimum period of heat exchange. Understandably the greater contact area provided in slinky configuration allows more heat transfer compared to straight configuration. It can be also stated that pipe material with low thermal resistance provides high temperature difference at the interface between water flow and pipe. At the same, pipe material with low thermal resistance encourages the presence of small temperature gradient within the pipe wall.

Table 5.3 summarizes the mean specific heat exchange rate for both per pipe and trench length of all cases. The mean heat exchange rate per pipe length is slightly higher in straight configuration compared to in slinky configuration except in the cases using composite pipe albeit the small difference. The temperature difference between the GHE inlet and ground at 1.5 m deep when the operation began is about 5 °C. It is expected that the different in heat exchange rate per pipe length between straight and

Table 5.3. Summary of mean specific heat exchange rate.

Case	Configuration	Pipe material	Mean specific heat exchange rate (W/m)	
			Per pipe length	Per trench length
Case 1	Straight	HDPE	7.5	16.4
Case 2	Straight	Composite	14.2	30.8
Case 3	Slinky	HDPE	6.9	33.6
Case 4	Slinky	Composite	15.1	73.6

slinky configuration would be more significant when the temperature difference between water flow and ground is increased.

The pipe length ratio between slinky and straight configuration is 2.2. The mean heat exchange rate per trench length in slinky configuration using HDPE pipe increases to about 2.0 times higher in than in straight configuration. About 2.4 times improvement is observed for mean heat exchange rate per trench length in slinky configuration using composite pipe than in straight configuration. Hence it can be said that composite pipe exploits the additional pipe length in slinky configuration better compared to HDPE pipe. This is evident as the thermal performance in composite pipe in different configuration is increased more than the straight-to-slinky pipe length ratio.

It is worth noting that the LDPE coating presents 40% of the overall thickness and has major influence on the overall thermal resistance of composite pipe. While LDPE has inferior thermal properties than HDPE, composite pipe with LDPE coating still performs relatively superior than HDPE pipe. The specific heat exchange rate is 1.9 times higher in straight configuration using composite pipe than using HDPE pipe. In slinky configuration using composite pipe, the specific heat exchange rate is increased to 2.2 times than using HDPE pipe.

HDPE pipe is commonly preferable by GSHP installers as GHE due to the high strength-to-density ratio in addition to its characteristic of high flexibility and durability. Nowadays as the variation of copper pipes being produced includes with protective coating, GSHP installers may opt to GHE with superior thermal properties as pipe material for higher efficiency system.

5.4 Conclusions

Despite GSHP system provides high efficiency, high installation cost hinders homeowners and small-medium enterprises from opting to this system. In promoting this system, cheaper installation cost can be introduced by using horizontal GHE. In this work, thermal performance of horizontal GHE in straight and slinky configuration was modelled. This includes simulating the operation by using pipe materials with different thermal resistance.

Based on the analysis, whilst heat exchange rate per pipe length in straight configuration is higher than in slinky configuration, the heat exchange rate per trench length of the latter is significantly improved compared to the former. It is also found that the greater surface area and pipe material of superior thermal properties are capable in delaying the thermal saturation effect. This lengthens GHE performance at optimum range. GHE configuration that provides high surface area and pipe material with superior thermal properties contributes to high efficiency system. This can be interpreted as lower operating cost thus increasing the desirability for such installation.

This improvement is necessary to overcome the drawback of shallow GHE installations that is prone to unstable thermal performance due to temporal weathers and seasonal variations. However this would have an impact on initial cost of such installation. An economic analysis is required to determine the cost effectiveness and return of investment of the proposed installation.

CHAPTER

6

ANALYSIS OF HORIZONTAL GHE MODELS WITH DIFFERENT LAYOUTS AND PIPE MATERIALS

6.1 Introduction

Energy is rejected to or absorbed from the Earth in ground source heat pump (GSHP) systems through ground heat exchangers (GHE). Basically, GHE are pipes buried in the ground either in deep boreholes or shallow horizontal trenches. Installations of horizontal GHE mainly involve excavation of shallow trenches 1–2 m deep where pipes are laid and buried. That being said, horizontal GHE installations would be convenient where land area is not limited.

Horizontal GHE in slinky configuration provides greater thermal performance compared to straight pipe [81,96,111,112]. Such layout is advantageous in comparable trench length by boosting amount of heat transfer. Slinky or coil-like pipe geometry also enhances flow characteristics by inducing secondary flow due to action of centrifugal force [113–116].

GSHP system owners can choose to install slinky GHE either in horizontal or vertical orientations [32,69,82]. The loop diameter determines trench width in horizontal slinky GHE. In vertical slinky GHE, narrower trench is required whereby the bottom of the loop sits deeper in the ground. Due to slinky GHE placement in shallow trenches, the thermal performance is prone to the influence of varying conditions at ground surface [34,41,100].

Knowledge of climate interaction and ground thermal properties are increasingly

important in designing such installations. Designs that can yield the highest thermal performance permitted by the land availability for trenching are desirable. Conversely, the designs should possess sensible balance between thermal performance and cost-effectiveness i.e., initial and operating costs.

Despite the growing number of GSHP systems in developed countries [33,101,117–120], efforts in promoting its usage in other parts of the world are essential. High efficiency slinky GHE designs may also appeal small businesses and homeowners to apply GSHP systems. Design and operating strategies to further elevate the efficiency of slinky GHE are valuable to accomplish this cause.

Enhanced-surface pipes yield better heat transfer by inciting turbulent eddies in heat exchangers in addition to increasing contact area [110,121–125]. Corrugated plastic pipes are reported to be used in Earth-air heat exchangers (EAHE) [78,126] and direct expansion GHE [127] for agricultural and residential buildings acclimatization. Meanwhile, corrugated [128] and twisted [129] metal pipes are used as heat pipe to conduct terrestrial heat onto surface of the ground.

GHE constructed from high thermal conductivity materials such as copper [107,130] show thermal performance enhancement compared to the widely used plastic materials. GHE using copper pipe have also been studied for EAHE [131] and direct expansion GHE [132] as well. Copper pipe is reliable with manufacturers provide up to 50-year warranty on their products. However, it may be problematic for applications underneath the ground surface.

Alternatively, composite copper pipes can be used as it is commercially available nowadays. This warrants the durability whereby coating layer provides protection against deterioration in harsh ground conditions. Nevertheless, the coating is expected to render the effective thermal conductivity of composite pipe. Combination of slinky-shape pipe with enhanced-surface and high thermal conductivity materials could prompt such studies to be undertaken.

Numerical modelling concerning horizontal GHE can be found in several studies but mostly were performed using straight configuration. On the contrary, studies on slinky GHE modelling are limited. The ones that are available were carried out by either in miniature-scale, representative geometry, two-dimensional, or cross sections containing one or two loops. However, real-scale spiral borehole GHE models were often studied as the geometry is easier to construct.

To the authors' best knowledge, there has not been any study carried out in

modelling real-scale slinky horizontal GHE. Apart from complex interaction at ground surface boundary, the models construction is extremely difficult and time-consuming to begin with [83]. Another challenge is the expensive computational requirements such as CPU, GPU, physical memory and data storage.

The present work is an elaborate attempt to conduct real-scale modelling of moderate-size horizontal GHE. The three-dimensional numerical model employed is based on finite volume method. Numerical models performed using this method shows better stability on unstructured grids [133]. Comparative analysis on thermal performance was carried out by modelling horizontal GHE using different layouts. Additionally, the effect of thermal properties of different pipe materials was also investigated.

6.1.1 GHE analysis methods

Analytical and numerical methods are used to aid the design and sizing of a proposed GHE installation. While both have its pros and cons, these methods are able to provide reliable solutions with reasonable accuracy [42,72]. Analytical method is computationally efficient and provides a fast approach in obtaining solutions based on developed mathematical models.

Analytical models are preferable over numerical models due to the latter would have high potential to be computationally expensive. This is especially true during simulating models with large numbers grid elements over extended operation period. There are numerous commercial and open source numerical solvers available that are robust and able to handle complex geometry. Depending on scale of geometry, huge generated grid size is sometimes inevitable that would later affect solving time. As a result, numerical modelling could be very time consuming.

Numerical models present its own merits in GHE thermal analysis, especially when horizontal configuration is involved. Numerical models are capable in producing realistic solutions compared to analytical models as it is flexible and can easily handle complex boundary conditions. Due to horizontal GHE placement in shallow trenches, spatial and temporal changes at ground surface would affect its thermal performance.

Such dynamics interactions between horizontal GHE and ground surface can be incorporated in numerical models to mimic an accurate analysis. Apart from near-

surface effect, numerical models are convenient in incorporating (1) seasonal ground freezing or thawing around the pipe; (2) moisture transport; (3) snow cover and permafrost; and (4) rain infiltration and groundwater advection [68,134].

6.1.2 Thermal interference influence

Heat flow from adjacent pipes in the same borehole or trench causes the overall thermal performance to be affected. This thermal inference or short-circuiting phenomena also occurs between multiple boreholes or trenches. The separation distance between pipes and boreholes or trenches dictates the significance of this effect [135]. Although studies that elaborately describe thermal interference are limited, the ones available are centered on the effect in borehole GHE.

Classic analytical models for GHE thermal analysis consider thermal interference effect between boreholes in their solutions [136]. However, heat flow circuiting from adjacent pipes is not incorporated [38]. Recent analytical models based on quasi-three-dimensional were developed to account for heat flow from adjacent pipes. For example, analytical models for borehole GHE incorporating fluid axial convective heat transfer and thermal interference among U-tube legs have been derived [49,59,109,137,138]. In addition, recent moving ring source models for spiral or slinky GHE were proposed to include heat flow effect in the ground [35,65,68,69,138].

On the other hand, numerical models include heat flow effect within the analysis domain. Mei [139] solved numerically thermal interference in horizontal GHE loop with one pipe on top of the other using a three-dimensional explicit finite difference model. Muraya [140] investigated the thermal interference between the U-tube legs in boreholes GHE using a transient two-dimensional finite element model. Xing [134] attributed the difference when comparing analytical and numerical results for a foundation heat exchanger system due to thermal inferences between the pipe and convective nature of the basement.

U-tube configuration is commonly applied in borehole GHE installations. Recently, vertical spiral coil configuration is also gaining interest. In comparison, horizontal GHE offer more freedom in the choice of design layouts e.g. straight, slinky or serpentine; single- or double-layer; and in horizontal or vertical orientations. Hence it is not practical to apply generic analytical models for a unique horizontal GHE layout.

Unless specific analytical methods are developed, the existing ones are unable to consider thermal interference as effective as in numerical models. Additionally, numerical models consider the effect of exact geometry shapes and its interactions. The interactions would include between adjacent pipes and vertical connecting pipes to ground surface.

6.2 Description of numerical modelling

6.2.1 GHE models

For ease of reference, the GHE models tested are distinguished according to configurations, orientations and pipe materials as cases listed in Table 6.1. Pressure distribution as given in Fig. 6.1 can be used to describe the cases using different layouts including its flow path. GHE in straight configuration as in Case 1 is basically horizontal U-tube pipe placed at the trench bottom. The trench is 1.5 m deep with 1 m pipe separation distance was given.

Table 6.1. GHE models according to configurations, orientations and pipe materials.

Case	Configuration	Orientation	Pipe material
1	Straight	Horizontal	HDPE
2	Slinky	Horizontal	HDPE
3	Slinky	Horizontal	Composite
4	Slinky	Horizontal	Copper
5	Slinky	Vertical	Composite
6	Slinky	Inverted vertical	Composite

Meanwhile, slinky configuration comprises a series of seven non-overlapping loops followed by straight return pipe as in Case 2–6. The loop diameter for each slinky loop is 1 m. In Case 1–4, the GHE were positioned inside the trench in a similar depth and orientation as in Case 1. In contrast, GHE in vertical orientation were laid upright in 2 m deep trenches as in Case 5 and 6. Perceivably, the loops center is at the same 1.5 m deep as the GHE laid in horizontal configuration. The return pipe is at the top in Case 5 as opposed to at the bottom in Case 6. Vertical pipes connect the GHE to ground

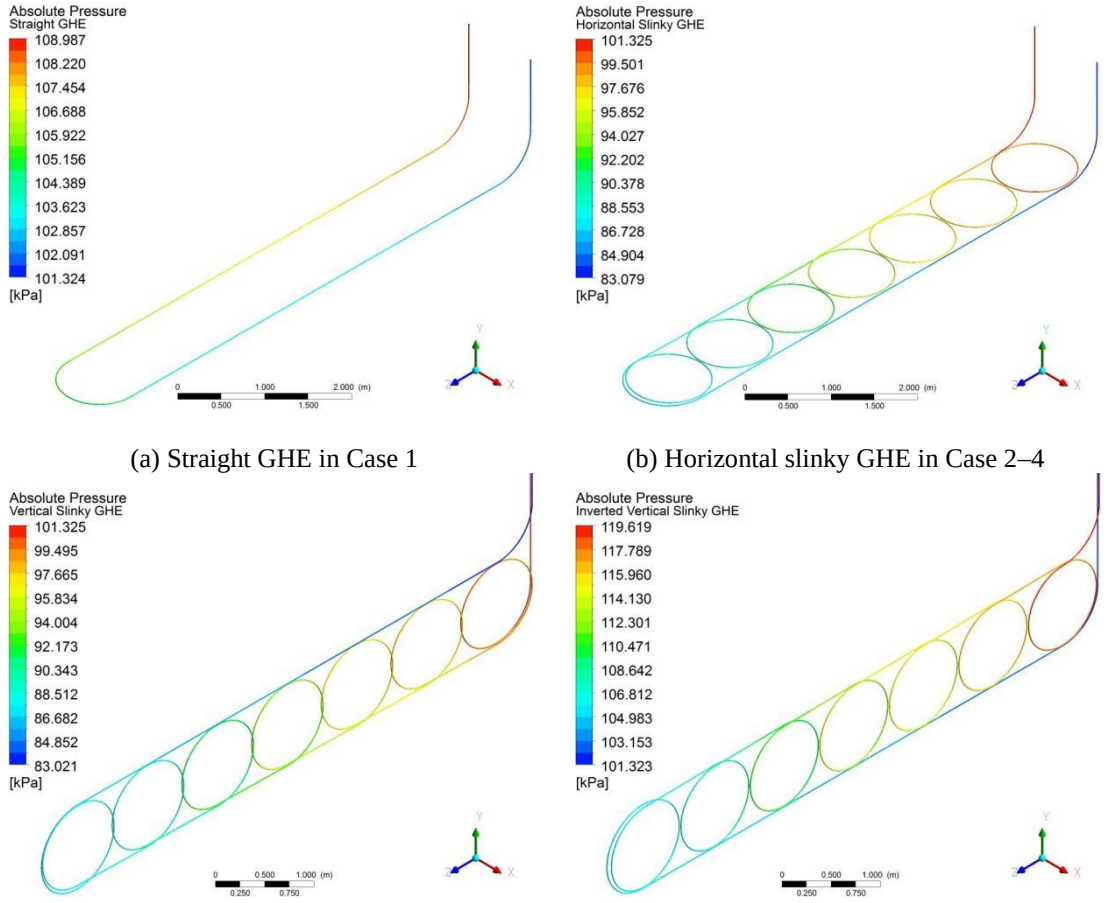

(a) Straight GHE in Case 1

(b) Horizontal slinky GHE in Case 2–4

(c) Vertical slinky GHE in Case 5

(d) Inverted vertical slinky GHE in Case 6

Fig. 6.1. Pressure distribution in the four main GHE layouts.

surface in all cases.

The total pipe length for straight and slinky GHE is 17 m and 39 m, respectively. The dimensions for each analysis domain are 10 m length × 10 m wide × 5 m deep. The trench is symmetrical on both length and width directions of the analysis domain. An example of the three-dimensional unstructured grid and GHE positioning is given in Fig. 6.2.

Table 6.2 summarizes important grid parameters in all GHE layouts. Same grid sizing method for grid generation such as element or cell size and growth rate was used in all cases. GHE region employs fine cells and the cell size grows coarser along the ground region towards the outer boundaries.

Table 6.3 lists the thermal properties of pipe materials and ground. The pipe inner diameter is 12.7 mm (0.5 inch) in all cases. The wall thickness for HDPE pipe in Case 1 and 2 is 1.75 mm. For composite pipe in Case 3, 5 and 6, the overall wall thickness is of HDPE pipe equivalent. The layer thickness for inner copper and LDPE coating is

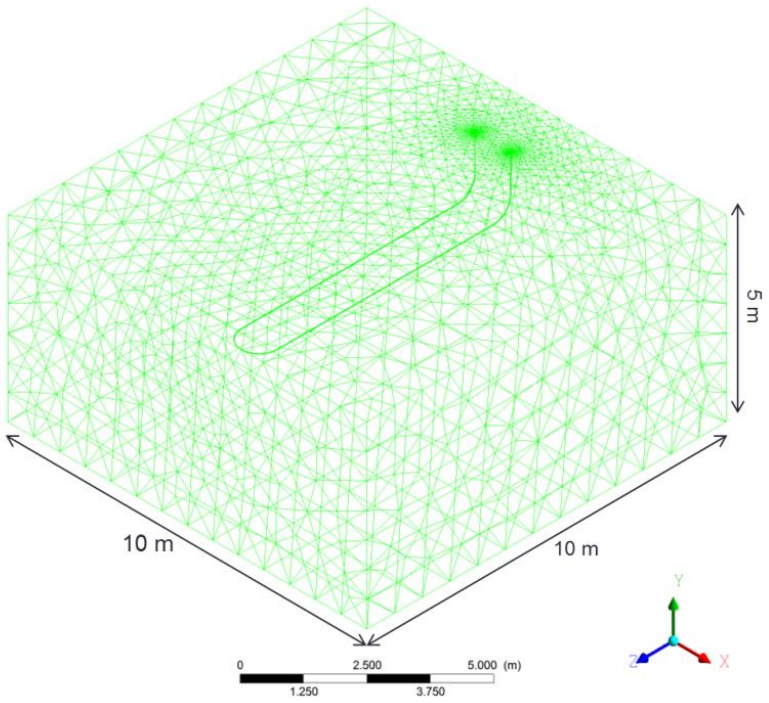

Fig. 6.2. Example of analysis domain for Case 1.

Table 6.2. Summary of grid parameters.

Parameter	Value
Boundary meshing	
GHE region	Hexahedral
GHE-ground interface region	Hexahedral
Ground region	Tetrahedral
Number of grid cells	
Straight GHE (Case 1)	18,081,872
Horizontal slinky GHE (Case 2–4)	38,926,045
Vertical slinky GHE (Case 5)	37,794,259
Inverted vertical slinky GHE (Case 6)	38,784,521

1.25 mm and 0.5 mm, respectively.

The dual layer of composite pipe was treated as single wall thickness in the modelling. This was to avoid convoluted layer grid thus aid solution convergence. Therefore, effective properties for composite pipe as given in Table 6.3 were obtained and applied. For reference, the density, specific heat and thermal conductivity of LDPE used are 920 kg/m3, 3400 J/kg.K and 0.34 W/m.K, respectively. Bare copper pipe is used in Case 4 where the wall thickness is the same as the inner copper layer of composite pipe.

Table 6.3. Thermal properties of pipe materials and ground.

Pipe material	Density (kg/m^3)	Specific heat (J/kg.K)	Thermal conductivity (W/m.K)
HDPE	955	2300	0.461
Copper	8978	381	387.6
Composite	6475	514	1.19
Clay	1700	1800	1.2

6.2.2 Initial and boundary conditions

Ground heat flux is the process where heat is being transported between the Earth's atmosphere and ground surface. Subsequently, the heat is transported through conduction that in turn governs the ground temperature profile [98]. Ground heat flux has strong influence on horizontal GHE operation due to the position at shallow depth. For simplicity or lack of data availability reasons, many analytical or numerical models tend towards regarding the surface as a constant or imposed temperature boundary where the heat flux are allowed to vary [81,82,96,141–143].

Fig. 6.3 shows the varying near-surface air temperature at a test site in Saga University on Kyushu Island, Japan. The outer boundaries distance was assumed sufficient to eliminate influence of ground surface temperature on top of the trench. This allows generic transient temperature to be imposed as surface boundary condition. The temperature on the far-field boundaries can be safely assumed has no effect on ground region near the GHE, and vice versa. Thus all side walls were treated as

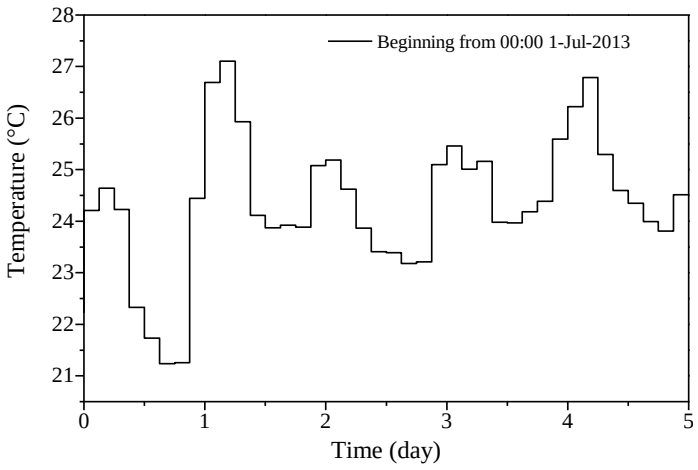

Fig. 6.3. 3-hourly near-surface air temperature at Saga University test site (Source: GES DISC).

adiabatic boundaries.

Analysis domain depth of 5 m was selected because the temperature at this distance maintains relatively constant throughout the year. A constant geothermal heat flux of 65 mW/m^2 [144] was defined at the bottom boundary. The analysis domains were initialized using the following fitted equation, as illustrated in Fig. 6.4, of recorded ground temperature profile at the test site.

$$T_y = 16.1 - 0.0027y^3 + 7.2e^y \tag{6.6}$$

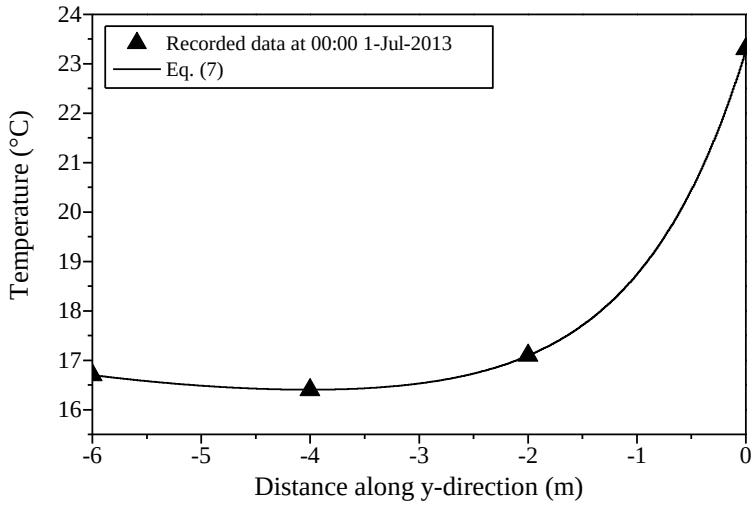

Fig. 6.4. Ground temperature profile applied as analysis domain initial condition.

6.2.3 CFD simulation setup

CFD simulation of all cases was performed under cooling mode in continuous 5-day operation. Water was used as working fluid with a constant flow rate of 4 LPM and entering water temperature of 27 °C. This corresponds to turbulence flow with Reynold number of 6660. The effect of contact thermal resistance, rain infiltration and groundwater flow were not considered in the simulation.

The simulation was carried out using commercial finite volume CFD software Fluent 14.5. The software obtains the heat transfer solution by solving conservation equations for continuity, momentum and energy. Realizable *k*-*ε* model with enhanced wall treatment option enabled was applied in the turbulence model. The numerical scheme adopted segregated coupled algorithm with second order upwind discretization. The calculation time step was in minute basis.

6.3 Results and discussion

Numerical solution of horizontal GHE models obtained were analyzed and compared. The comparison covers the effect of using different configurations, pipe materials and orientations. Thermal performance criteria include heat exchange rate, effective period and thermal interference. The impact on initial and operating costs are also discussed.

6.3.1 Pre-analysis

Pipe length as well as curvature affects flow behavior inside GHE in different layouts. Therefore, simulation under steady condition to investigate its effect on pressure drop was carried out. The results of pressure distribution for the four main GHE layouts are as previously shown in Fig. 6.1. The pressure drop is 7.7 kPa in straight configuration and about 18 kPa regardless of orientations in slinky configuration. This information is discussed in subsection 3.4 when comparing thermal performance improvement against increase in circulation work.

The simulation results can also be used to validate the selection of analysis domain dimensions. Fig. 6.5 shows an example of isotherm generated at the end of operation for Case 4. It is observed that heat flow near GHE region does not affect the far-field and bottom boundaries. Temperature of the ground affected by GHE heat flow is within 0.8 m from the pipe edge.

6.3.2 Heat exchange rate

Heat transfer between GHE and ground was determined by examining the amount of heat loss through water flow. Thus, based on Eq. (5.4), heat exchange rate of GHE for each case, expressed per meter length of trench, is calculated using:

$$HER = HER_{LT} = \dot{m} c_p \Delta T / L_T \tag{6.7}$$

where $\dot{m}$ denotes the mass flow rate; ΔT is the difference between entering water temperature (EWT) and leaving water temperature (LWT); and L_T is the trench length which is 7 m in all cases.

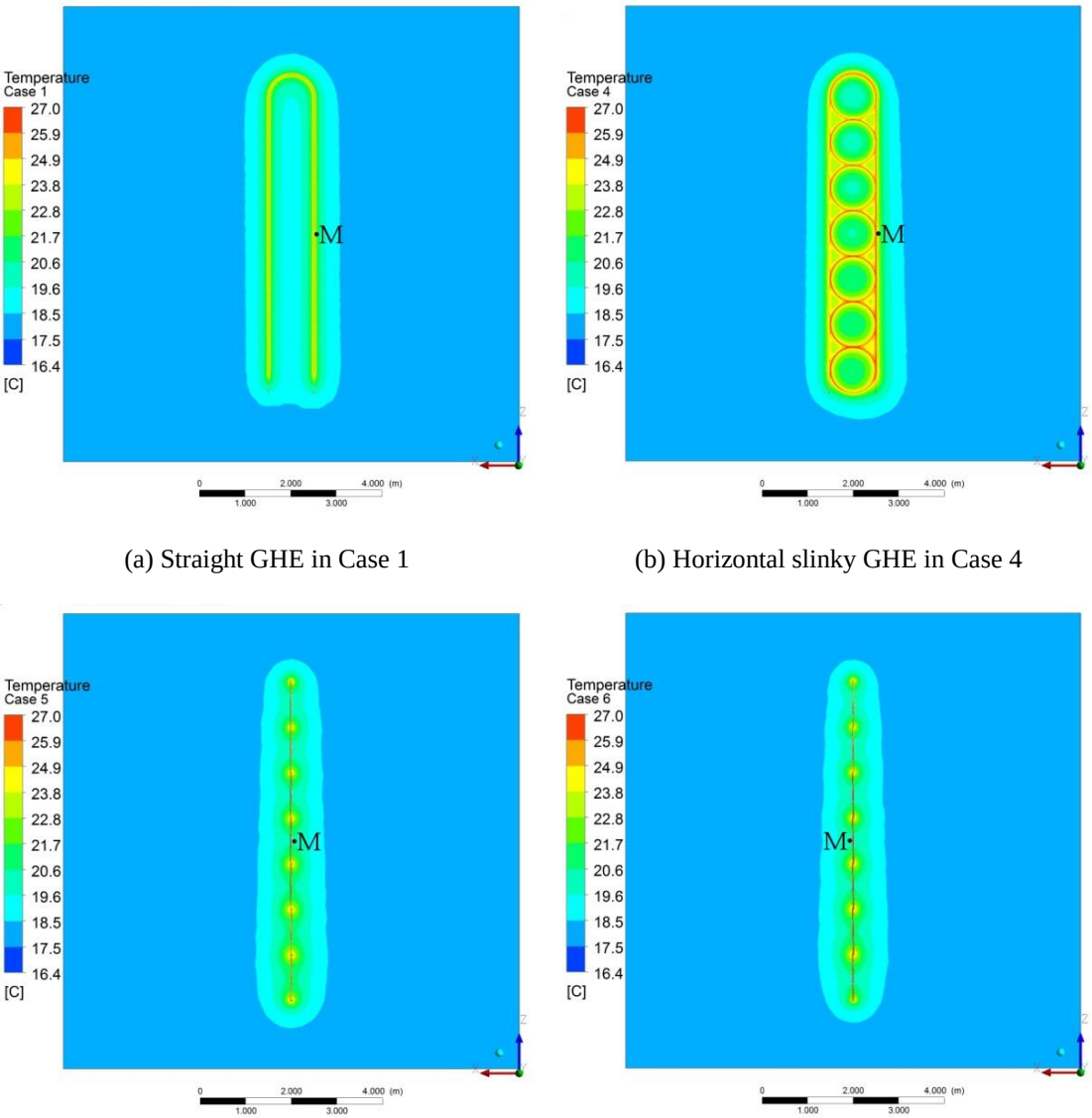

(a) Straight GHE in Case 1

(b) Horizontal slinky GHE in Case 4

(c) Vertical slinky GHE in Case 5

(d) Inverted slinky GHE in Case 6

Fig. 6.5. Example of isotherm generated (ZX plane at y = -1.5 m) at 120 h elapsed time. Point M indicates the location of monitoring well for ground temperature profile for the four main GHE layouts.

Fig. 6.6 shows the simulation results of predicted LWT over continuous 120 h operation in cooling mode. The corresponding transient heat exchange rate calculated using Eq. (6.7) is shown in Fig. 6.7. Heat transfer rises within the first 2 to 3 hours of operation until maximum rate is reached. The heat exchange rate is then sustained and said to be in effective operation up to this period. Subsequently, heat exchange rate decreases with much less thermal performance towards the end of operation. It is observed that vertical slinky cases do not strictly follow this trend as in other cases.

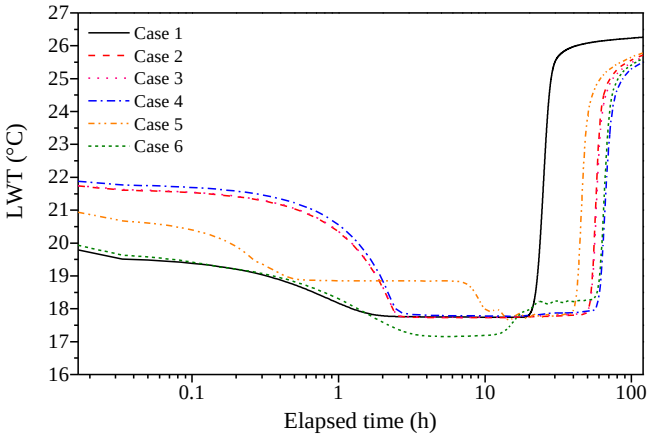

Fig. 6.6. Leaving water temperature versus elapsed time.

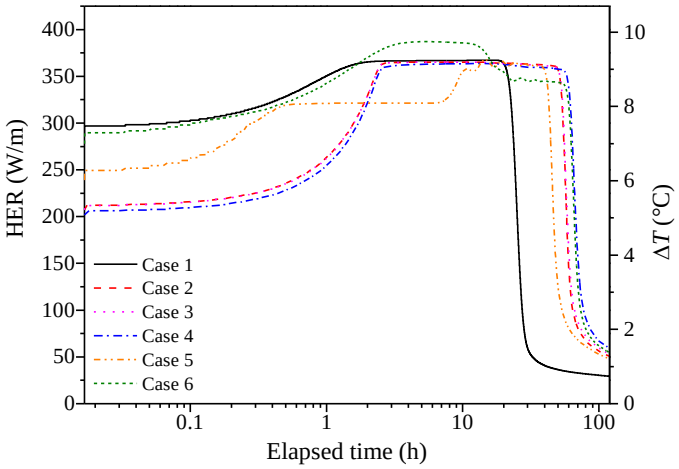

Fig. 6.7. Heat exchange rate and EWT-LWT difference versus elapsed time.

It is apparent that GHE response to operation start-up varies among the cases. As soon as the operation begins, Case 1 yields the highest heat exchange rate close to 300 W/m. The heat exchange rate differs from the lowest response as in Case 4 by approximately 100 W/m. The difference among the cases gradually reduces as heat exchange rate draws near to maximum. Temperature of the ground surrounding vertical leaving pipe influences the LWT during initial operation period. In addition, GHE configuration plays an important factor on thermal performance during this period.

High heat exchange rate in Case 1 is obviously because thermal interference from adjacent pipe is non-existent in straight configuration. Also, HDPE higher thermal resistance allows higher temperature difference to be sustained between inner pipe wall and water flow. As for Case 4, copper pipe wall warms up quicker as heat is transported by water flow. The resulting lower temperature difference at inner wall-water interface

during initial operation period contributes to lesser heat exchange rate.

Although straight GHE performs significant higher during initial operation, heat exchange rate drops much sooner than in slinky configuration. Among horizontal slinky cases, heat exchange rate difference is observed to be marginal during initial operation. Between Case 2 and 3, the difference is virtually indistinguishable even during the entire operation. Case 4 performs slightly lower than other horizontal slinky cases during initial operation but maintains longer afterward.

Evidently, all GHE cases are equally capable of exploiting ground temperature by rejecting heat at a comparable maximum rate. The maximum heat exchange rate is independent of layouts and pipe materials but rather dependent on ground temperature. LWT during this period corresponds to the initial temperature of ground region near GHE. EWT-LWT difference is kept above 9 °C during this period but not strictly in vertical slinky cases. Influence from the ground surrounding leaving pipe reduces as this region cools off along with operation.

GHE in horizontal orientation cases sit flat at trench bottom 1.5 m deep. Contrastingly, the return pipe in vertical slinky cases was placed at 1 m and 2 m deep in Case 5 and 6, respectively. LWT in these cases is strongly influenced by ground temperature where the return pipe is positioned. The closely positioned vertical connecting pipes from ground surface may interact with each other as well.

Ground surface heat flux affects heat dissipation rate at shallower ground region. This region is exposed to relatively warmer ground and near-surface interaction. The heat dissipation rate imbalance along the depth causes heat exchange rate in vertical orientation cases to vary. Noticeably, about half of the pipe in vertical orientation was positioned less than 1.5 m deep.

Ground temperature where the return pipe is positioned in vertical orientation influences GHE response to operation start-up. Case 6 shows higher heat exchange rate during initial operation and also lasts significantly longer than Case 5. Heat exchange rate in Case 5 takes the shortest time to reach planar but performs the worst initially. However, the heat exchange rate is boosted comparable to other cases after about 7 h of operation.

The exact opposite can be observed in Case 6. The maximum heat exchange rate is the highest of all cases. After about 10.5 h of operation, it shrinks to lower than any other cases. The effect of different layouts and pipe materials on thermal performance is discussed in elaborate details in the following subsections.

6.3.3 Effective period

A GSHP system is said to operate at its highest efficiency when circulating water inside heat pump is at the highest temperature difference. LWT is received by heat pump which later rejects it as EWT. Therefore, GHE should be designed to allow heat rejection or extraction as much as it can for as long as possible. As it is evident in Fig. 6.7, heat exchange rate plummets, varies upon cases, within 1 to 3 days of operation.

After that, the decrease is more settled and the GHE is considered to cease in rejecting heat effectively. This is due to thermal saturation at ground region near the GHE. Heat accumulates at this region resulted by the lesser rate of heat dissipation in the ground compared to heat rejected by GHE. Towards the end of operation, EWT-LWT difference is about 1 °C in Case 1 and 2 °C for the rest.

To further investigate thermal saturation effect, heat transfer coefficient of the GHE was examined. Fig. 6.8 shows the simulation results of surface heat transfer coefficient along GHE-ground interface region. It is worth noting that the software calculates these values using a fixed reference temperature instead of bulk fluid temperature. Hence, the surface heat transfer coefficient is merely an indication rather than expression of an actual condition.

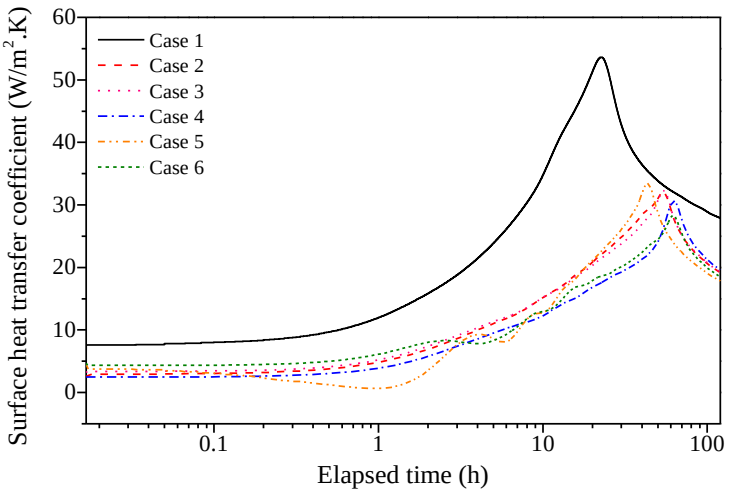

Fig. 6.8. Surface heat transfer coefficient from Fluent solution versus elapsed time.

Essentially, heat transfer coefficient increases steadily in all cases except in vertical slinky cases. As discussed previously, varying ground temperature profile causes amount of heat transfer to vary in the latter. Soon after reaching its peak, heat

transfer coefficient gradually decreases. Elapsed time when heat transfer coefficient peaks is considered as an indication that thermal saturation begins to halt GHE effective thermal performance.

Fig. 6.9 shows elapsed time before thermal saturation becomes dominating, or simply effective period denoted as t_{eff}. Case 1 has the lowest effective period compared to other cases. This relates to Case 1 pipe length is much shorter than in all other cases. Clearly, effective period is dependent on pipe length when results from Case 1 and Case 2 are compared. Heat is rejected and dissipated to more ground volume impeding heat accumulation thus prolonging effective thermal performance.

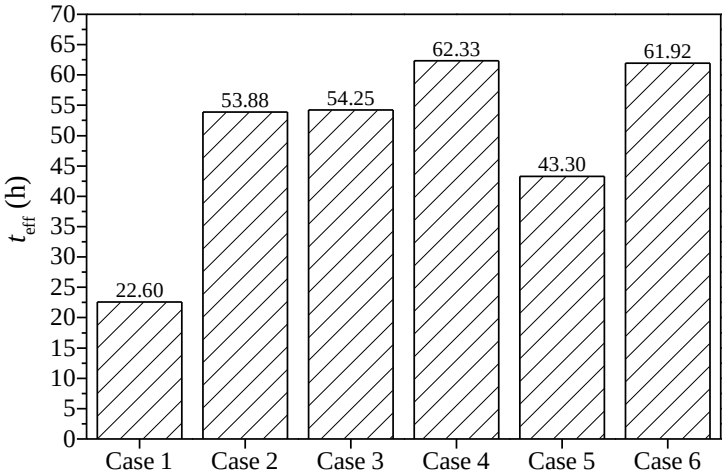

Fig. 6.9. Effective period of all cases tested.

GHE pipe length in slinky configuration cases is more or less the same. However, the effective period is noticeably different among these cases except in Case 2 and 3. This suggests that pipe materials and orientations also influence effective period. GHE using copper pipe as in Case 4 yields the highest effective period. High thermal conductivity materials would minimize heat build-up inside the pipe wall itself. Heat can travel efficiently in the presence of low temperature gradient along the pipe wall.

The effective period in Case 3 only improves slightly compared to Case 2. Apparently, effective thermal conductivity of composite pipe is largely limited by the outer coating. The advantage of highly conductive inner layer is nullified, thus rendering the effective thermal conductivity close to the ground thermal conductivity. After all, this study supports the common claim that GHE thermal performance is primarily dictated by thermal conductivity of the ground.

Fig. 6.10 shows ground temperature profile at a monitoring well at various elapsed times. The location of the monitoring well indicated by point M is about 0.005 m from nearest pipe edge. At 24 h elapsed time, Case 1 that has already beyond effective period yields the highest ground temperature near GHE. Case 4 shows the lowest temperature rise as heat travels efficiently along the pipe wall and ground region. The pipe layouts in Case 5 and 6 show a significant temperature difference inside the trench. This can be associated with the position of the return pipe and water flow path.

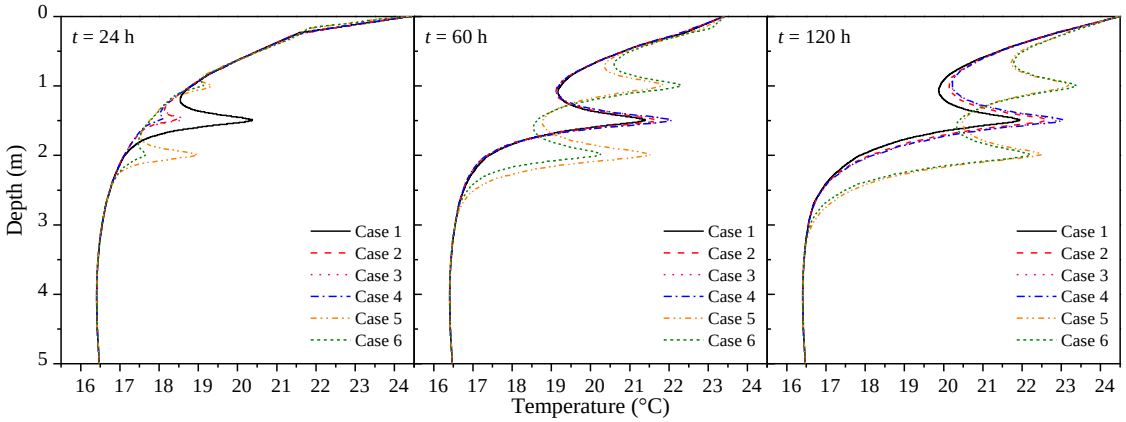

Fig. 6.10. Ground temperature profile at monitoring well along point M at 24 h, 60 h and 120 h elapsed time.

At 60 h elapsed time, most cases have reached thermal saturation except for Case 4 and 6. At this point, Case 4 it is still rejecting the highest amount of heat compared to that in other cases. This emphasizes the presence of low temperature gradient along the pipe wall although heat accumulation at surrounding ground is high. It is worth mentioning that ground temperature exceeding 3.5 m deep remains unchanged throughout the operation. At the end of operation, Case 1 shows the lowest ground temperature near GHE. As Case 1 is the earliest to cease operating effectively, the amount of heat rejected is explicably reduced.

In judging GHE thermal performance, heat exchange rate should be considered hand in hand with effective period. Fig. 6.11 shows the average of effective and overall heat exchange rate for all cases. Again here, the difference in effective heat exchange rate among cases albeit marginal indicates the presence of interactions with surface

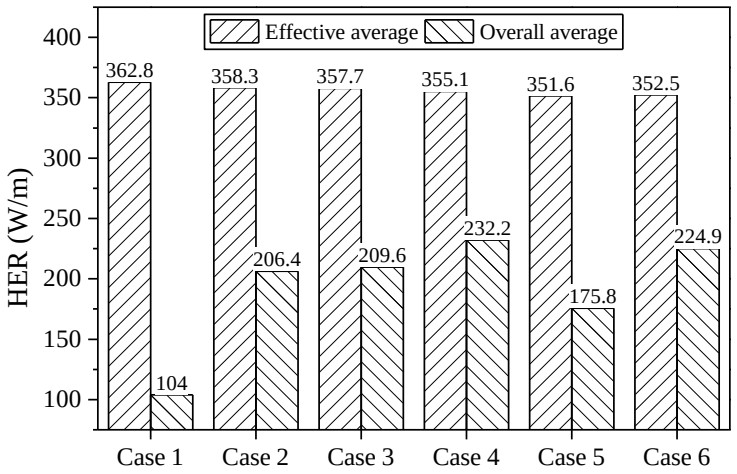

Fig. 6.11. Average effective and overall heat exchange rate.

boundary and between adjacent pipes. As highlighted before, effective heat exchange rate is largely independent of layouts or pipe materials but rather on ground temperature surrounding GHE.

On the other hand, overall heat exchange rate takes into account how long the effective heat exchange rate would last. As Case 1 has the lowest effective period, it is reflected by the poorest overall thermal performance. Of all cases, Case 4 shows the highest thermal performance. However, if the pipe material in Case 6 were to be substituted for copper as in Case 4, the thermal performance is expected to surpass the latter. This is speculated based on Case 4-to- Case 3 overall heat exchange rate ratio if it were to be used a hint.

6.3.4 Effectiveness and feasibility

The merits of installing GHE using different layouts and pipe materials were examined by comparisons among compatible cases. Fig. 6.12 shows the comparisons for cases using different configurations i.e., straight and slinky. GHE in both cases are of HDPE pipe in horizontal orientation. Slinky configuration requires significant amount of pipe material and circulation work to maintain equivalent flow rate about 130% and 138%, respectively.

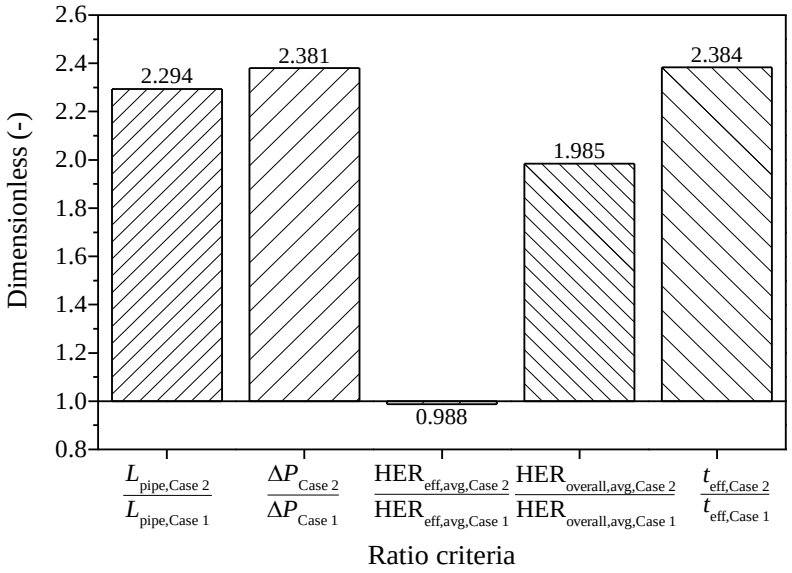

Fig. 6.12. Comparisons for cases using straight (Case 1) and slinky (Case 2) configurations.

The resulting thermal interference from adjacent pipe causes effective heat exchange rate denotes as HER_{eff} to reduce. As such, this is considered to be minimal. Overall heat exchange rate denotes as $\text{HER}_{\text{overall}}$ improvement is not impressive compared to the increase in initial and operating costs. Nevertheless, the costs are equally compensated by longer effective period. For equal trench length comparison, slinky configuration is considered to be worthwhile.

Thermal interference can be defined quantitatively as a complement of heat effectiveness [140]. In our work, heat effectiveness is taken as effective heat exchange rate ratio between slinky and straight configurations i.e., Case 2-to-Case 1. Sufficient pipe separation distance was provided in Case 1 in a way that effective heat exchange rate of Case 1 is considered isolated. Therefore, thermal interference for an equal trench length is calculated by:

$$\Lambda = 1 - \text{HER}_{\text{eff}}\,\text{ratio} = 0.012 \tag{6.8}$$

Such small 1.2% thermal interference is alleged to only some areas where the pipe is closely adjacent to the other in slinky configuration. Hence the effect is not as severe as in closely separated parallel pipes, for example U-tube legs in borehole GHE. Slinky-shape pipe is expected to induce secondary flow by centrifugal force action that in turn enhances heat transfer. However, the results prove somewhat counterproductive as the enhancement leads to thermal interference.

Thermal interference is expected to increase in overlapping slinky loops. Although admittedly by not much, the effect would be more noticeable as the loop pitch

decreases. As pointed earlier, thermal interference is more prevalent during the initial period of operation. The heat exchange rate is about the same in all cases as heat begins to accumulate at ground region near the GHE.

Fig. 6.13 shows the comparisons for cases using different pipe materials i.e., HDPE, composite and copper pipes. The GHE are all in horizontal slinky configuration. Significant improvement is observed when comparing copper to any other pipe material. The effective period and overall heat exchange rate improve by 14.9–15.7% and 10.8–12.5%, respectively.

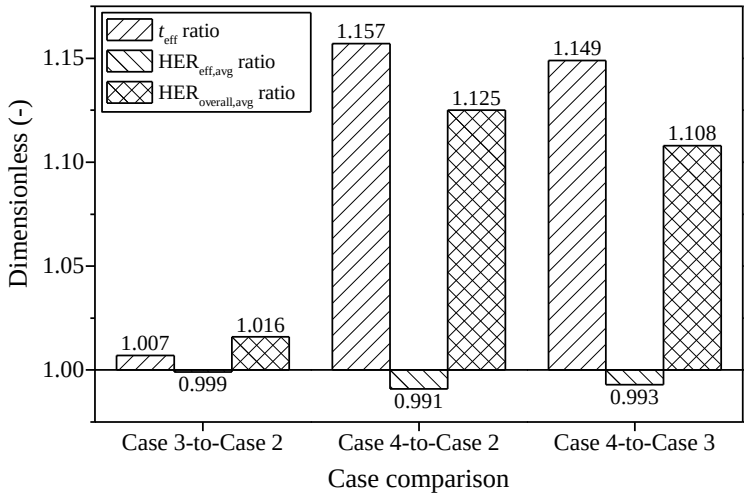

Fig. 6.13. Comparisons for cases using HDPE (Case 2), composite (Case 3) and copper (Case 4) pipes.

It can be safely said that pipe material has negligible influence on effective heat exchange rate with less than 1% difference between any two cases. Thermal performance of composite pipe improves over HDPE pipe ever so slightly. This is due to insignificant difference between thermal conductivity of these pipe materials. On top of that, effective thermal conductivity of composite pipe is close to thermal conductivity of the ground.

Installing GHE using different configurations and pipe materials may have implication on initial or operating costs or both. However, it is not overstating to say that installation using different orientations has insignificant financial difference. The amount of deeper excavation work can be compensated by narrower trench required in vertical orientation.

Fig. 6.14 shows the comparisons for cases using different orientations i.e., horizontal, vertical and inverted vertical. The GHE are in slinky configuration and using

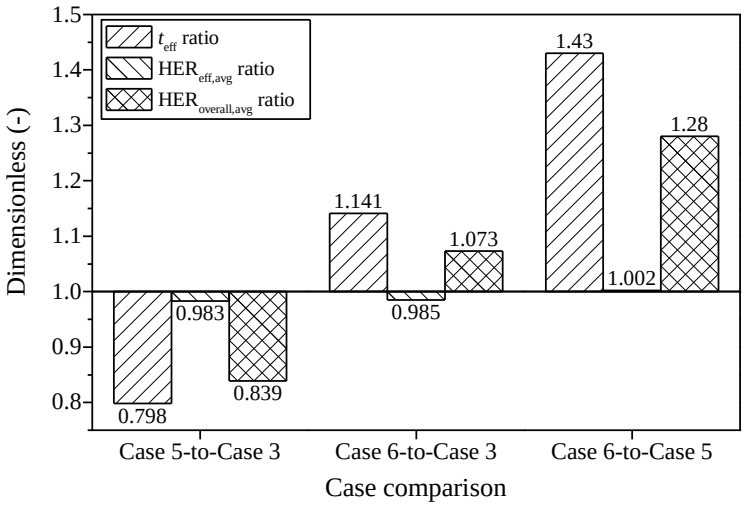

Fig. 6.14. Comparison for cases using horizontal (Case 3), vertical (Case 5) and inverted vertical (Case 6) orientations.

composite pipe. If vertical slinky GHE were to be installed, layout such in Case 5 where the return pipe is located at the top should be avoided.

Evidently, GHE layout in Case 5 brings significant detrimental effect on thermal performance. The effective period in Case 5 is reduced by 20.2% compared to using horizontal orientation as in Case 3. Contrarily, Case 6 where the return pipe sits at the bottom is able to manipulate cooler temperature at deeper ground. Enhancement of 14.1% and 7.3% for effective period and overall heat exchange rate, respectively compared to using horizontal orientation are observed.

6.3.5 Thermal interference between connecting pipes

The connecting pipes in horizontal slinky cases are well separated whereas in vertical slinky cases, they are close to each other. This might suggest strong thermal interference in the latter as it can be visually compared in Fig. 6.15. Obviously, thermal interference effect between connecting pipes can be dismissed in Case 3 at any period of operation. However, thermal interference can be observed since early operation in Case 6.

Heat flow interaction between connecting pipes in Case 6 is actually beneficial towards heat exchange process during initial operation period. This is supported in Fig. 6.7 where vertical slinky cases show superior response to operation start-up. In fact, thermal performance of Case 6 is just slightly off that in Case 1 during that period. The

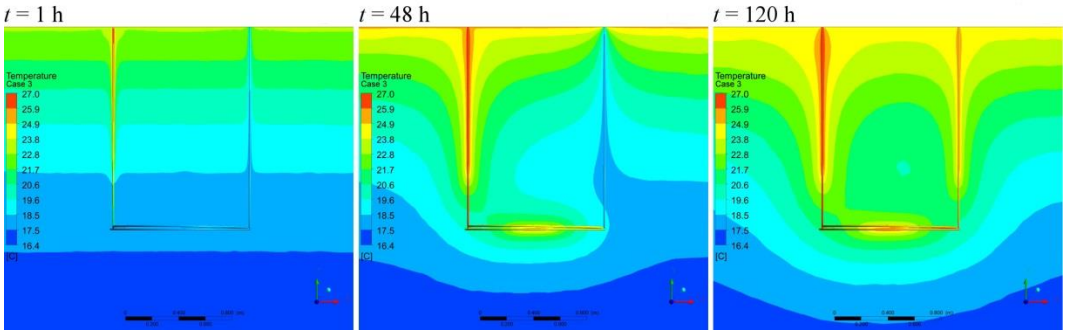

(a) Case 3

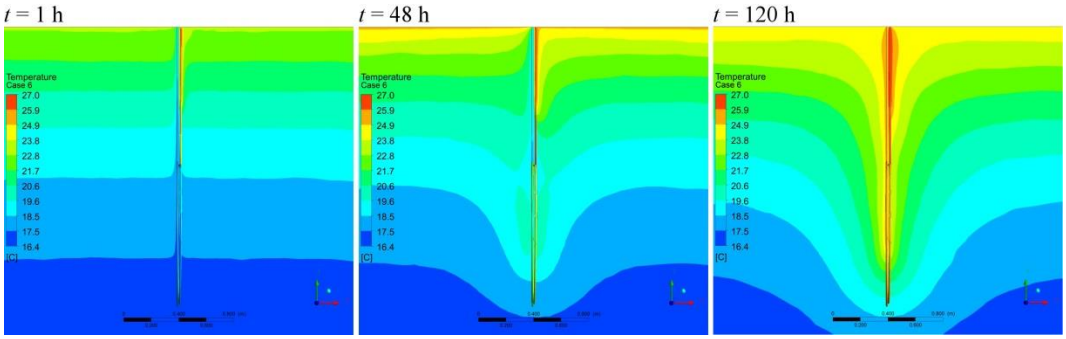

(b) Case 6

Fig. 6.15. Connecting pipes section view (Plane XY from tail end) for temperature distribution at 1 h, 48 h and 120 h elapsed time.

connecting pipes exchange heat with each other causing GHE inside the trench to receive water at a lower temperature. Consequently, this enhances heat exchange rate.

Heat exchange between connecting pipes becomes less advantageous as heat is being accumulated at this region. Heat accumulation near the entering pipe brings adverse effect to the adjacent leaving pipe. At this point, heat exchange rate deteriorates but is still operating within effective period. This is due to thermal saturation has yet to become dominant at inside the trench. The lowest effective heat exchange rate differs from the highest in Case 6 by about 24%.

In comparing thermal performance without heat flow interaction between connecting pipes, heat exchange rate for water flow inside the trench was investigated. Hourly flow temperature at two points, one at each end of connecting pipes inside the trench was acquired. The results were compared against heat exchange rate at ground surface as calculated using EWT-LWT difference. The comparisons are shown in Fig. 6.16. There is almost no thermal performance difference during effective period between inside the trench and at ground surface in Case 3.

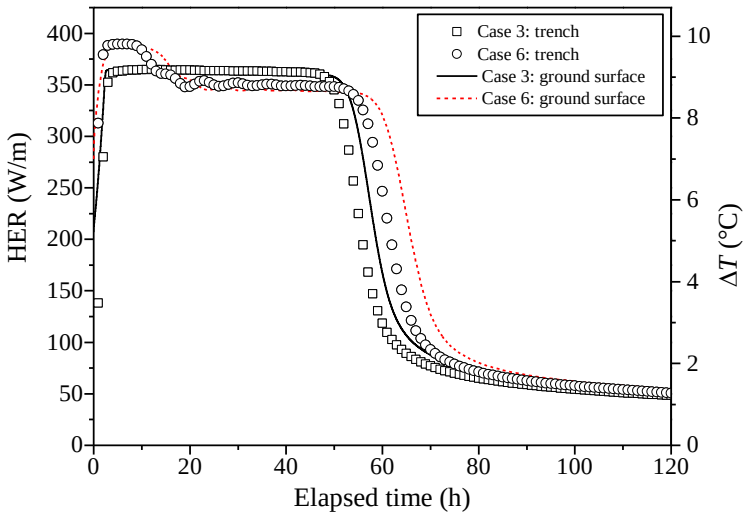

Fig. 6.16. Comparisons of HER and temperature difference between inside the trench and at ground surface versus elapsed time.

Noticeable heat exchange rate difference between inside the trench and at ground surface is observed between 10 to 20 h in Case 6. This supports that interaction between connecting pipes is beneficial towards heat exchange process. Hence, heat exchange rate decline at 10 h elapsed time can be attributed to GHE interaction with ground surface boundary alone.

Heat exchange rate inside the trench is slightly higher than at ground surface after 20 h elapsed time. The overall heat exchange rate inside the trench was 198.2 W/m and 214.1 W/m in average for Case 3 and 6, respectively. Thus, the overall heat exchange rate inside the trench ratio for Case 6-to-Case 3 is 1.08. This is a slight increase than in that shown in Fig. 6.14.

Nevertheless, vertical slinky GHE thermal performance is expected to increase when thermal interference between connecting pipes is minimized. This can be rectified, for example, by providing adequate spacing between the two pipes or by means of insulation. Adequate spacing may also be applicable at other areas such as at GHE tail end to avoid pipes overlapping.

6.3.6 Ground thermal recovery

Thermal balance in the surrounding ground is affected as a result of GHE operation. Beyond the operation effective period, thermal saturation in the ground

reduces significantly the thermal performance of GHE. Thus, it is sensible to halt the operation allowing the ground to recuperate its thermal balance before the next cycle resumes. Further investigation was carried out to analyze ground thermal behavior specifically during off period.

A slice of the ground profile cross-section where monitoring well is located was modeled for each case as shown in Fig. 6.17. These simplified models help in reducing computational requirements thus expediting the CFD solutions [82]. The flow temperatures at respective inlets of the simplified models where extracted from the real-scale models solution and applied as the flow boundary conditions as shown in Fig. 6.18. The same initial, ground surface and bottom boundary conditions as for real-scale models were applied. Both lateral walls adjacent to the GHE were assumed as adiabatic boundaries, as well as the far-field boundaries.

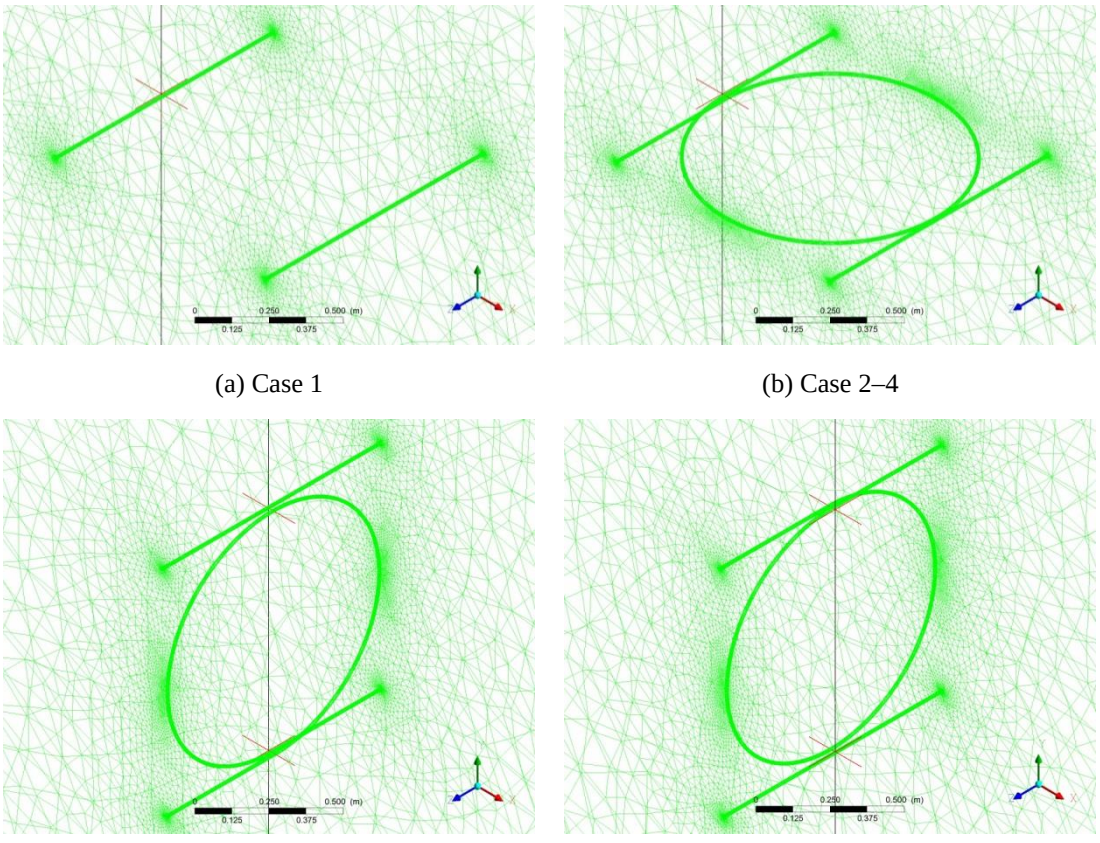

(a) Case 1 (b) Case 2–4

(c) Case 5 (d) Case 6

Fig. 6.17. Slice of the ground profile cross-section used as simplified model. The vertical lines denote monitoring well where measurement points at 1.5 m for Case 1–4 and 1.0 m and 2.0 m for Case 5 and 6.

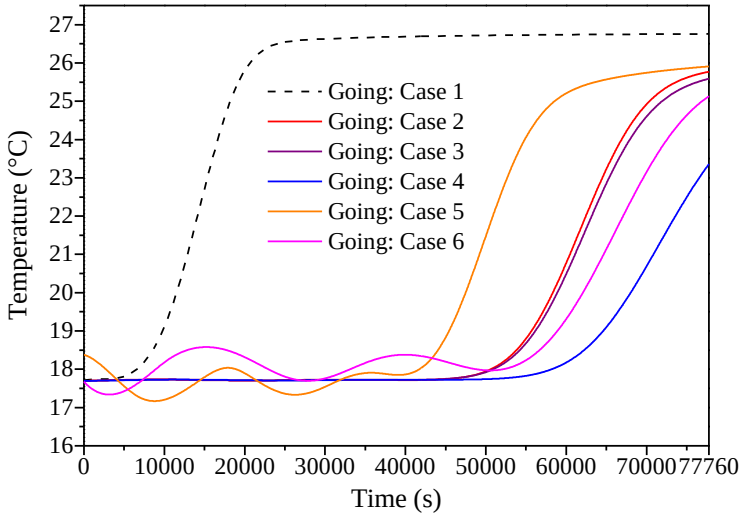

(a) Going pipe

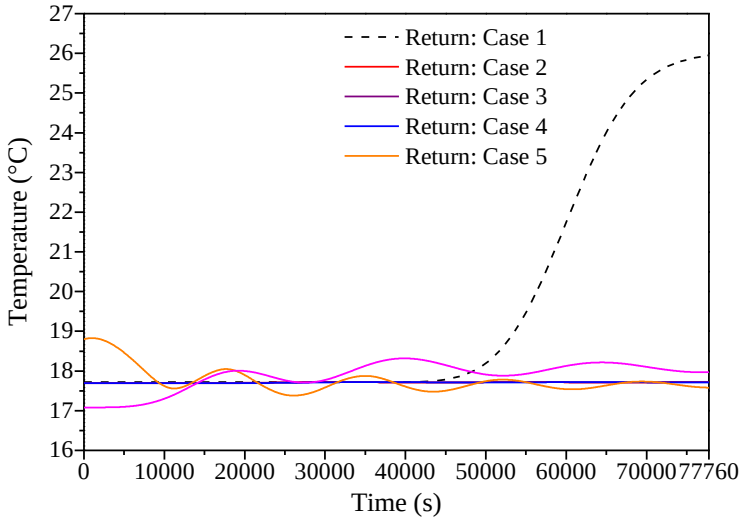

(b) Return pipe

Fig. 6.18. Inlet temperature set as boundary condition for simplified models.

The flow in all cases was stopped at 22.6 h, which is the end of effective period of Case 1 observed from the real-scale modelling. The ground temperature at measurement points along monitoring well, 1.5 m deep for Case 1–4 and 1.0 m and 2.0 m deep for Case 5 and 6 were obtained. These results were compared against undisturbed ground condition of Case 1, where the flow rate set to 0 LPM the entire time.

It is observed in Fig. 6.19 that ground temperature recovers the quickest in Case 2 while Case 4 the slowest. At the end of day-5, temperature difference at measurement point is about 0.4 °C higher than that in undisturbed condition except for Case 4. This is due to the fact that Case 4 injects the highest amount of heat to the ground per pipe

length. On a side note, as has been discovered, Case 4 is able to show longer effective operation due to minimal heat build-up within copper pipe wall. Comparison between Case 5 and 6 shows that thermal recovery rates are observed in reversed order as can be observed in Figs. 6.20 and 6.21. However, Case 6 clearly presents an advantage over Case 5 at shallower depth due to steeper temperature decrease and at deeper depth due to smaller ground temperature rise.

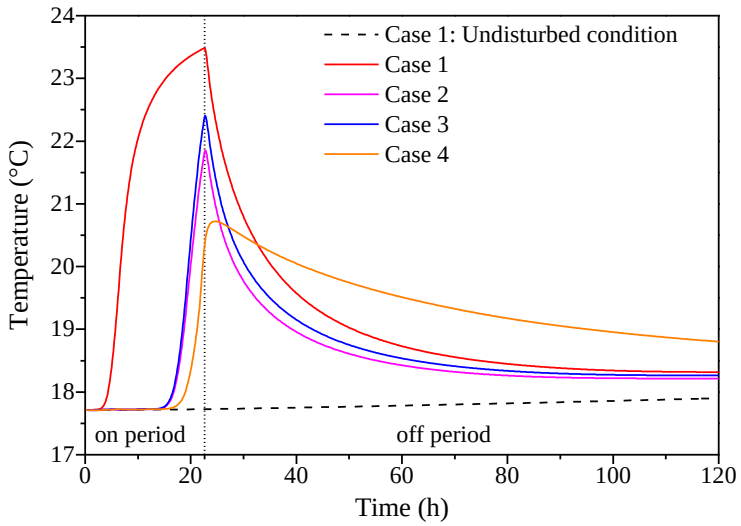

Fig. 6.19. Ground temperature at measurement point along monitoring well at 1.5 m deep.

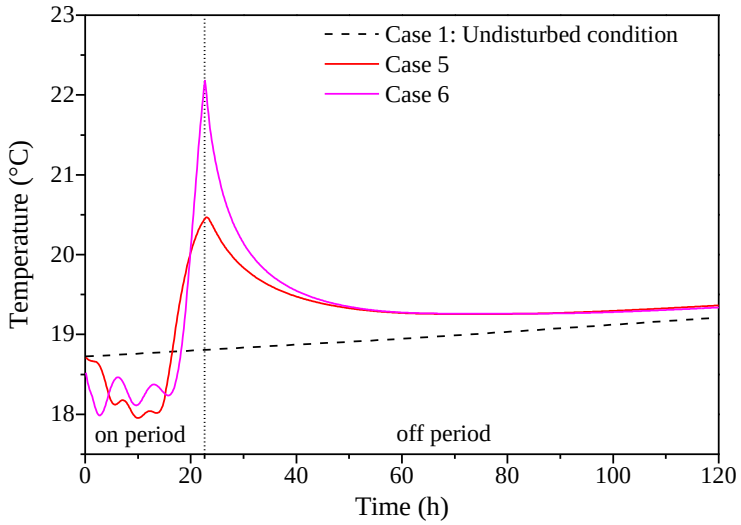

Fig. 6.20. Ground temperature at measurement point along monitoring well at 1.0 m deep.

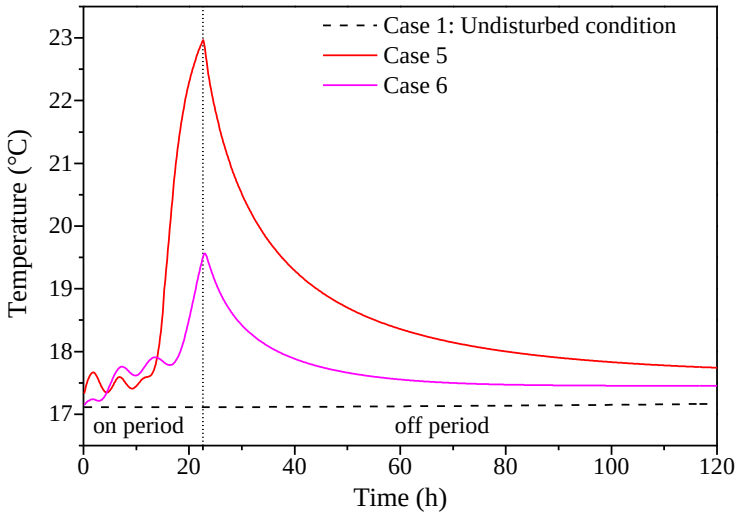

Fig. 6.21. Ground temperature at measurement point along monitoring well at 2.0 m deep.

It should be noted that these simplified models come at the expense of accuracy of CFD solution. The solution could be an artefact of boundary conditions of lateral walls being adjacent to GHE. This could explain the reason of slight temperature deviation from undisturbed condition even after the flow has stopped after a while. Nonetheless, the approach would provide a comparable indication on ground thermal recovery in the cases tested.

6.4 Conclusions

Usage of GSHP systems is blooming but rather concentrated in developed countries. To promote such usage, ways on how to reduce capital cost and overhead are essential. Horizontal GHE installed in shallow trenches are convenient low-cost solution to exorbitant boreholes drilling. Nonetheless, its shortcoming in occupying large land area as well as requires huge amount of pipe materials needs to be addressed.

The feasibility of horizontal GHE in different layouts and pipe materials was investigated for equal trench length comparison. This was carried out using CFD simulation of real-scale GHE models suited for residential or small commercial buildings installation. Potential ways of optimization are proposed as an outcome of this work.

GHE operate at an effective heat exchange rate before thermal saturation in the ground becomes dominant. Understandably, it is pointless to operate GHE beyond its

effective period. While effective heat exchange rate is fairly comparable in all cases tested, for how long they can operate effectively is a different matter. It is somewhat intriguing since there are not many studies that emphasize on such crucial parameter.

Most thermal performance prediction models are concerning the magnitude but rarely from the time perspective. This is important as thermal performance of horizontal GHE is prone to limitation by thermal saturation in the ground region. Heat accumulation is signified in moderate-sized designs like the ones being investigated in this work.

Based on simulation results, additional amount of pipe material and circulation work are compensated by prolonged effective period for GHE in slinky configuration. Heat build-up within pipe wall can be delayed by using materials with superior thermal conductivity. Copper pipe improves effective period by 16% over HDPE pipe. This brings a challenge find comparable materials or other coating techniques that are suitable for application underneath the ground.

The effective heat exchange rate in vertical orientation is 14% longer when it is installed appropriately compared to its horizontal counterpart. However, any heat transfer enhancement would cause thermal interference in slinky loops that is noticeable especially during initial operation. Even the enhanced flow behavior is somewhat counterproductive on the effective heat exchange rate.

Over time, thermal interference effect diminishes as heat being accumulated in the ground. But further improvement is expected in vertical orientation when heat flow interaction between connecting pipes is anticipated and rectified.

CHAPTER

7

CONCLUSIONS AND RECOMMENDATIONS

7.1 Conclusions

Horizontal ground heat exchangers (GHE) installed in shallow trenches help in reducing ground source heat pump (GSHP) systems installation cost. This would promote such systems usage among homeowners and small-medium enterprises. However, horizontal GHE are prone to unstable thermal performance due to temporal weathers and seasonal variations. This drawback coupled with the needs of large land area as well as piping in great length requires the designs to be scrutinized to ensure the shortest possible return of investment.

In this work, horizontal GHE models in several configurations and pipe materials were simulated for thermal performance investigation. Time- and position-varying parameters were used in the analysis to predict realistically the thermal performance of each operation. The investigation can be divided into two stages: (1) preliminary modelling involving a slice of ground profile cross-section containing only a unit of GHE and (2) real-scale modelling of moderate-size installations suited for residential or small commercial buildings installation.

Based on the preliminary analysis, it was observed that the effect of different GHE orientations is negligible on thermal performance. The thermal performance for vertical orientation provides a slight improvement of 0.8% in mean heat exchange rate compared to horizontal orientation. However, the preliminary analysis does not account

for heat transfer contribution from the return pipe. The real-scale analysis reveals that the positioning or the return pipe has significant effect on thermal performance especially in vertical orientation. Adverse effect is reported when the return pipe is positioned at the top portion. In contrast, the effective heat exchange rate is 14% longer when the return pipe is placed at the bottom compared to its horizontal orientation.

In reality, GHE is more convenient to be installed in horizontal orientation where it can be laid flat at the trench bottom and later buried. Conventionally, GHE installed in vertical orientation is an alternative option in locations where land space is limited. As suggested based on the findings, higher efficiency can be achieved through vertical orientation. Although vertical orientation requires deeper excavation as the depth increases by one-third, a narrower trench width is needed for the installation. It is safe to presume that GHE in vertical orientation is worthy the additional cost for the installation. However, thermal interference between surface connecting pipes should be minimized to benefit the most from GHE in vertical orientation.

It is a common understanding that better thermal performance comes with greater GHE length. This would allow more heat to be rejected to or extracted from more ground volume. The thermal saturation effect in the ground is delayed as heat is dissipated along greater contact area. Thus, thermal performance at optimum range is extended. GHE in slinky configuration can meet this objective while keeping the trench length to be minimal. Within optimum thermal performance range, all cases studied show comparable heat exchange rate. Nonetheless, for how long they can operate effectively or simply effective period differs from one another.

The effective period is a crucial parameter especially in shallow GHE installations where near-surface interaction and higher ground temperature variation exist. GHE operation strategies are beneficial when dealing with thermal saturation in the ground. The ground should be allowed to recuperate its thermal balance or some of it before the next cycle. Hence, it is sensible to operate GHE in cycles or alternate cooling-heating modes for domestic hot water supply. Alternating operation between (among) multiple trenches that are well-spaced could be another option where the resources e.g., land availability and capital cost permit.

In a nutshell, the analysis supports the common claim that the ground thermal resistance has more significant effect on GHE thermal performance compared to the pipe thermal resistance. It is observed that copper pipe with over 800 times the thermal conductance than HDPE pipe shows disproportionate increase in heat exchange rate.

Low pipe thermal resistance is associated with longer effective period as the heat build-up within pipe wall is delayed. Copper composite pipes are commercially-available in the market that suitable for application in harsh conditions such as GHE. However, coating material increases the effective thermal resistance making it about the same as the ground thermal resistance. Thus, superior coating materials or techniques that would not compromise the effective thermal properties of the pipes are preferable.

The proposed optimizations using different GHE configurations, orientations and pipe materials or in combination could be used a guide in designing such installations. However, it is worth noting that any heat transfer enhancement would also cause thermal interference especially in slinky configuration during initial operation. In the end, factors such as heat pump loading, time of use and available resources should be weigh in for a fine balance between systems efficiency and cost-effectiveness. An economic analysis is required to determine the cost effectiveness and return of investment of the proposed installation.

7.2 Recommendations for future works

Some recommendations for future works based on the present work are as follows:

1. The possibility of further reducing trench size by using smaller loop diameter as well as loop pitch of slinky coil and its effects on thermal performance should be investigated.
2. The modelling should include the effects of moisture transport and, if applicable, groundwater advection to improve the reliability of the analysis.
3. It is recommended to extend the size of GHE models suited for application in large building complex involving high heating and cooling demands.
4. The CFD analysis should be supported by experimental validation. At the point of writing up this thesis, experimental investigation of identical slinky GHE modelled in this work is currently on-going. The experimental work carried out by the research group involves GHE installed in both horizontal and vertical orientations.

REFERENCES

[1] Agency of Natural Resources and Energy Energy Conservation and Renewable Energy Department. Energy conservation policies of Japan 2012. http://www.meti.go.jp/english/policy/energy_environment/energy_efficiency/pdf/121003.pdf (accessed October 1, 2015).

[2] Agency of Natural Resources and Energy Energy Conservation and Renewable Energy Department. Comprehensive Energy Statistics (Preliminary Report for 2012). 2012.

[3] Ministry of the Environment Japan. Heat-island mitigation technology field (Heat pump air conditioning systems using underground heat, wastewater, etc.) 2004. http://www.env.go.jp/policy/etv/en/technologies/s05_c3.html (accessed October 1, 2015).

[4] Akbari H, Rosenfeld A, Taha H. Summer heat islands, urban trees, and white surfaces. ASHRAE Symp., vol. 96, 1990.

[5] Akbari H, Pomerantz M, Taha H. Cool surfaces and shade trees to reduce energy use and improve air quality in urban areas. Sol Energy 2001;70:295–310. doi:10.1016/S0038-092X(00)00089-X.

[6] Summary for policymakers (SPM) of the Working Group I contribution to the IPCC Fifth Assessment Report. Climate Change 2013: The Physical Science Basis. 2013.

[7] IEA. Redrawing the energy-climate map. World energy outlook special report 2013a OECD/IEA Paris. 2013.

[8] UNFCCC. Kyoto Protocol to the United Nations Framework Kyoto Protocol to the United Nations Framework. vol. 7. 1998. doi:10.1111/1467-9388.00150.

[9] Ministry of the Environment Japan. Overview of the Bill of the Basic Act on Global Warming Countermeasures (Provisional Translation). 2010.

[10] Genchi Y, Kikegawa Y, Inaba A. CO2 payback-time assessment of a regional-scale heating and cooling system using a ground source heat-pump in a high energy-consumption area in Tokyo. Appl Energy 2002;71:147–60. doi:10.1016/S0306-2619(02)00010-7.

[11] Ministry of Environment Japan. Survey result of geothermal heat pump system installation. 2013.

[12] Sasada M. Current trend in ground source heat pumps in Japan 2012. http://www.aist.go.jp/Portals/0/fukushima/images/shiryou/10-18/01_Sasada IEA141019.pdf (accessed October 1, 2015).

[13] JFE Technical Report. Geothermal air-conditioning system using the Tsubasa pile 2012:70–1. http://www.jfe-steel.co.jp/research/giho/029/pdf/029-13.pdf (accessed October 1, 2015).

[14] Mitsubishi Materials Techno. Why are geothermal heat pump systems getting more attention? n.d. http://www.mmtec.co.jp/en/stories/consulting/heatpump_b.html (accessed October 1, 2015).

[15] Atam E, Helsen L. Ground-coupled heat pumps: Part 2—Literature review and research challenges in optimal design. Renew Sustain Energy Rev 2015:1–17. doi:10.1016/j.rser.2015.07.009.

[16] Axelsson G, Stefánsson V, Björnsson G, Liu J. Sustainable management of geothermal resources and utilization. Proc. World Geotherm. Congr., Antalya, Turkey: 2005, p. 1–8.

[17] Howe JC, Gerrard M. Regulatory and legal issues in design, construction, operations, and financing. Chicago, Illinois, USA: American Bar Association; 2010.

[18] Howe JC. Overview of Green Buildings. In: Howe JC, Gerrard M, editors. law Green Build. Regul. Leg. issues Des. Constr. Oper. Financ., Chicago, Illinois, USA: American Bar Association; 2010, p. 3.

[19] Sarbu I, Sebarchievici C. General review of ground-source heat pump systems for heating and cooling of buildings. Energy Build 2014;70:441–54. doi:10.1016/j.enbuild.2013.11.068.

[20] Oughton D, Wilson A. Faber & Kell's heating & air-conditioning of buildings. 11th ed. New York, NY, US: Routledge; 2015.

[21] Kurevija T, Vulin D, Krapec V. Influence of Undisturbed Ground Temperature and Geothermal Gradient on the Sizing of Borehole Heat Exchangers. World Renew. Energy Congr., Linköping, Sweden: 2011, p. 1360–7.

[22] Swenka MJ. An Energy and Cost Analysis of Residential Ground-source Heat Pumps in Iowa. Master Thesis. Iowa State University (USA), 2008.

[23] Natural Resources Canada. Heating and cooling with a heat pump. Rev. Gatineau, Québec, Canada: Energy Publications; 2004.

[24] Harvey D. A handbook on low-energy buildings and district-energy systems: Fundamentals, techniques and examples. New York, NY, USA: Routledge; 2006.

[25] Sarbu I, Sebarchievici C. Ground-source heat pumps: Fundamentals, experiments and applications. London Wall, London, UK: Academic Press; 2015.

[26] Ochsner K. Geothermal heat pumps: A guide for planning and installing. New York, NY, USA: Routledge; 2012.

[27] Dincer I, Kanoglu M. Refrigeration aystems and applications. 2nd ed. Chicester, West Sussex, UK: John Wiley & Sons; 2011.

[28] Ewings SK. Geothermal heat pumps: Installation guide. www.global-greenhouse-warming.com; 2008.

[29] Goswami DY, Kreith F. Energy Efficiency and Renewable Energy Handbook. 2nd ed. Boca Raton, Florida, USA: CRC Press; 2015.

[30] UK Enviroment Agency (EA). Environmental good practice guide for ground source heating and cooling. 2010.

[31] Voss K. Earth-to-air heat exchangers. In: Hastings R, Wall M, editors. Sustain. Sol. Hous. Ex. Build. Technol. Vol. 2, London, UK: Earthscan; 2007.

[32] Mustafa Omer A. Ground-source heat pumps systems and applications. Renew Sustain Energy Rev 2008;12:344–71. doi:10.1016/j.rser.2006.10.003.

[33] Self SJ, Reddy BV, Rosen MA. Geothermal heat pump systems: Status review and comparison with other heating options. Appl Energy 2013;101:341–8. doi:10.1016/j.apenergy.2012.01.048.

[34] Florides G, Kalogirou S. Ground heat exchangers-A review of systems, models and applications. Renew Energy 2007;32:2461–78. doi:10.1016/j.renene.2006.12.014.

[35] Xiong Z. Development and validation of a slinky ground heat exchanger model. Master thesis. Oklahoma State University (USA), 2010. doi:10.1016/j.farmac.2004.11.004.

[36] Nam Y, Ooka R, Hwang S. Development of a numerical model to predict heat exchange rates for a ground-source heat pump system. Energy Build 2008;40:2133–40. doi:10.1016/j.enbuild.2008.06.004.

[37] Popiel., Wojtkowiak. B. Measurements of temperature distribution in ground. Exp Therm Fluid Sci 2001;25:301–9. doi:10.1016/S0894-1777(01)00078-4.

[38] Yang H, Cui P, Fang Z. Vertical-borehole ground-coupled heat pumps: A review of models and systems. Appl Energy 2010;87:16–27. doi:10.1016/j.apenergy.2009.04.038.

[39] Ball D, Fischer R, Hodgett D. Design methods for ground-source heat pumps. ASHRAE Trans 1983;89:416–40.

[40] Javed S, Fahlén P, Claesson J. Vertical ground heat exchangers: a review of heat flow models. Proc. 11th Int. Conf. Therm. energy storage - Effstock2009, Stockholm, Sweden: 2009, p. 53–78. doi:10.1017/CBO9780511974885.006.

[41] Soni SK, Pandey M, Bartaria VN. Ground coupled heat exchangers: A review and applications. Renew Sustain Energy Rev 2015;47:83–92. doi:10.1016/j.rser.2015.03.014.

[42] Li M, Lai ACK. Review of analytical models for heat transfer by vertical ground heat exchangers (GHEs): A perspective of time and space scales. Appl Energy 2015;151:178–91. doi:10.1016/j.apenergy.2015.04.070.

[43] Bear J. Dynamics of fluids in porous media. New York, NY, USA: American Elsevier Publishing Company Inc; 1972.

[44] ASHRAE. ASHRAE handbook: HVAC applications. Atlanta, USA: ASHRAE Inc; 2011.

[45] Luikov AV. Systems of differential equations of heat and mass transfer in capillary-porous bodies (review). Int J Heat Mass Transf 1975;18:1–14. doi:10.1016/0017-9310(75)90002-2.

[46] Carslaw H, Jaeger J. Conduction of heat in solids. Oxford UK: Claremore Press; 1946.

[47] Lee CK. Effects of multiple ground layers on thermal response test analysis and

ground-source heat pump simulation. Appl Energy 2011;88:4405–10. doi:10.1016/j.apenergy.2011.05.023.

[48] Claesson J, Eskilson P. Conductive heat extraction to a deep borehole: Thermal analyses and dimensioning rules. Energy 1988;13:509–27. doi:10.1016/0360-5442(88)90005-9.

[49] Eskilson P. Thermal analysis of heat extraction boreholes. Doctoral thesis. Department of Mathematical Physics, University of Lund (Sweden), 1987.

[50] Lee CK, Lam HN. A modified multi-ground-layer model for borehole ground heat exchangers with an inhomogeneous groundwater flow. Energy 2012;47:378–87. doi:10.1016/j.energy.2012.09.056.

[51] Bose J, Parker J, McQuiston F. Design/data manual for closed-loop ground coupled heat pump systems. Oklahoma State Univ for ASHRAE; 1985.

[52] Ingersoll L, Zobel O, Ingersoll A. Heat conduction with engineering, geological, and other applications. Revised ed. Madison: The University of Wisconsin Press; 1954.

[53] Hart D, Couvillion R. Earth coupled heat transfer. National Water Well Association; 1986.

[54] Fang Z, Diao N, Cui P. Discontinuous operation of geothermal heat exchangers. Tsinghua Sci Technol 2002;7:194–7.

[55] Hackner R, Hughes P, O'Neil R. Design of ECHP Systems in northern climates. ASHRAE Trans 1987;93.

[56] Kavanaugh S. Simulation and experimental verification of vertical groundcoupled heat pump systems. Doctoral thesis. Oklahoma State University, USA, 1985.

[57] Deerman J, Kavanaugh S. Simulation of vertical U-tube ground coupled heat pump systems using the cylindrical heat source solution. ASHRAE Trans 1991;97:287–95.

[58] Bernier M. Ground-coupled heat pump system simulation. ASHRAE winter Meet. CD, Tech. Symp. Pap., 2001, p. 739–50.

[59] Hellström G. Ground heat storage: thermal analysis of duct storage systems. Doctoral thesis. Department of Mathematical Physics, University of Lund (Sweden), 1991.

[60] Liu XL, Wang DL, Fang ZH. Modeling of heat transfer of a vertical bore in ground-source heat pumps. J Shandong Inst Archit Eng 2001:47–51.

[61] Zeng HY, Diao NR, Fang ZH. A finite line-source model for boreholes in geothermal heat exchangers. Heat Transf - Asian Res 2002;31:558–67. doi:10.1002/htj.10057.

[62] Gu Y, O'Neal DL. Development of an equivalent diameter expression for vertical U-tubes used in ground-coupled heat pumps. ASHRAE Trans 1998;104:347–55.

[63] Zeng HY, Diao NR, Fang ZH. Efficiency of vertical geothermal heat exchangers in ground source heat pump systems. J Therm Sci 2003;12:77–81.

[64] Man Y, Yang H, Diao N, Cui P, Lu L, Fang Z. Development of spiral heat source model for novel pile ground heat exchangers. HVAC&R Res 2011;17:1075–88. doi:10.1080/10789669.2011.610281.

[65] Park SK, Lee SR, Park H, Yoon S, Chung J. Characteristics of an analytical solution for a spiral coil type ground heat exchanger. Comput Geotech 2013;49:18–24. doi:10.1016/j.compgeo.2012.11.006.

[66] Man Y, Yang H, Diao N, Liu J, Fang Z. A new model and analytical solutions for borehole and pile ground heat exchangers. Int J Heat Mass Transf 2010;53:2593–601. doi:10.1016/j.ijheatmasstransfer.2010.03.001.

[67] Cui P, Li X, Man Y, Fang Z. Heat transfer analysis of pile geothermal heat exchangers with spiral coils. Appl Energy 2011;88:4113–9. doi:10.1016/j.apenergy.2011.03.045.

[68] Li H, Nagano K, Lai Y. Heat transfer of a horizontal spiral heat exchanger under groundwater advection. Int J Heat Mass Transf 2012;55:6819–31. doi:10.1016/j.ijheatmasstransfer.2012.06.089.

[69] Xiong Z, Fisher DE, Spitler JD. Development and validation of a Slinky ™ ground heat exchanger model. Appl Energy 2015;141:57–69. doi:10.1016/j.apenergy.2014.11.058.

[70] Kabashnikov VP, Danilevskii LN, Nekrasov VP, Vityaz IP. Analytical and numerical investigation of the characteristics of a soil heat exchanger for ventilation systems. Int J Heat Mass Transf 2002;45:2407–18. doi:10.1016/S0017-9310(01)00319-2.

[71] Ruan W, Horton WT. Literature review on the calculation of vertical ground heat exchangers for geothermal heat pump systems. Int. High Perform. Build. Conf., 2010, p. 1–5.

[72] Aslam Bhutta MM, Hayat N, Bashir MH, Khan AR, Ahmad KN, Khan S. CFD applications in various heat exchangers design: A review. Appl Therm Eng 2012;32:1–12. doi:10.1016/j.applthermaleng.2011.09.001.

[73] De Paepe M, Janssens A. Thermo-hydraulic design of earth-air heat exchangers. Energy Build 2003;35:389–97. doi:10.1016/S0378-7788(02)00113-5.

[74] Shonder J, Beck J. Determining effective soil formation thermal properties from field data using a parameter estimation technique. ASHRAE Trans 1999;105:458–66.

[75] Bojic M, Trifunovic N, Papadakis G, Kyritsis S. Numerical simulation, technical and economic evaluation of air-to-earth heat exchanger coupled to a building. Energy 1997;22:1151–8. doi:10.1016/S0360-5442(97)00055-8.

[76] Bi Y, Chen L, Wu C. Ground heat exchanger temperature distribution analysis and experimental verification. Appl Therm Eng 2002;22:183–9. doi:10.1016/S1359-4311(01)00073-4.

[77] Rottmayer SP, Beckman WA, Mitchell JW. Simulation of a single vertical U-tube ground heat exchanger in an infinite medium. ASHRAE Trans 1997;103:651–9.

[78] Gauthier C, Lacroix M, Bernier H. Numerical simulation of soil heat exchanger-

storage systems for greenhouses. Sol Energy 1997;60:333–46. doi:10.1016/S0038-092X(97)00022-4.

[79] De Paepe M, Willems N. 3D unstructured modelling technique for ground-coupled air heat exchanger. Clima 2000/Napoli World Congr., Napoli, Italy: 2001, p. 15–8.

[80] Piechowski M. Heat and mass transfer model of a ground heat exchanger : Theoretical development. Int J Energy Res 1999;23:571–88. doi:10.1002/(SICI)1099-114X(19990610)23:7<571::AID-ER462>3.0.CO;2-6.

[81] Wu Y, Gan G, Verhoef A, Vidale PL, Gonzalez RG. Experimental measurement and numerical simulation of horizontal-coupled slinky ground source heat exchangers. Appl Therm Eng 2010;30:2574–83. doi:10.1016/j.applthermaleng.2010.07.008.

[82] Chong CSA, Gan G, Verhoef A, Garcia RG, Vidale PL. Simulation of thermal performance of horizontal slinky-loop heat exchangers for ground source heat pumps. Appl Energy 2013;104:603–10. doi:10.1016/j.apenergy.2012.11.069.

[83] Fujii H, Nishi K, Komaniwa Y, Chou N. Numerical modeling of slinky-coil horizontal ground heat exchangers. Geothermics 2012;41:55–62. doi:10.1016/j.geothermics.2011.09.002.

[84] Cui P, Yang H, Fang Z. Numerical analysis and experimental validation of heat transfer in ground heat exchangers in alternative operation modes. Energy Build 2008;40:1060–6. doi:10.1016/j.enbuild.2007.10.005.

[85] Garber D, Choudhary R, Soga K. Risk based lifetime costs assessment of a ground source heat pump (GSHP) system design: Methodology and case study. Build Environ 2013;60:66–80. doi:10.1016/j.buildenv.2012.11.011.

[86] Ozgener O, Ozgener L, Tester JW. A practical approach to predict soil temperature variations for geothermal (ground) heat exchangers applications. Int J Heat Mass Transf 2013;62:473–80. doi:10.1016/j.ijheatmasstransfer.2013.03.031.

[87] Pulat E, Coskun S, Unlu K, Yamankaradeniz N. Experimental study of horizontal ground source heat pump performance for mild climate in Turkey. Energy 2009;34:1284–95. doi:10.1016/j.energy.2009.05.001.

[88] Naili N, Hazami M, Attar I, Farhat A. In-field performance analysis of ground source cooling system with horizontal ground heat exchanger in Tunisia. Energy 2013;61:319–31. doi:10.1016/j.energy.2013.08.054.

[89] Jalaluddin, Miyara A, Tsubaki K, Inoue S, Yoshida K. Experimental study of several types of ground heat exchanger using a steel pile foundation. Renew Energy 2011;36:764–71. doi:10.1016/j.renene.2010.08.011.

[90] Jalaluddin, Miyara A. Thermal performance investigation of several types of vertical ground heat exchangers with different operation mode. Appl Therm Eng 2012;33-34:167–74. doi:10.1016/j.applthermaleng.2011.09.030.

[91] Flaga-Maryanczyk A, Schnotale J, Radon J, Was K. Experimental measurements and CFD simulation of a ground source heat exchanger operating at a cold climate for a passive house ventilation system. Energy Build 2014;68:562–70.

doi:10.1016/j.enbuild.2013.09.008.

[92] Tarnawski VR, Leong WH, Momose T, Hamada Y. Analysis of ground source heat pumps with horizontal ground heat exchangers for northern Japan. Renew Energy 2009;34:127–34. doi:10.1016/j.renene.2008.03.026.

[93] Benazza A, Blanco E, Aichouba M, Río JL, Laouedj S. Numerical investigation of horizontal ground coupled heat exchanger. Energy Procedia 2011;6:29–35. doi:10.1016/j.egypro.2011.05.004.

[94] Rezaei-Bazkiaei A, Dehghan-Niri E, Kolahdouz EM, Weber a. S, Dargush GF. A passive design strategy for a horizontal ground source heat pump pipe operation optimization with a non-homogeneous soil profile. Energy Build 2013;61:39–50. doi:10.1016/j.enbuild.2013.01.040.

[95] Simms RB, Haslam SR, Craig JR. Impact of soil heterogeneity on the functioning of horizontal ground heat exchangers. Geothermics 2014;50:35–43. doi:10.1016/j.geothermics.2013.08.007.

[96] Congedo PM, Colangelo G, Starace G. CFD simulations of horizontal ground heat exchangers: A comparison among different configurations. Appl Therm Eng 2012;33-34:24–32. doi:10.1016/j.applthermaleng.2011.09.005.

[97] Ansys Fluent Theory Guide. Canonsburg, PA, USA: Ansys Inc.; 2011.

[98] Andersland OBB, Ladanyi B. Frozen Ground Engineering. 2nd ed. Hoboken, NJ, USA: John Wiley & Sons; 2003.

[99] JSME Data Book (in Japanese). 5th ed. Shinjuku, Tokyo, Japan: The Japan Society of Mechanical Engineers; 2009.

[100] Sanner B, Karytsas C, Mendrinos D, Rybach L. Current status of ground source heat pumps and underground thermal energy storage in Europe. Geothermics 2003;32:579–88. doi:10.1016/S0375-6505(03)00060-9.

[101] Lund J, Sanner B, Rybach L, Curtis R, Hellström G. Geothermal (ground-source) heat pumps a world overview. GHC Bull 2004:1–10.

[102] Yang W, Zhou J, Xu W, Zhang G. Current status of ground-source heat pumps in China. Energy Policy 2010;38:323–32. doi:10.1016/j.enpol.2009.09.021.

[103] Qi Z, Gao Q, Liu Y, Yan YY, Spitler JD. Status and development of hybrid energy systems from hybrid ground source heat pump in China and other countries. Renew Sustain Energy Rev 2014;29:37–51. doi:10.1016/j.rser.2013.08.059.

[104] Zachár a. Analysis of coiled-tube heat exchangers to improve heat transfer rate with spirally corrugated wall. Int J Heat Mass Transf 2010;53:3928–39. doi:10.1016/j.ijheatmasstransfer.2010.05.011.

[105] Bansal V, Misra R, Agrawal G Das, Mathur J. Performance analysis of earth–pipe–air heat exchanger for summer cooling. Energy Build 2010;42:645–8. doi:10.1016/j.enbuild.2009.11.001.

[106] Svec OJ, Goodrich LE, Palmer JHL. Heat transfer characteristics of in-ground heat exchangers. Int J Energy Res 1983;7:265–78. doi:10.1002/er.4440070307.

[107] Svec OJ, Palmer JHL. Performance of a spiral ground heat exchanger for heat

pump application. Int J Energy Res 1989;13:503–10. doi:10.1002/er.4440130502.

[108] Mihalakakou G, Santamouris M, Asimakopoulos D. On the cooling potential of earth to air heat exchangers. Energy Convers Manag 1994;35:395–402. doi:10.1016/0196-8904(94)90098-1.

[109] Zeng H, Diao N, Fang Z. Heat transfer analysis of boreholes in vertical ground heat exchangers. Int J Heat Mass Transf 2003;46:4467–81. doi:10.1016/S0017-9310(03)00270-9.

[110] Bharadwaj P, Khondge AD, Date AW. Heat transfer and pressure drop in a spirally grooved tube with twisted tape insert. Int J Heat Mass Transf 2009;52:1938–44. doi:10.1016/j.ijheatmasstransfer.2008.08.038.

[111] Adamovsky D, Neuberger P, Adamovsky R. Changes in energy and temperature in the ground mass with horizontal heat exchangers—The energy source for heat pumps. Energy Build 2015;92:107–15. doi:10.1016/j.enbuild.2015.01.052.

[112] Yoon S, Lee S-R, Go G-H. Evaluation of thermal efficiency in different types of horizontal ground heat exchangers. Energy Build 2015;105:100–5. doi:10.1016/j.enbuild.2015.07.054.

[113] Jalaluddin, Miyara A. Thermal performance and pressure drop of spiral-tube ground heat exchangers for ground-source heat pump. Appl Therm Eng 2015;90:630–7. doi:10.1016/j.applthermaleng.2015.07.035.

[114] Dravid AN, Smith KA, Merrill EW, Brian PL. Effect of secondary fluid motion on laminar flow heat transfer in helically coiled tubes. AIChE J 1971;17:1114–22. doi:10.1002/aic.690170517.

[115] Mokrani A, Castelain C, Peerhossaini H. The effects of chaotic advection on heat transfer. Int J Heat Mass Transf 1997;40:3089–104. doi:10.1016/S0017-9310(96)00361-4.

[116] Seader JD, Kalb CE, City SL. Heat and mass transfer for viscous phenomena flow. Int J Heat Mass Transf 1972;15:801–17.

[117] Barbier E. Geothermal energy technology and current status: An overview. Renew Sustain Energy Rev 2002;6:3–65. doi:10.1016/S1364-0321(02)00002-3.

[118] Blum P, Campillo G, Münch W, Kölbel T. CO2 savings of ground source heat pump systems - A regional analysis. Renew Energy 2010;35:122–7. doi:10.1016/j.renene.2009.03.034.

[119] Hepbasli A, Ozgener L. Development of geothermal energy utilization in Turkey: A review. Renew Sustain Energy Rev 2004;8:433–60. doi:10.1016/j.rser.2003.12.004.

[120] Lee JY. Current status of ground source heat pumps in Korea. Renew Sustain Energy Rev 2009;13:1560–8. doi:10.1016/j.rser.2008.10.005.

[121] Islamoglu Y, Parmaksizoglu C. The effect of channel height on the enhanced heat transfer characteristics in a corrugated heat exchanger channel. Appl Therm Eng 2003;23:979–87. doi:10.1016/S1359-4311(03)00029-2.

[122] Han H, He Y-L, Li Y-S, Wang Y, Wu M. A numerical study on compact

enhanced fin-and-tube heat exchangers with oval and circular tube configurations. Int J Heat Mass Transf 2013;65:686–95. doi:10.1016/j.ijheatmasstransfer.2013.06.049.

[123] Islam MA, Miyara A. Liquid film and droplet flow behaviour and heat transfer characteristics of herringbone microfin tubes. Int J Refrig 2007;30:1408–16. doi:10.1016/j.ijrefrig.2007.03.009.

[124] Webb RL. Performance evaluation criteria for use of enhanced heat transfer surfaces in heat exchanger design. Int J Heat Mass Transf 1981;24:715–26. doi:10.1016/0017-9310(81)90015-6.

[125] Masao F, Yu S, Goro Y. Heat transfer and pressure drop of perforated surface heat exchanger with passage enlargement and contraction. Int J Heat Mass Transf 1988;31:135–42. doi:10.1016/0017-9310(88)90230-X.

[126] Goswami DY BK. Use of underground air tunnels for heating and cooling agricultural and residential buildings. Fact Sheet EES 78, a series of the Florida Energy Extension Service, Florida Cooperative Extension Service, Institute of Food and Agricultural Sciences, Univers 1993:1–4.

[127] Ochsner K. Carbon dioxide heat pipe in conjunction with a ground source heat pump (GSHP). Appl Therm Eng 2008;28:2077–82. doi:10.1016/j.applthermaleng.2008.04.023.

[128] Sakaya M, Motai T, Mochizuki M, Mashiko K. Corrugated heat pipe. US4917175 A, 1990.

[129] Jensen R. Twisted conduit for geothermal heating and cooling systems. US8640765 B2, 2014.

[130] Badescu V. Simple and accurate model for the ground heat exchanger of a passive house. Renew Energy 2007;32:845–55. doi:10.1016/j.renene.2006.03.004.

[131] Santamouris M, Mihalakakou G, Argiriou A, Asimakopoulos D. On the performance of buildings coupled with earth to air heat exchangers. Sol Energy 1995;54:375–80. doi:10.1016/0038-092X(95)00016-K.

[132] Khedari J, Permchart W, Pratinthong N, Thepa S, Hirunlabh J. Field study using the ground as a heat sink for the condensing unit of an air conditioner in Thailand. Energy 2001;26:797–810. doi:10.1016/S0360-5442(01)00036-6.

[133] Nordström J, Forsberg K, Adamsson C, Eliasson P. Finite volume methods, unstructured meshes and strict stability for hyperbolic problems. Appl Numer Math 2003;45:453–73. doi:10.1016/S0168-9274(02)00239-8.

[134] Xing L. Analytical and numerical modeling of foundation heat exchangers. Master thesis. Oklahoma State University (USA), 2010.

[135] Niu F, Yu Y, Yu D, Li H. Investigation on soil thermal saturation and recovery of an earth to air heat exchanger under different operation strategies. Appl Therm Eng 2015;77:90–100. doi:10.1016/j.applthermaleng.2014.11.069.

[136] Cui P, Yang H, Fang Z. Heat transfer analysis of ground heat exchangers with inclined boreholes. Appl Therm Eng 2006;26:1169–75. doi:10.1016/j.applthermaleng.2005.10.034.

[137] Yang W, Shi M, Liu G, Chen Z. A two-region simulation model of vertical U-tube ground heat exchanger and its experimental verification. Appl Energy 2009;86:2005–12. doi:10.1016/j.apenergy.2008.11.008.

[138] Man Y, Cui P, Fang Z. Heat transfer modeling of the ground heat exchangers for the ground-coupled heat pump systems. In: Şencan A, editor. Model. Optim. Renew. Energy Syst., Rijeka, Croatia: InTech; 2012, p. 117–46.

[139] Mei VC. Heat pump ground coil analysis with thermal interference. J Sol Energy Eng 1988;110:67. doi:10.1115/1.3268247.

[140] Muraya NK. Numerical modeling of the transient thermal interference of vertical U-tube heat exchangers. Doctoral thesis. Texas A&M University (US), 1994. doi:10.1108/eb050773.

[141] Camdali U, Bulut M, Sozbir N. Numerical modeling of a ground source heat pump: The Bolu case. Renew Energy 2015;83:352–61. doi:10.1016/j.renene.2015.04.030.

[142] Gan G. Simulation of dynamic interactions of the earth–air heat exchanger with soil and atmosphere for preheating of ventilation air. Appl Energy 2015;158:118–32. doi:10.1016/j.apenergy.2015.08.081.

[143] Marcotte D, Pasquier P. The effect of borehole inclination on fluid and ground temperature for GLHE systems. Geothermics 2009;38:392–8. doi:10.1016/j.geothermics.2009.06.001.

[144] Pollack HN, Hurter SJ, Johnson JR. Heat flow from the Earth's interior: Analysis of the global data set. Rev Geophys 1993;31:267–80. doi:10.1029/93RG01249.